Interacting activity patterns in neural field models of working memory

Zachary Kilpatrick

Winter School on Deterministic and Stochastic Models in Neuroscience
Université Paul Sabatier, Toulouse, France
December 11, 2017

with Nikhil Krishnan (CU Boulder)
and Daniel Poll (Northwestern)

Working Memory

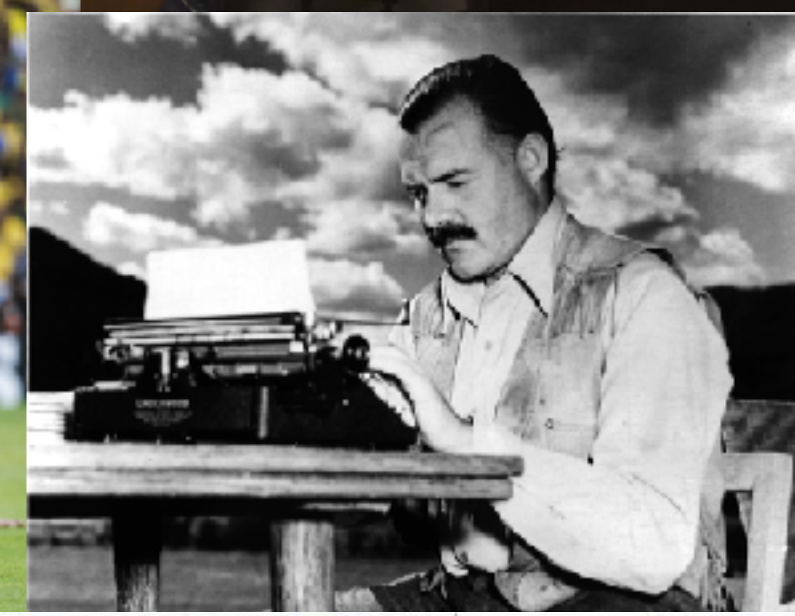

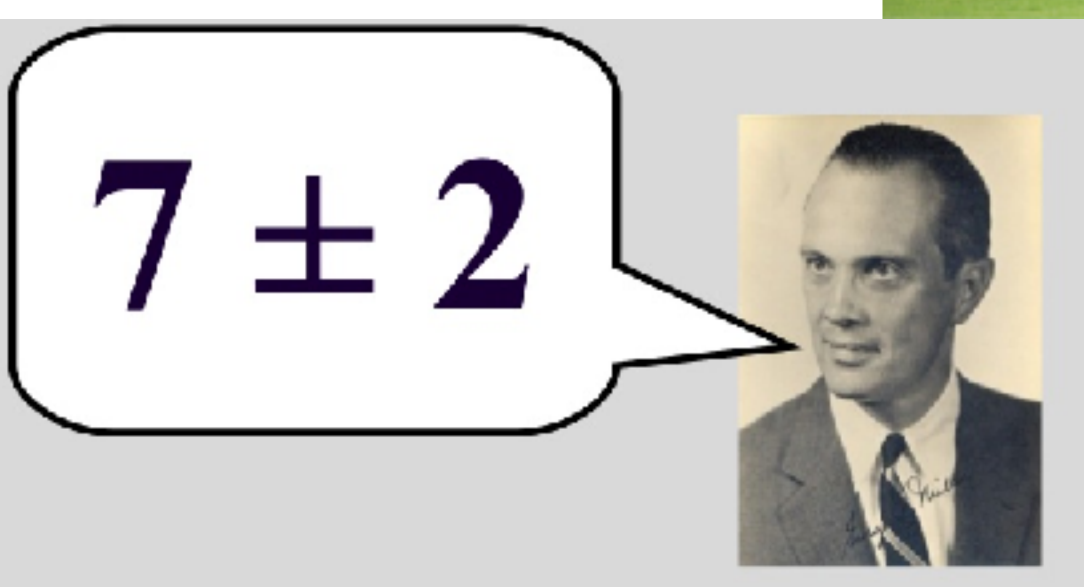

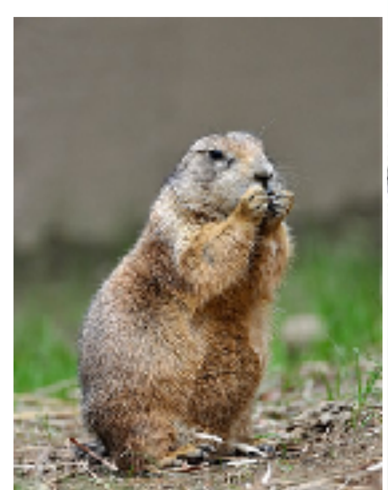

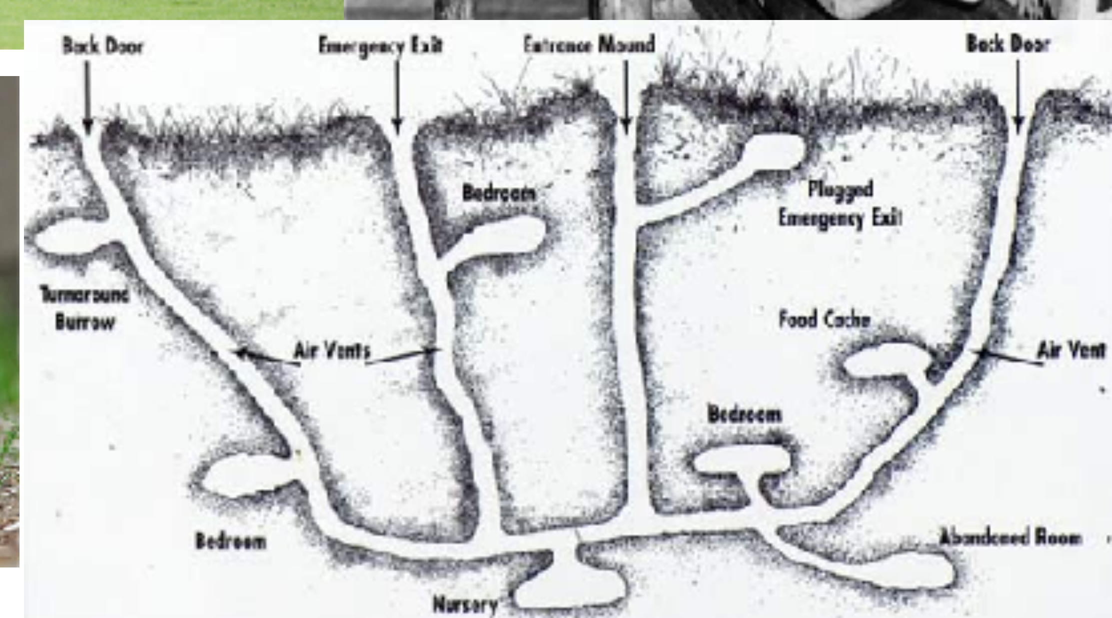

Outline

1. ***Continuous attractor models*** of parametric WM

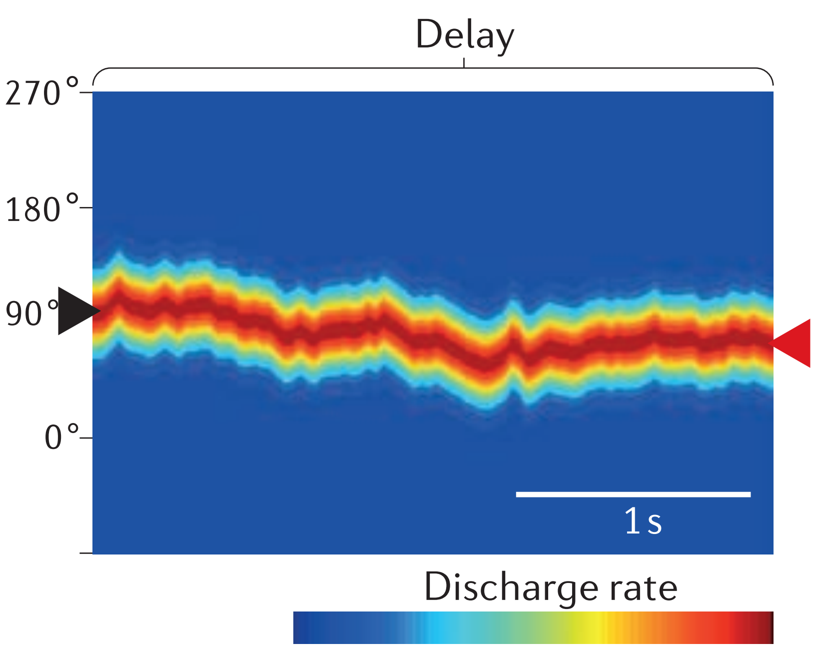

(Constantinidis & Klingberg 2016)

Outline

1. ***Continuous attractor models*** of parametric WM

2. Multi-item working memory: ***interacting bumps***

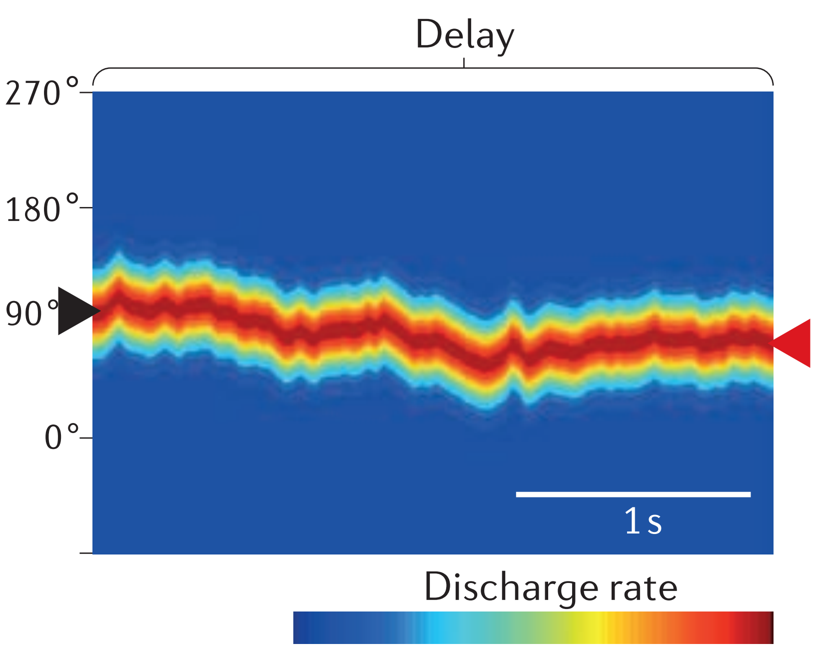

(Constantinidis & Klingberg 2016)

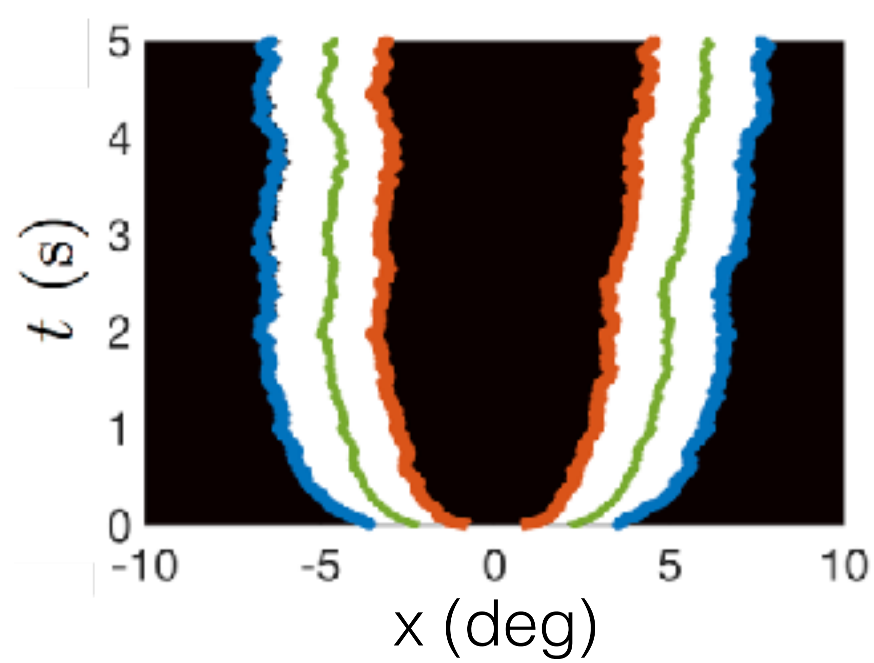

(Krishnan, Poll, and ZPK 2017)

Outline

1. ***Continuous attractor models*** of parametric WM

2. Multi-item working memory: ***interacting bumps***

3. Neural field model of ***memory-guided search***

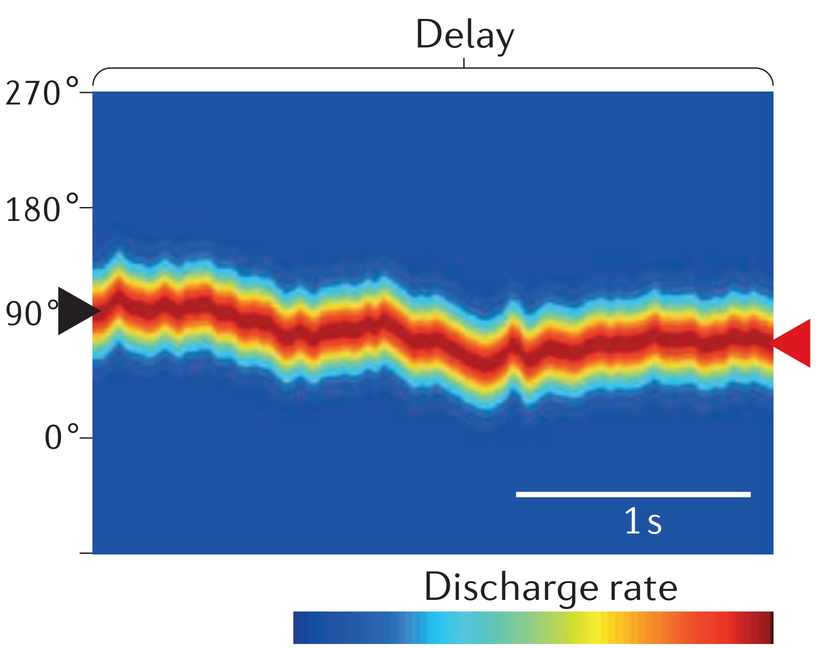

(Constantinidis & Klingberg 2016)

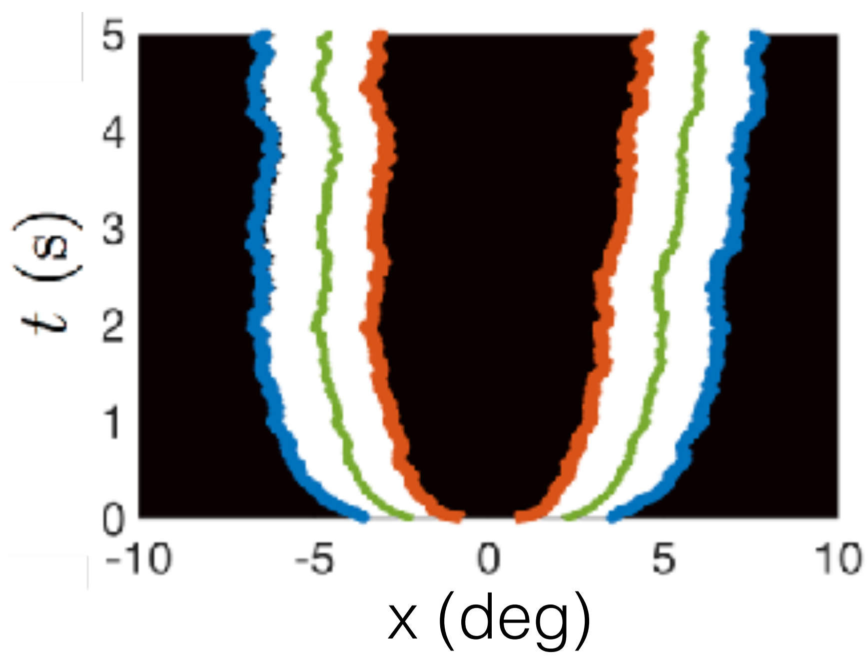

(Krishnan, Poll, and ZPK 2017)

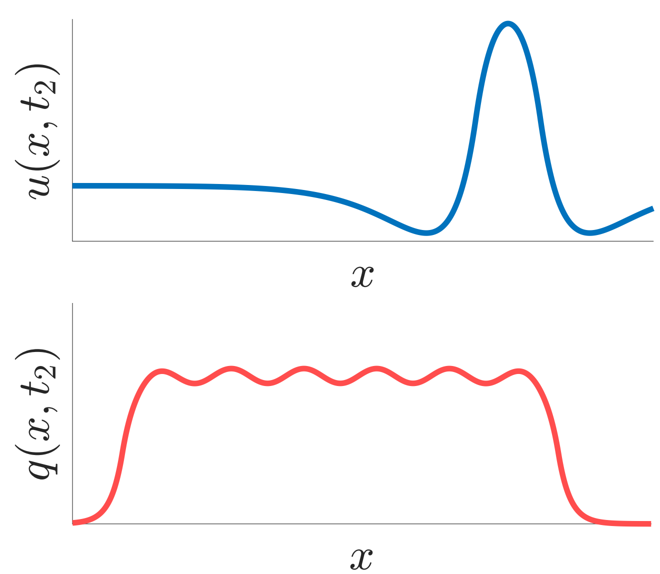

(ZPK and Poll 2017)

Visual spatial working memory experiments

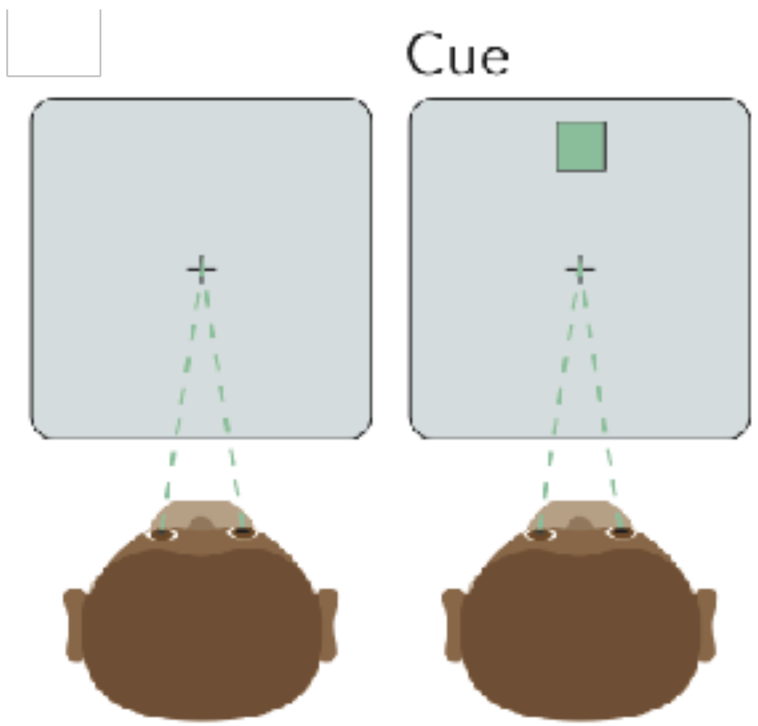

(Constantinidis & Klingberg 2016)

Visual spatial working memory experiments

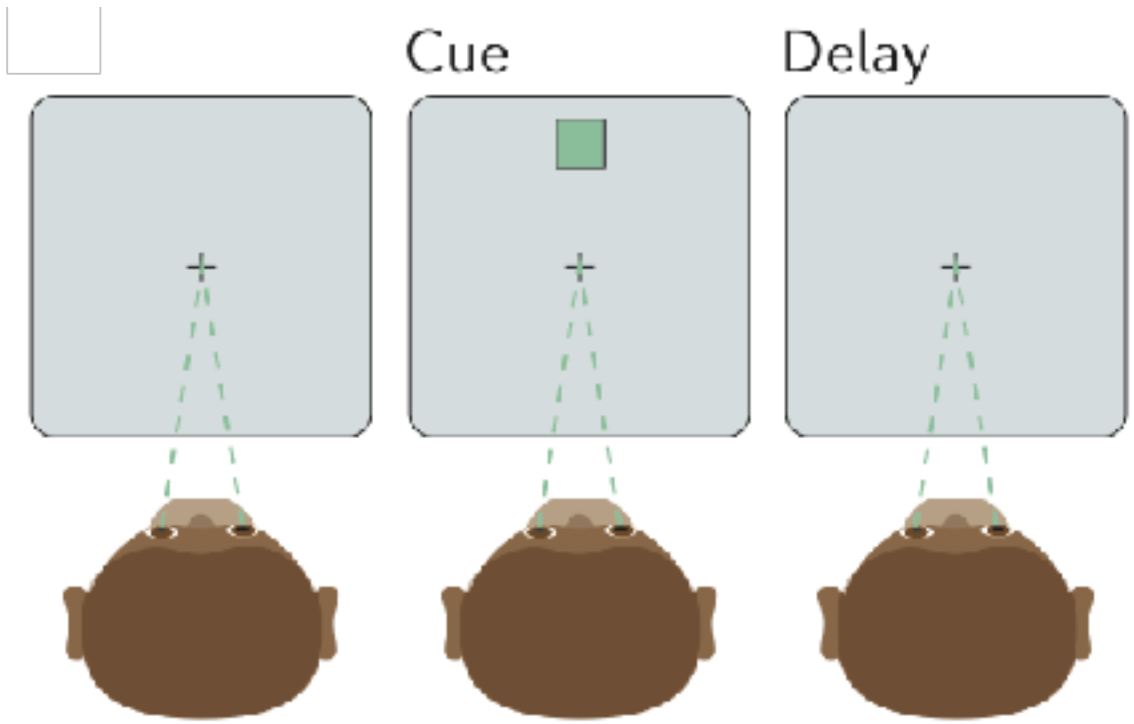

(Constantinidis & Klingberg 2016)

Visual spatial working memory experiments

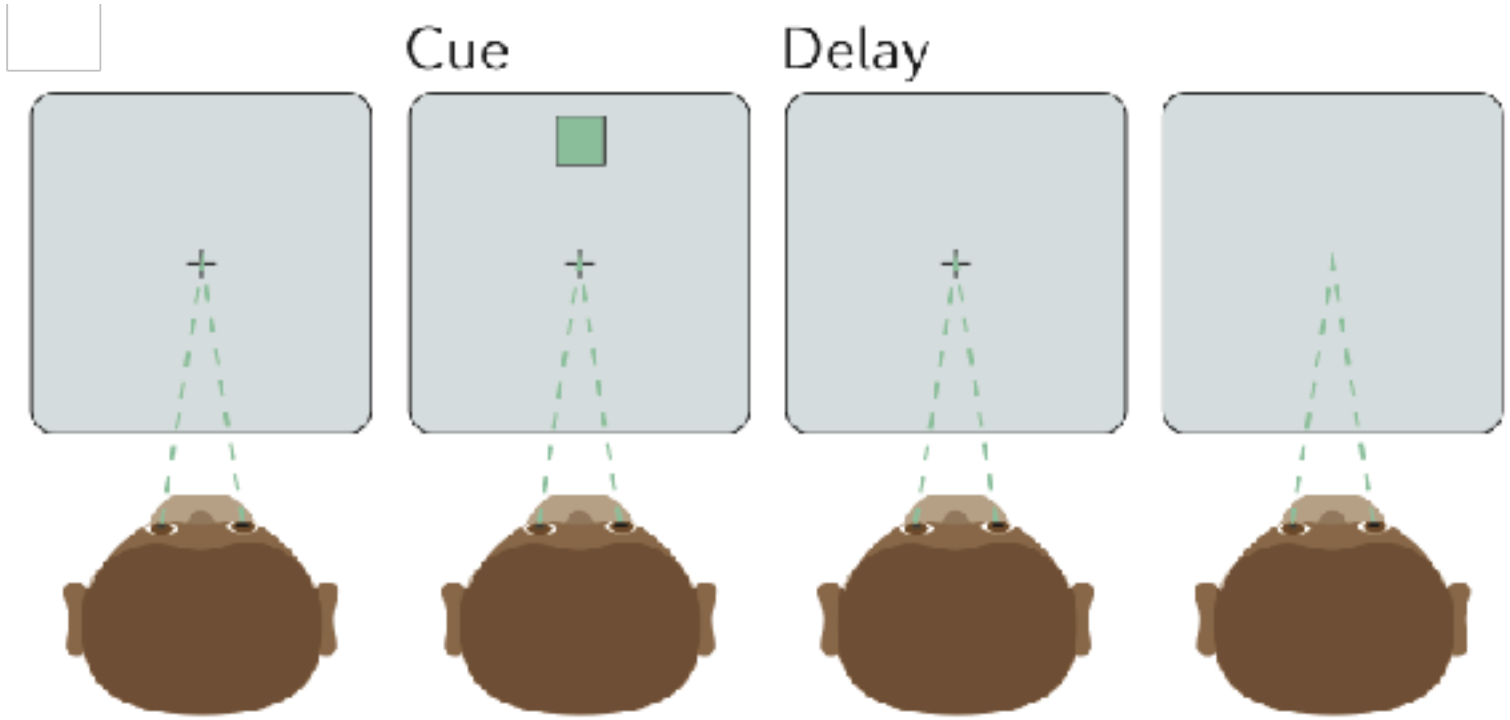

(Constantinidis & Klingberg 2016)

Visual spatial working memory experiments

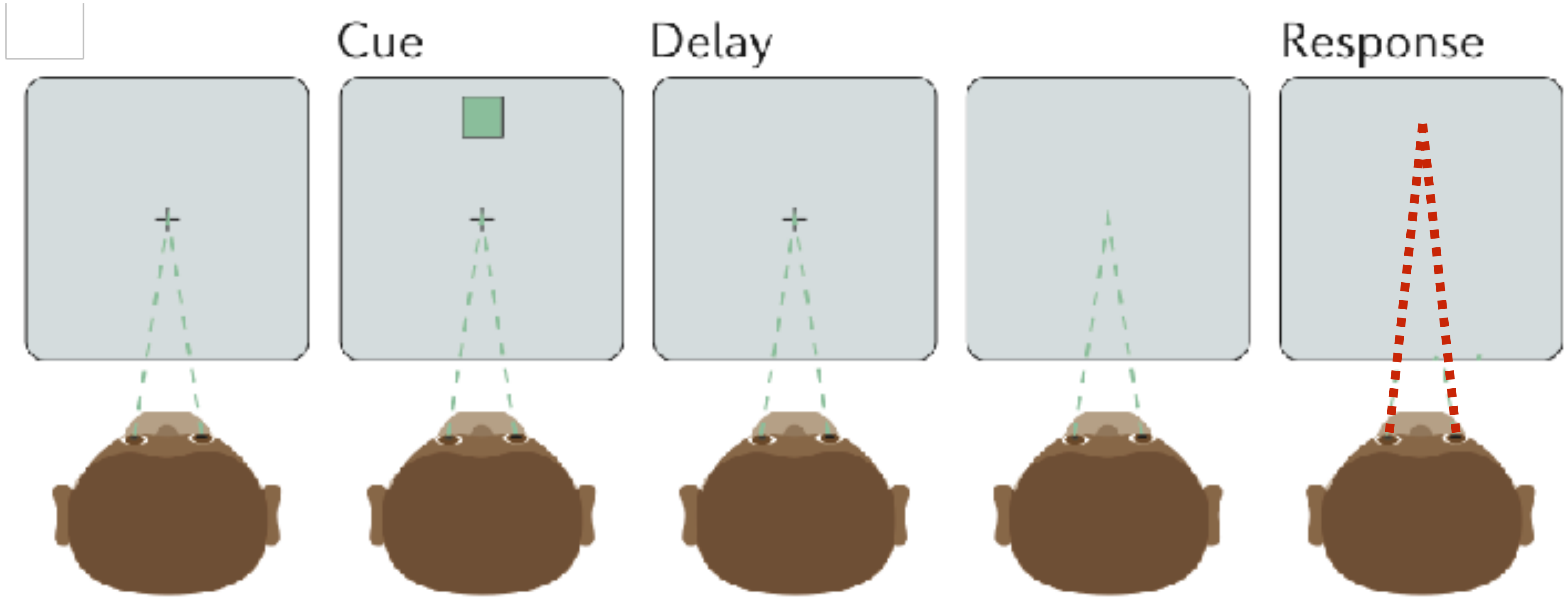

(Constantinidis & Klingberg 2016)

Visual spatial working memory experiments

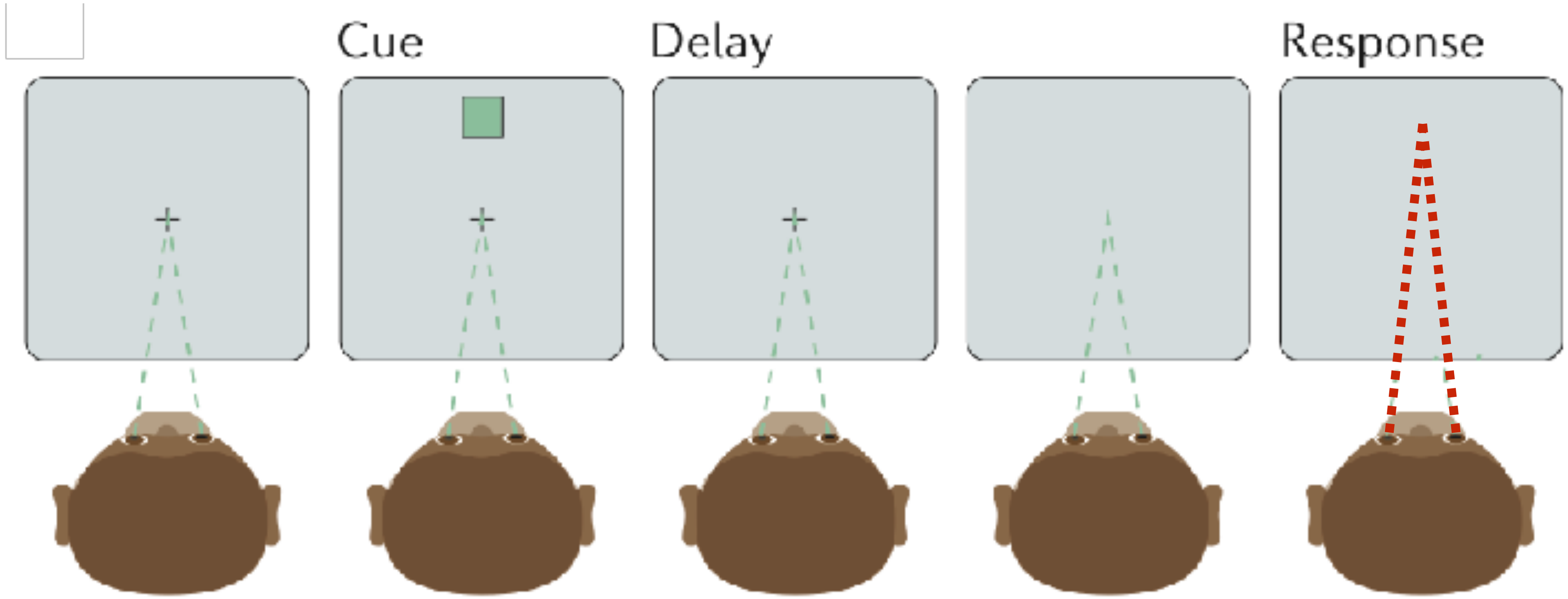

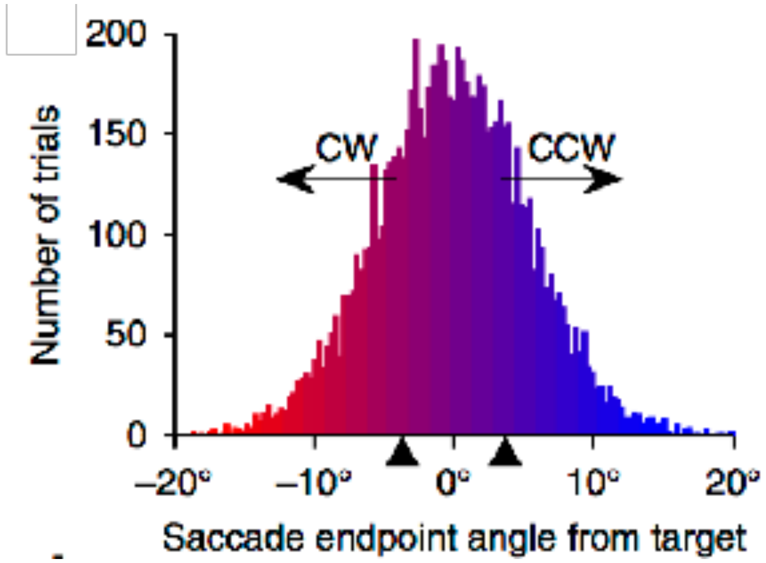

(Constantinidis & Klingberg 2016)

Visual spatial working memory experiments

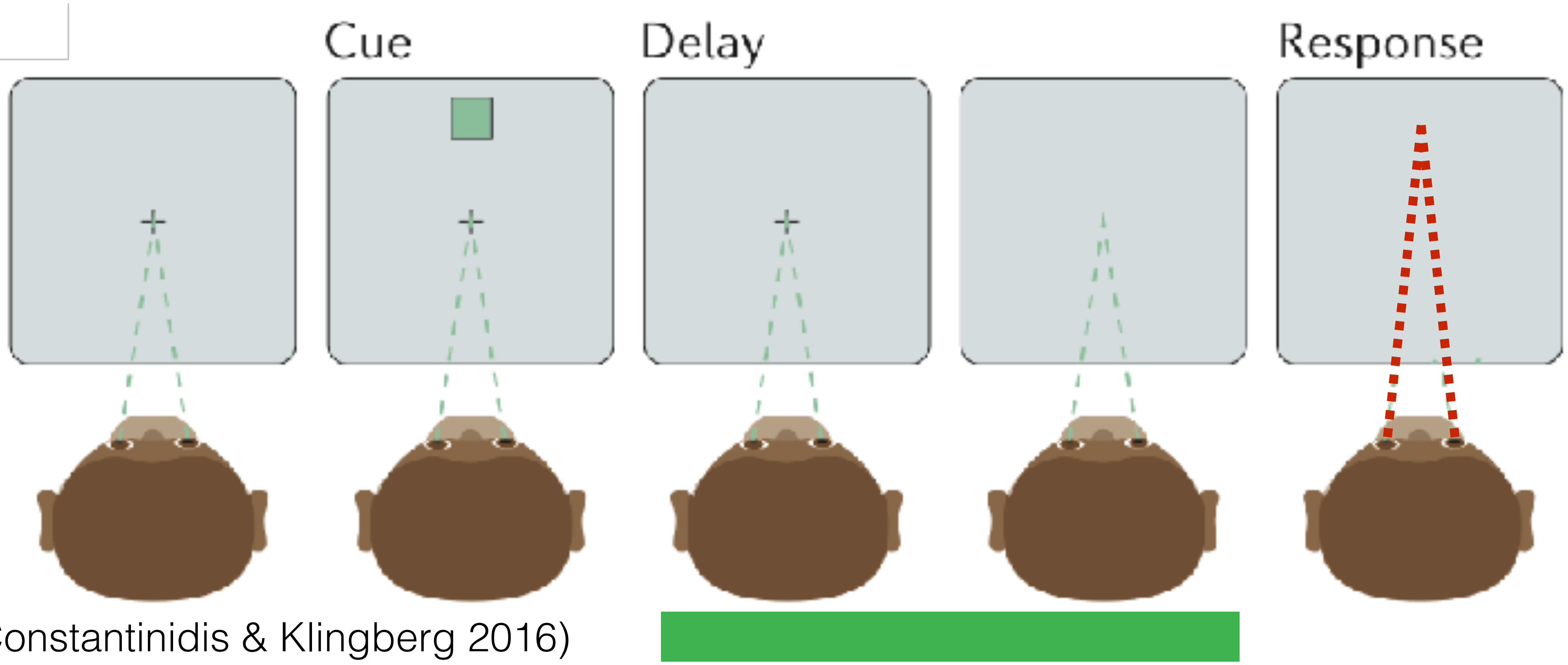

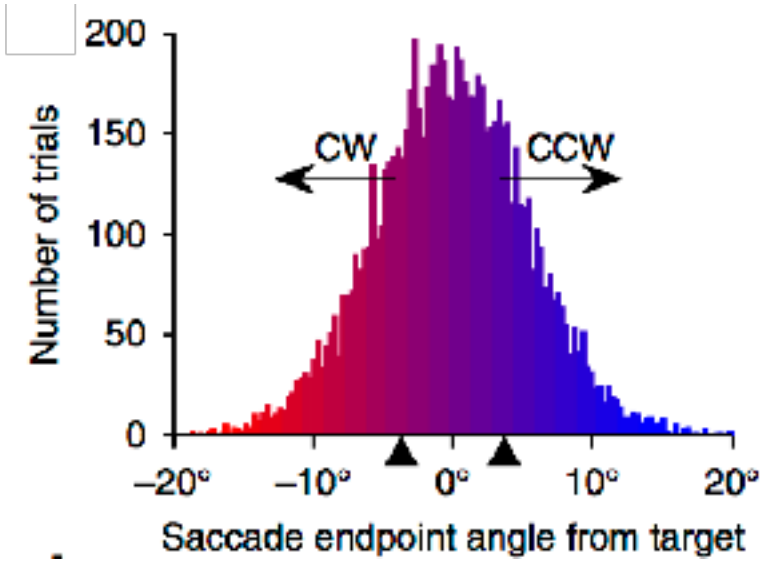

(Constantinidis & Klingberg 2016)

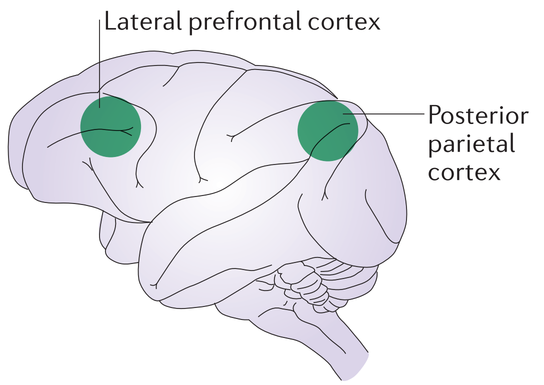

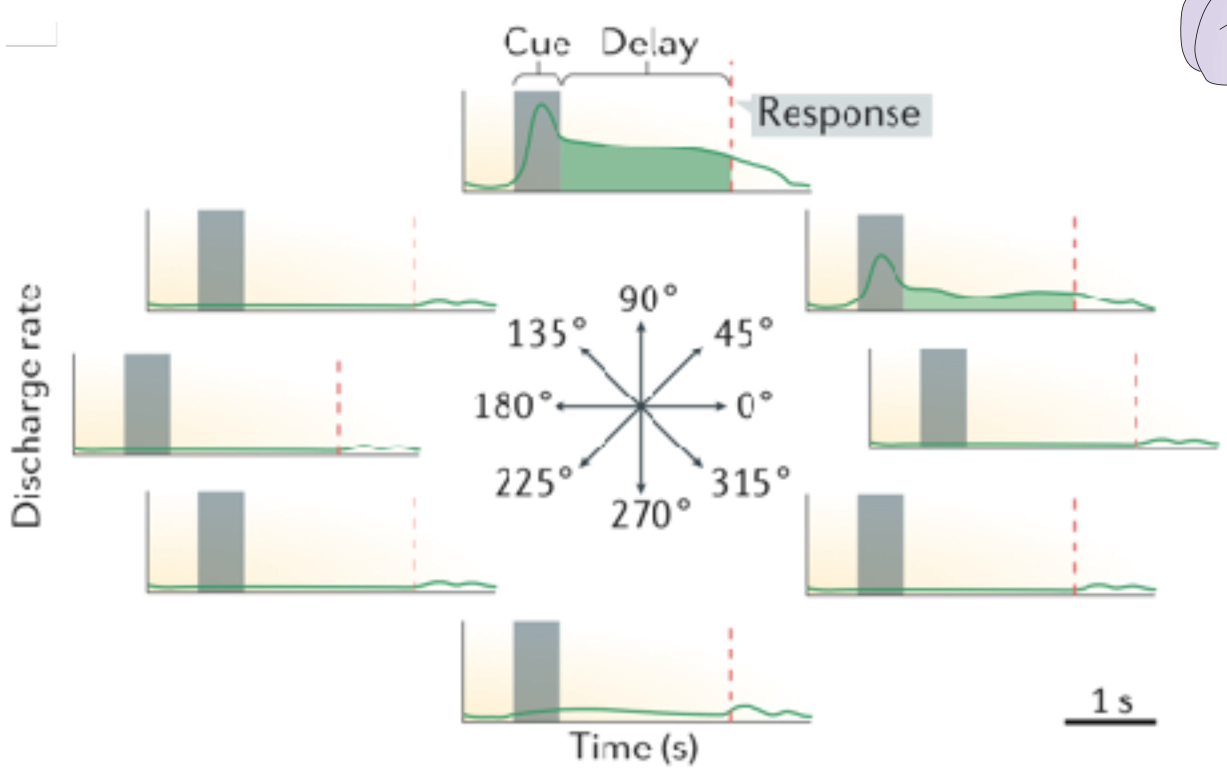

Visual spatial working memory experiments

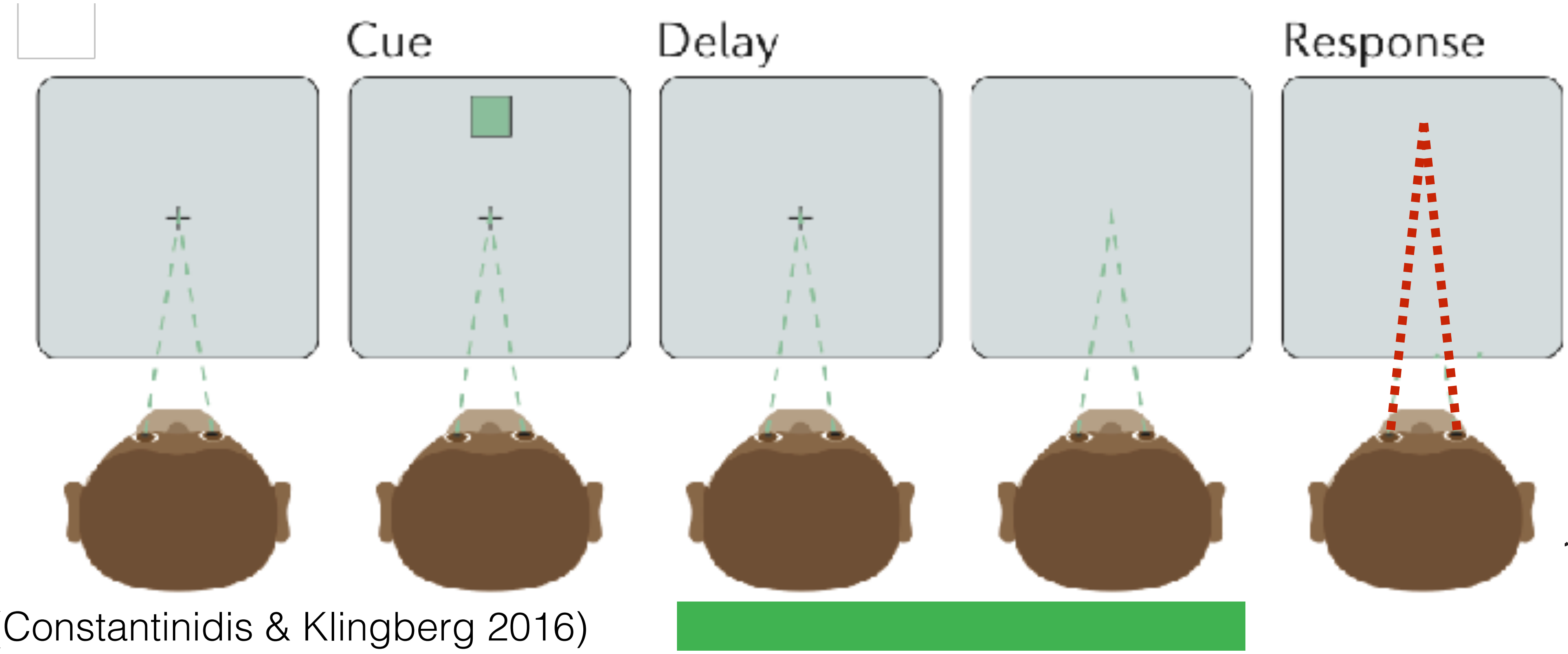

(Constantinidis & Klingberg 2016)

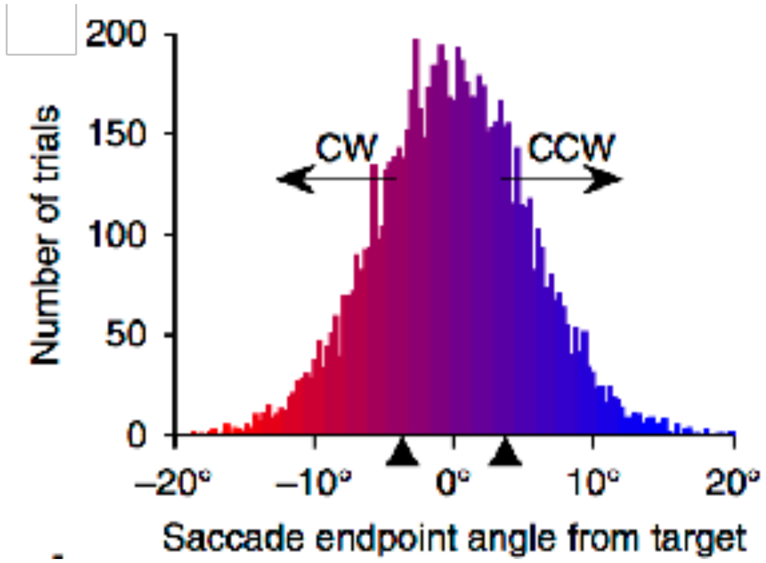

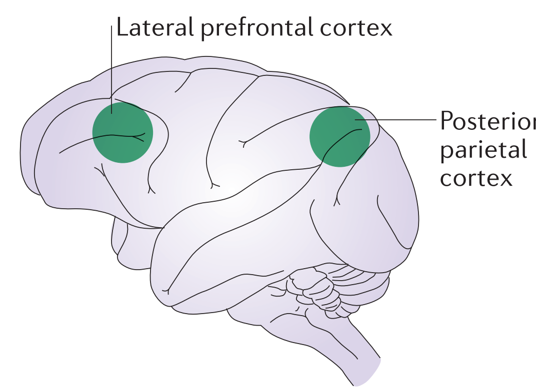

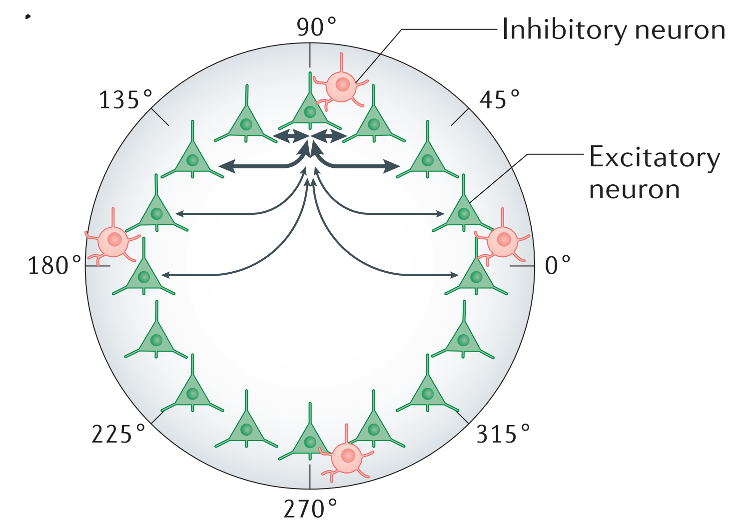

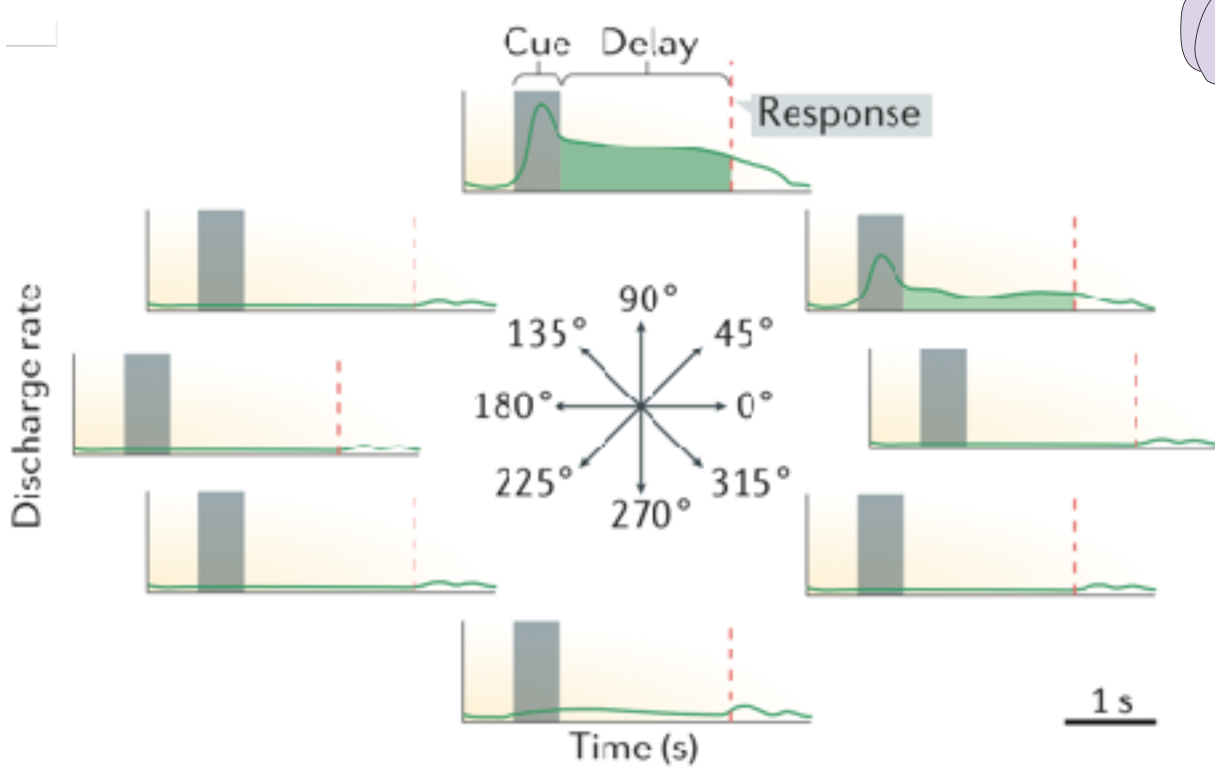

Visual spatial working memory experiments

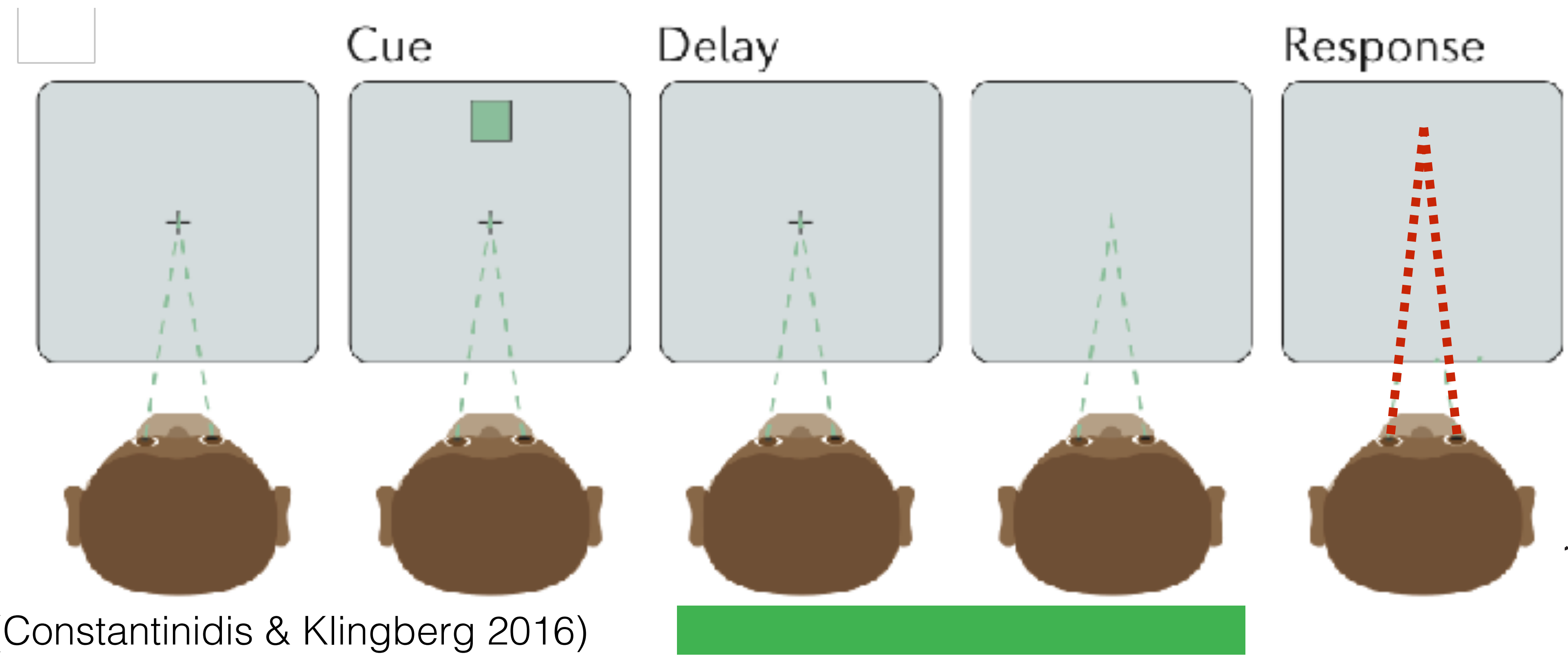

(Constantinidis & Klingberg 2016)

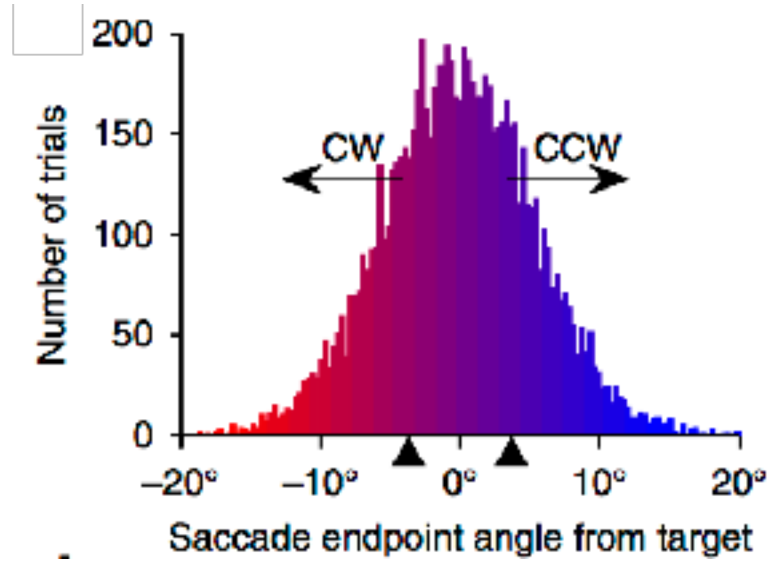

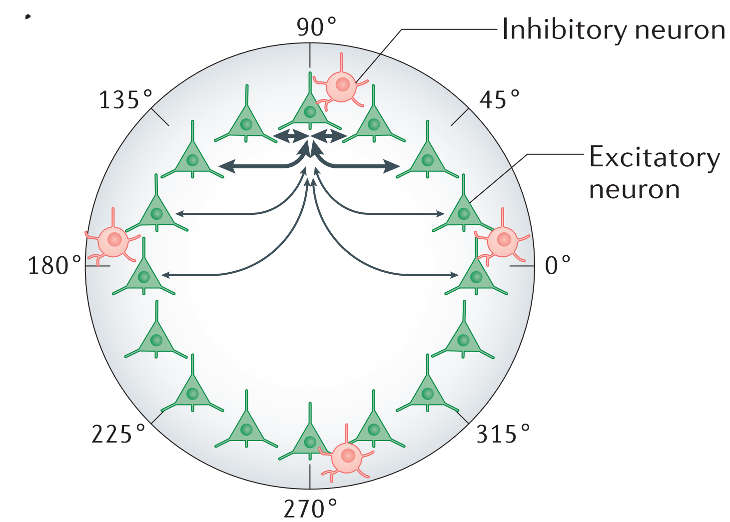

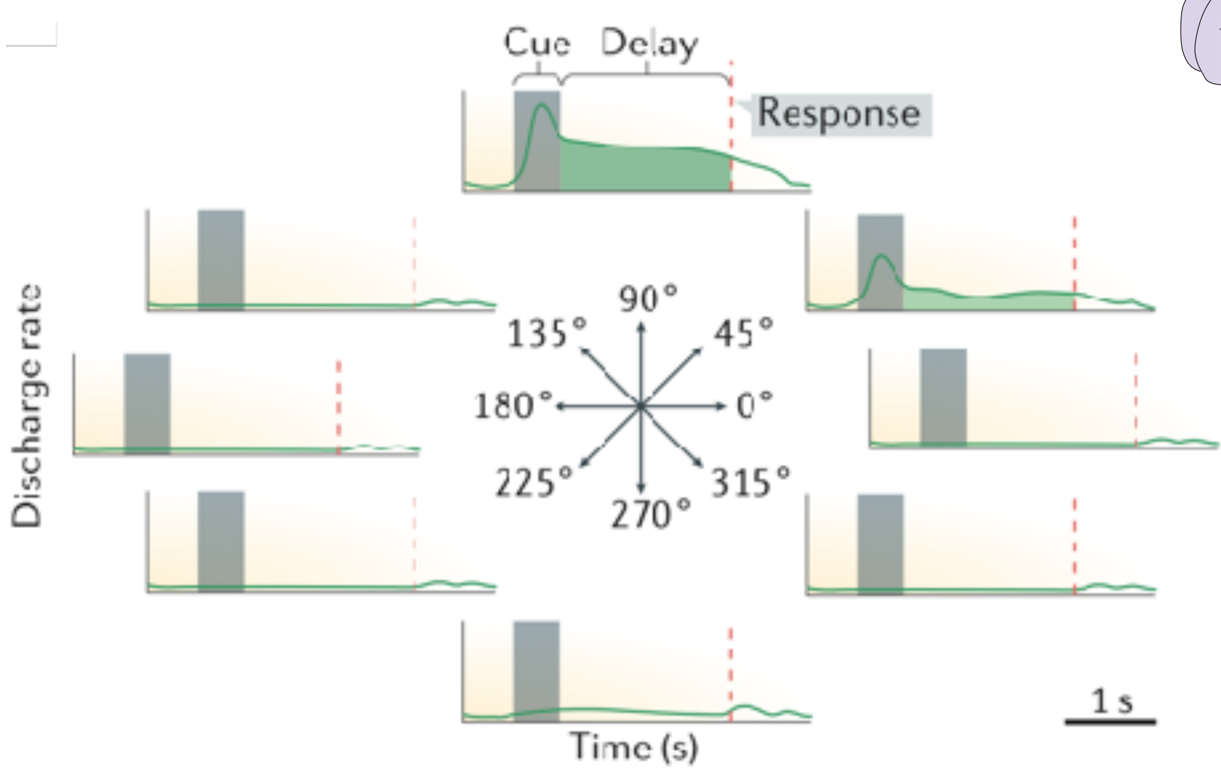

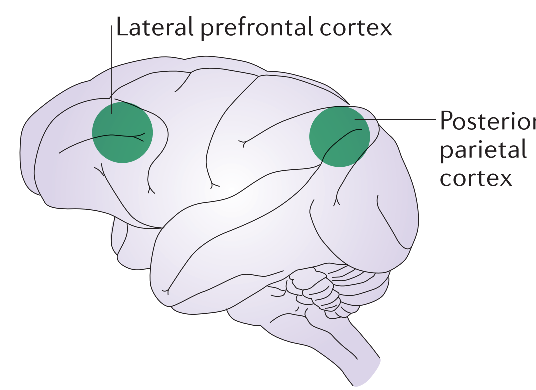

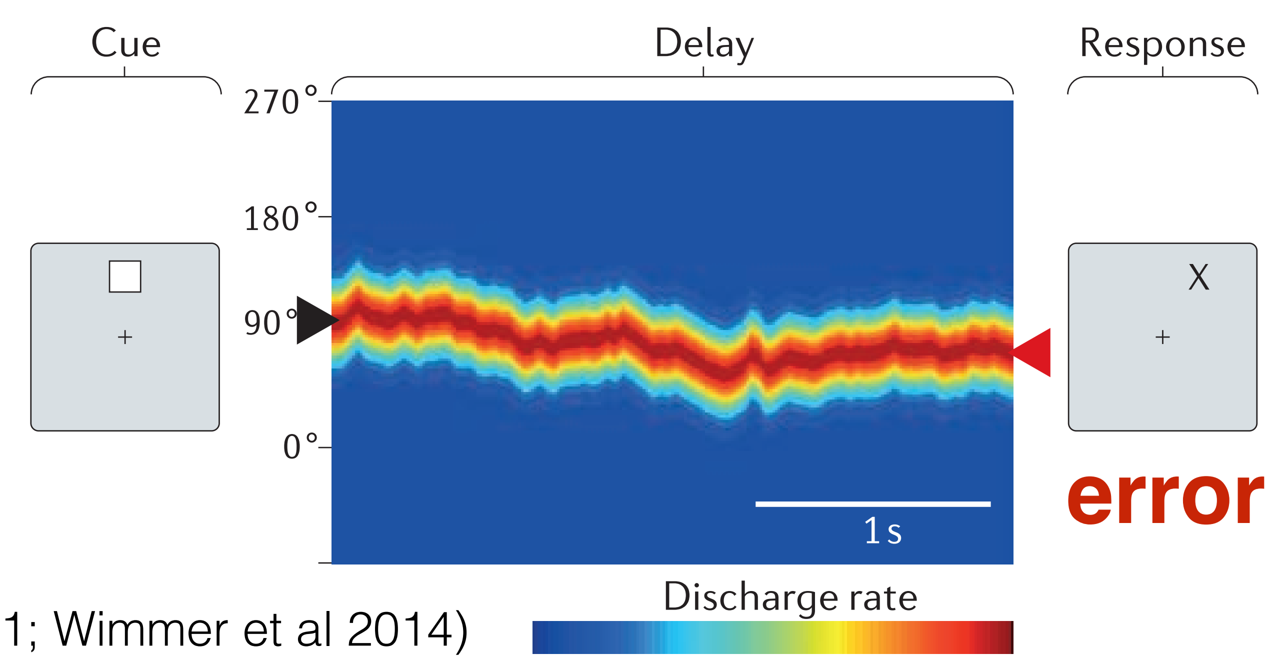

(Compte et al, 2001; Wimmer et al 2014)

Multi-item WM: Working memory is limited by “space”

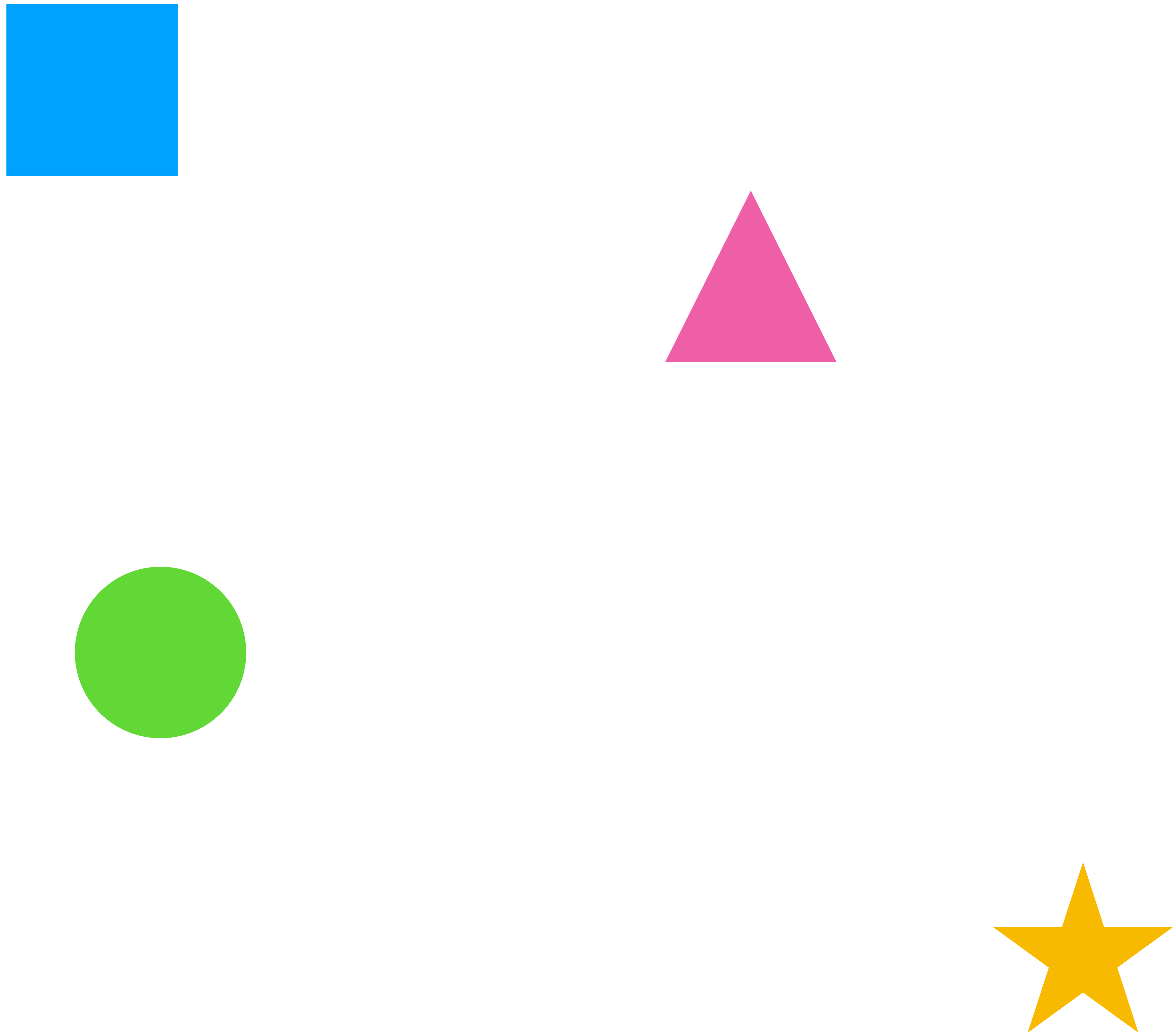

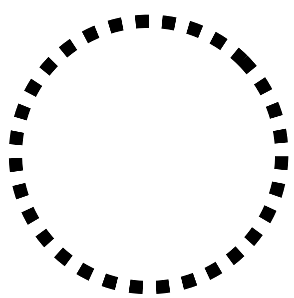

what color was this object

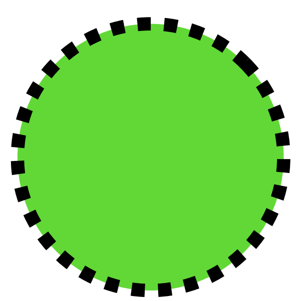

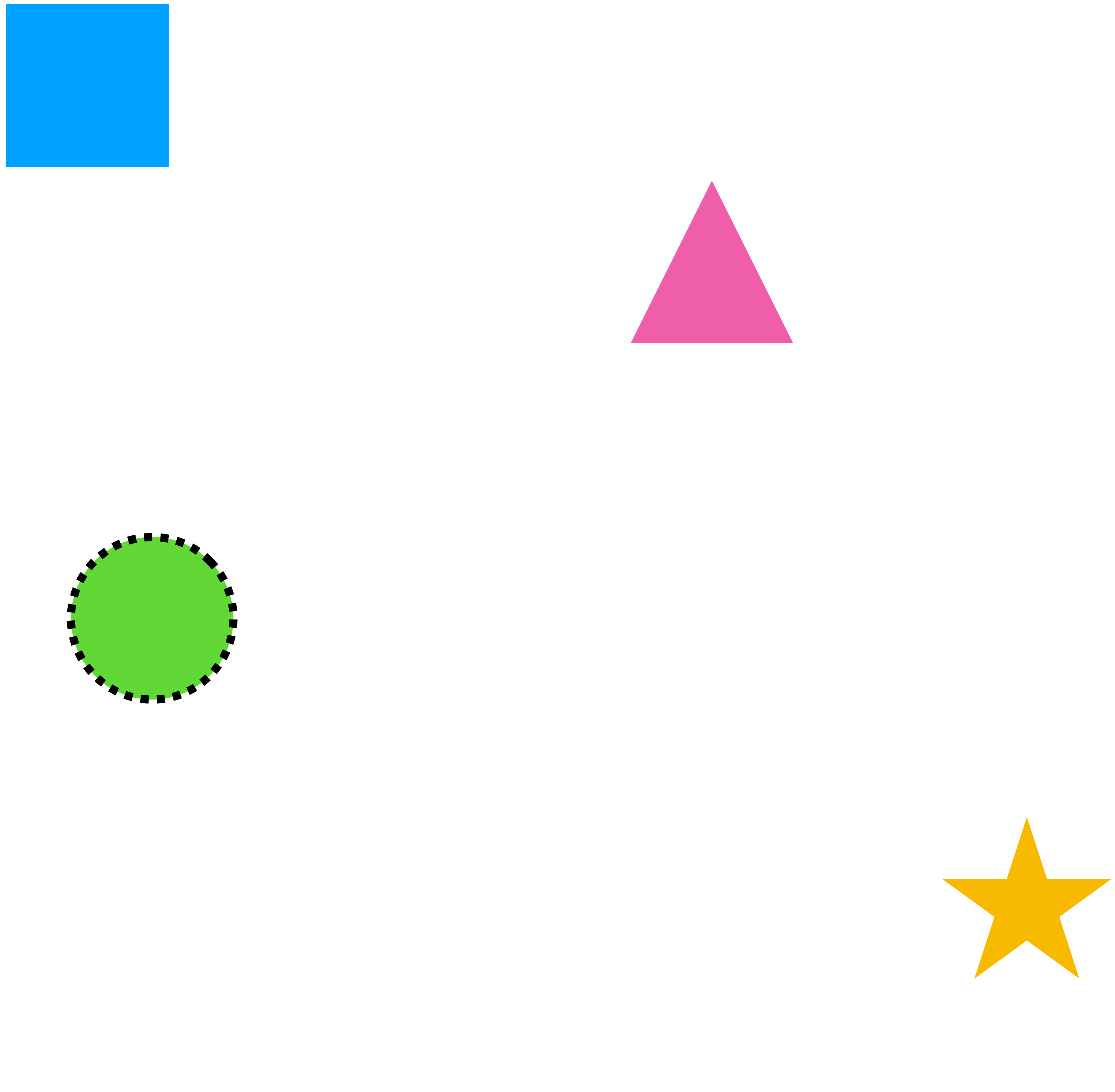

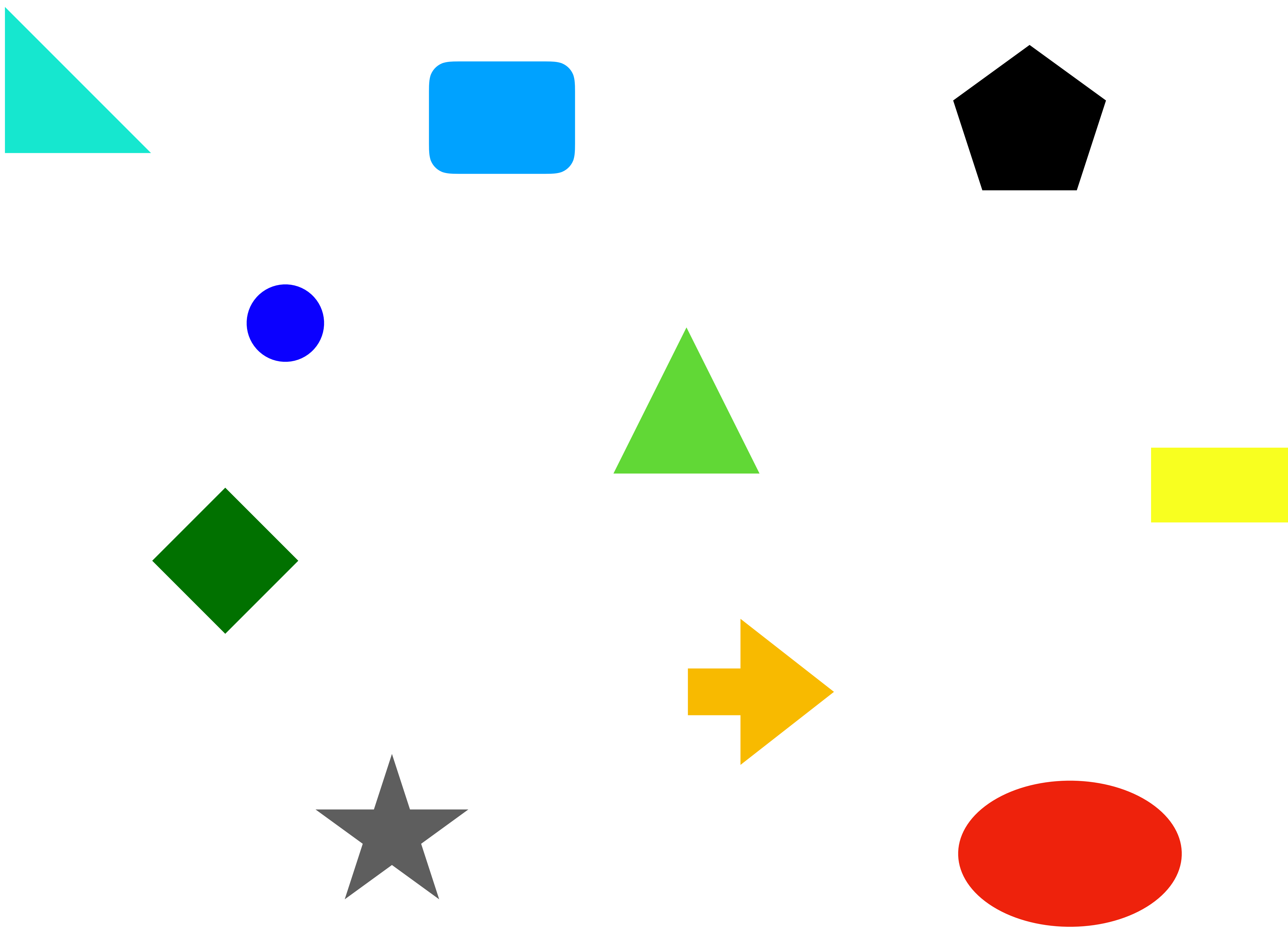

where was the pentagon?

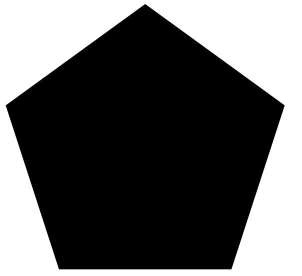

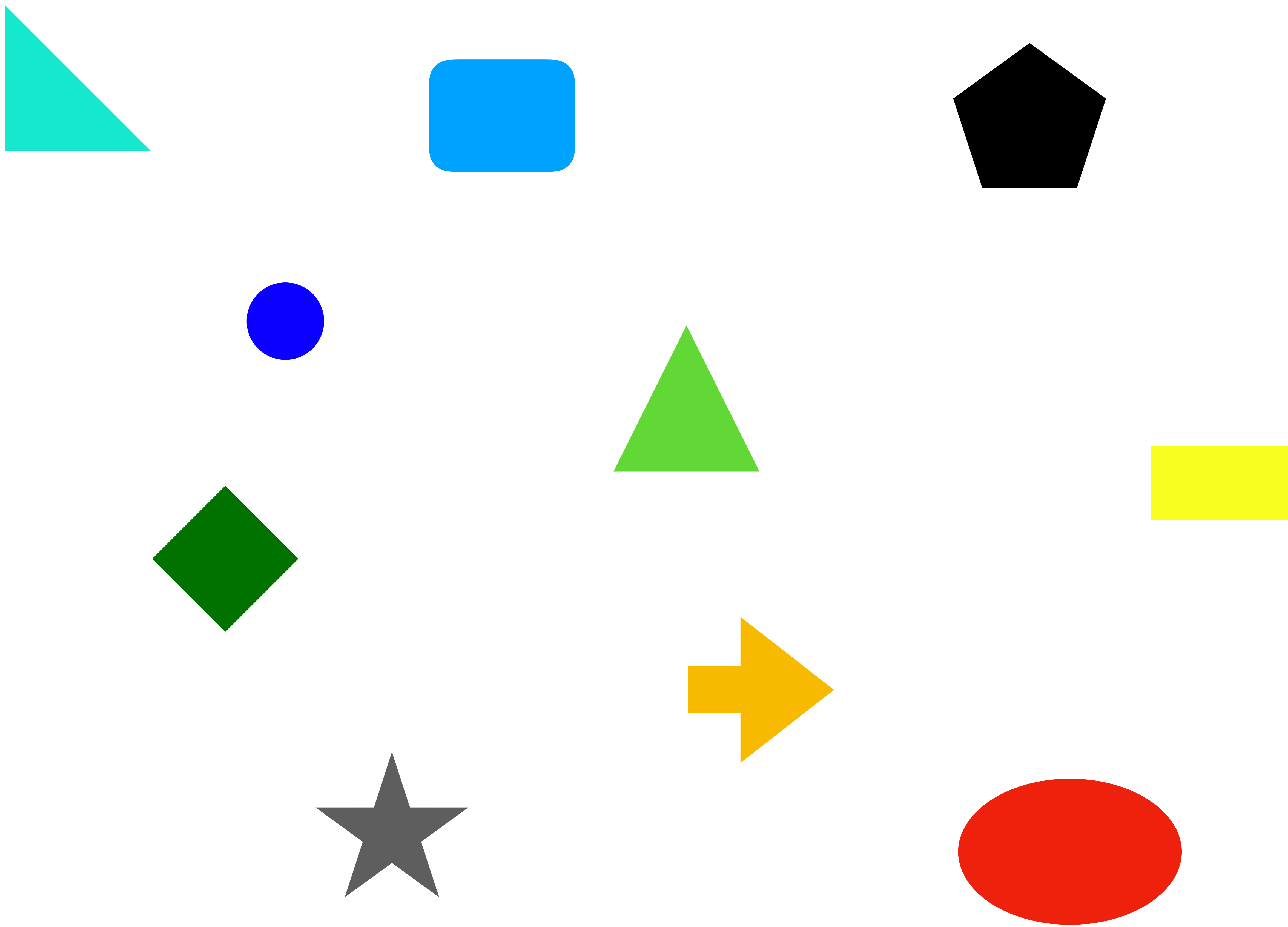

Recall error increases with item number

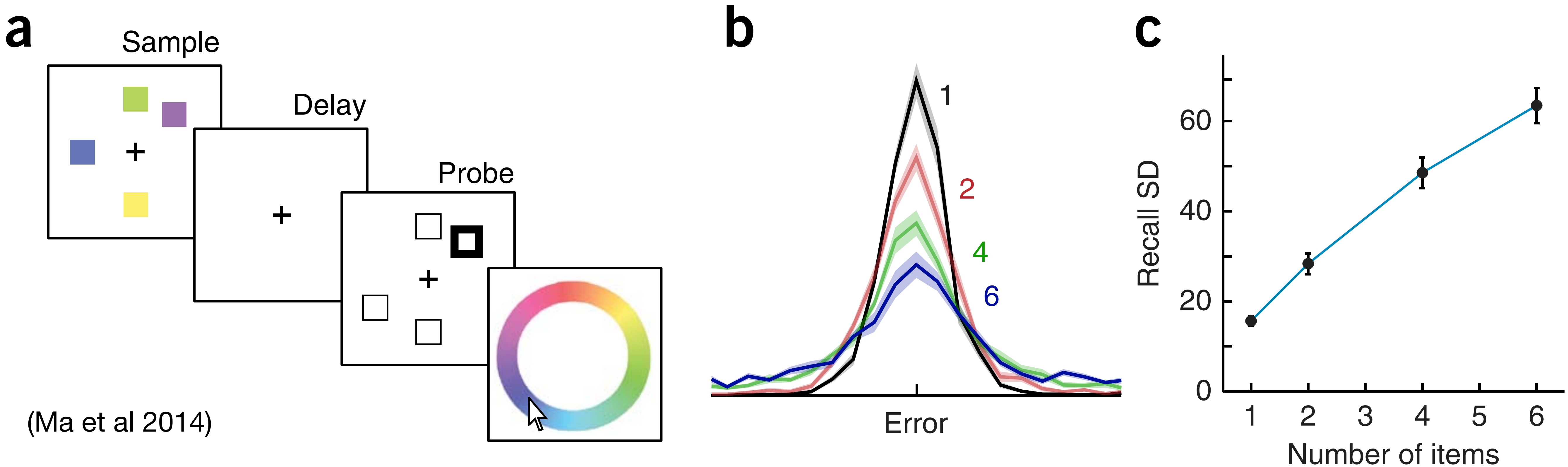

(Ma et al 2014)

Recall error increases with item number

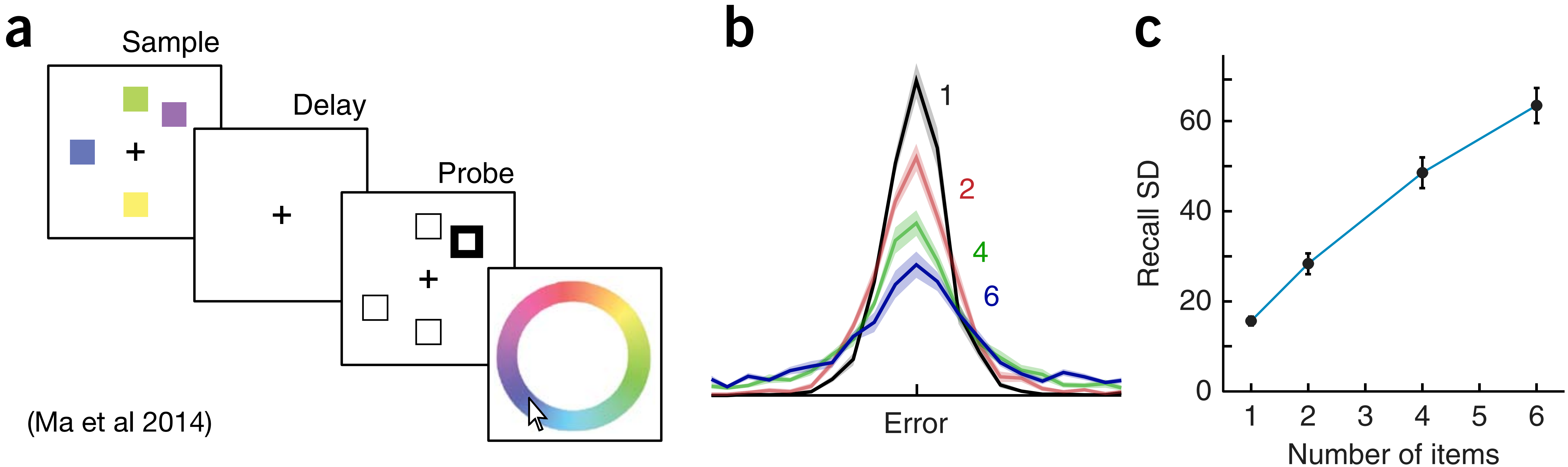

(Ma et al 2014)

- b) error: as the number of items is increased, the spread of the distribution of responses around the true color increases

Recall error increases with item number

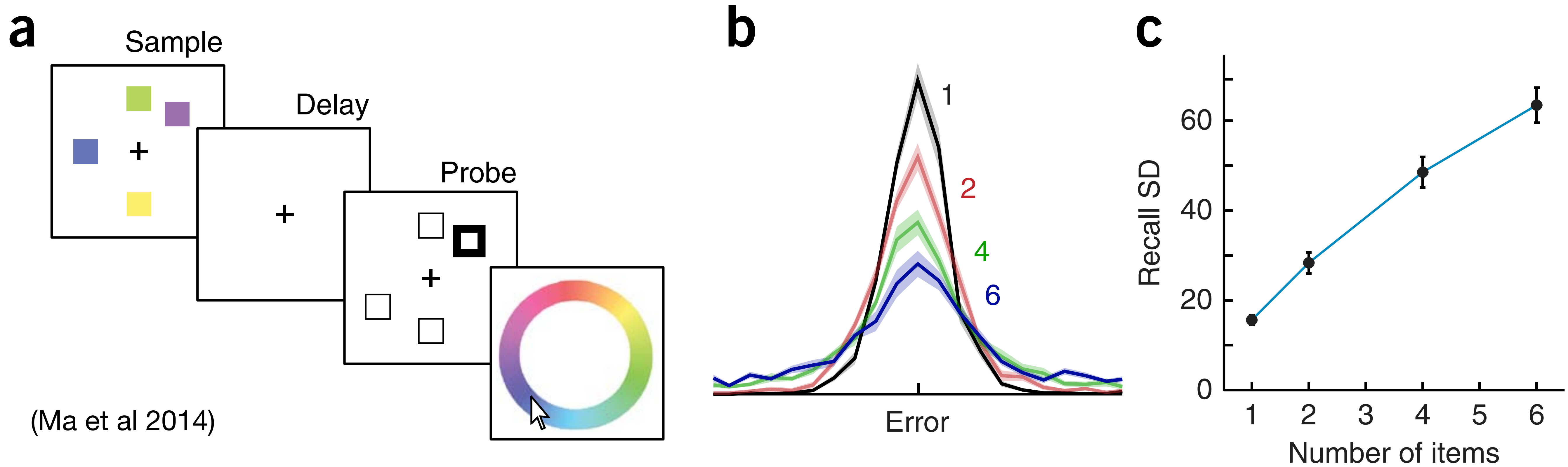

- b) error: as the number of items is increased, the spread of the distribution of responses around the true color increases
- c) *recall standard deviation* increases sublinearly with item number

Recall error increases with item number

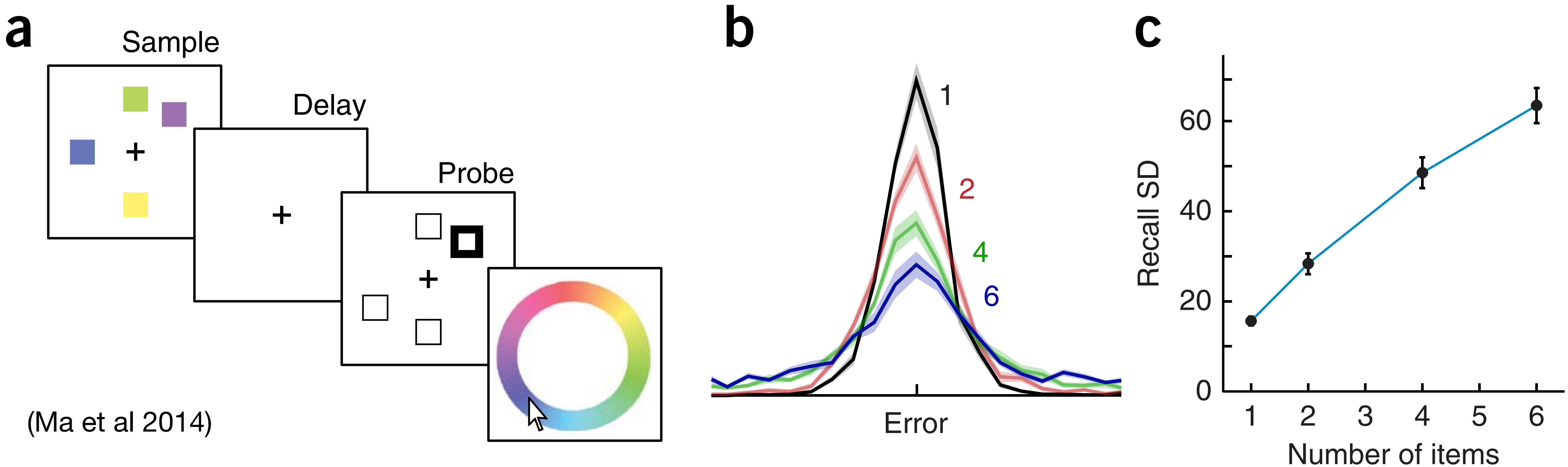

- b) error: as the number of items is increased, the spread of the distribution of responses around the true color increases
- c) *recall standard deviation* increases sublinearly with item number

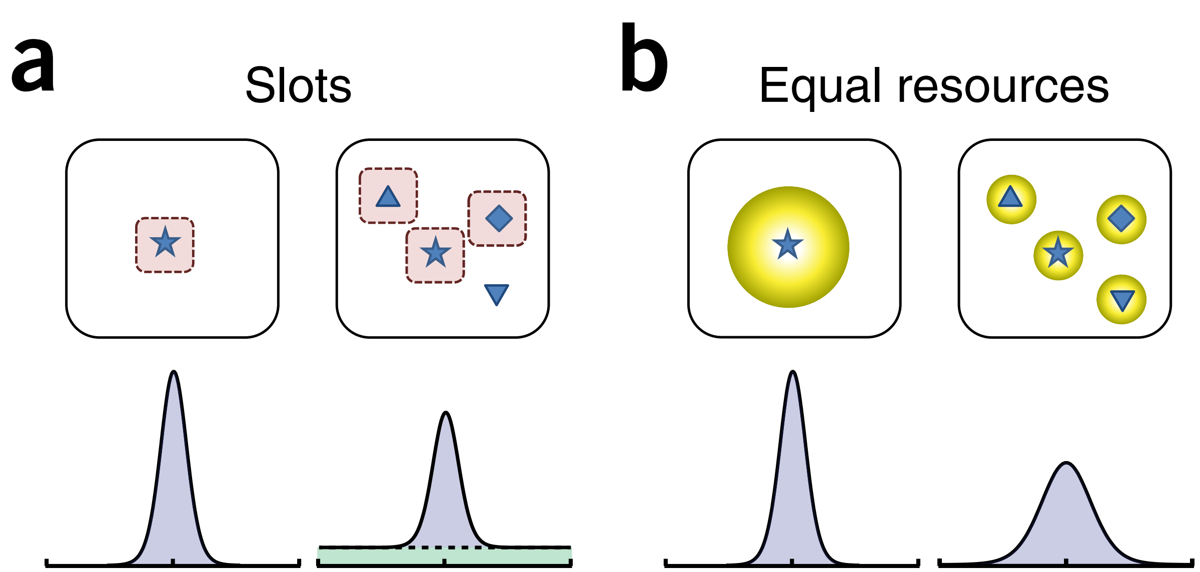

there is a debate about whether or not WM has a “finite capacity”

(Zhang and Luck 2008; Bays and Husein 2008)

Bump attractor models of working memory

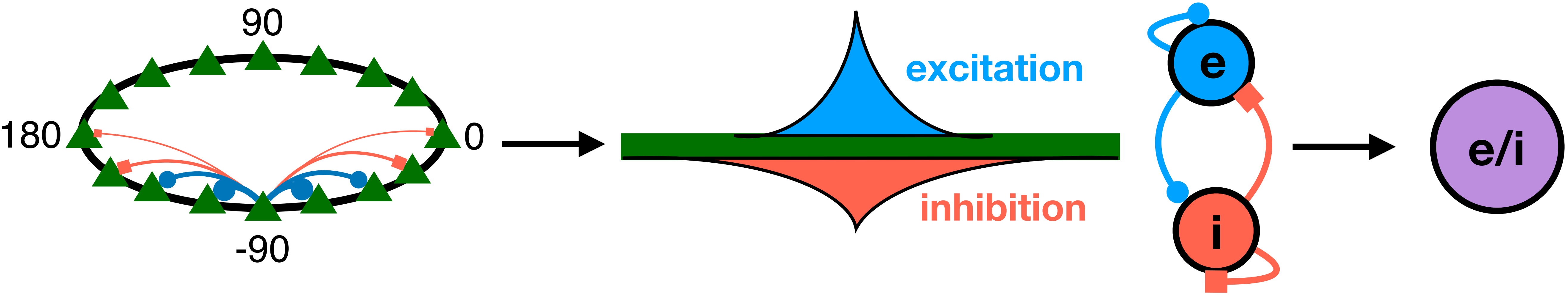

Bump attractor models of working memory

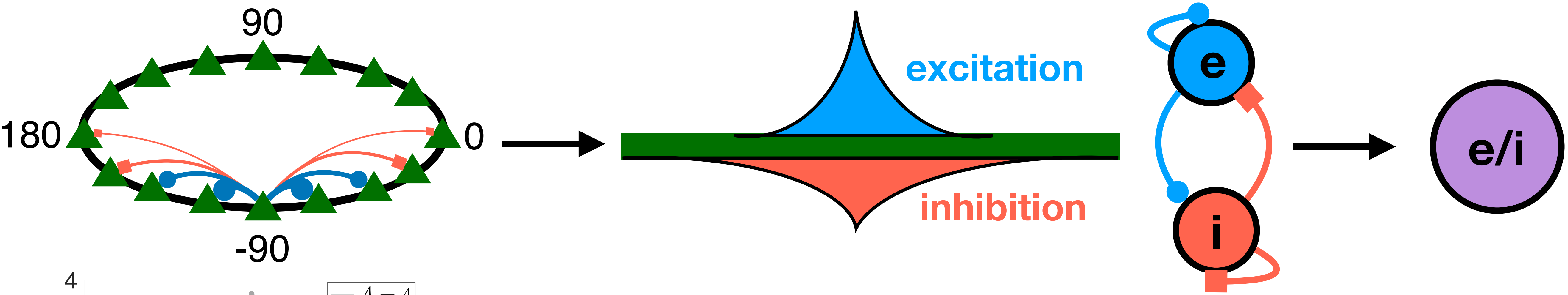

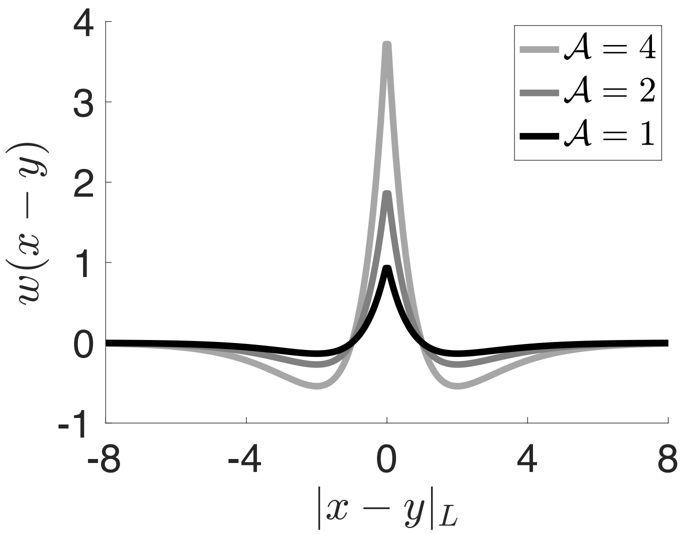

$$w(x) = \mathcal{A}(1 - |x|)\mathrm{e}^{-|x|}$$

Bump attractor models of working memory

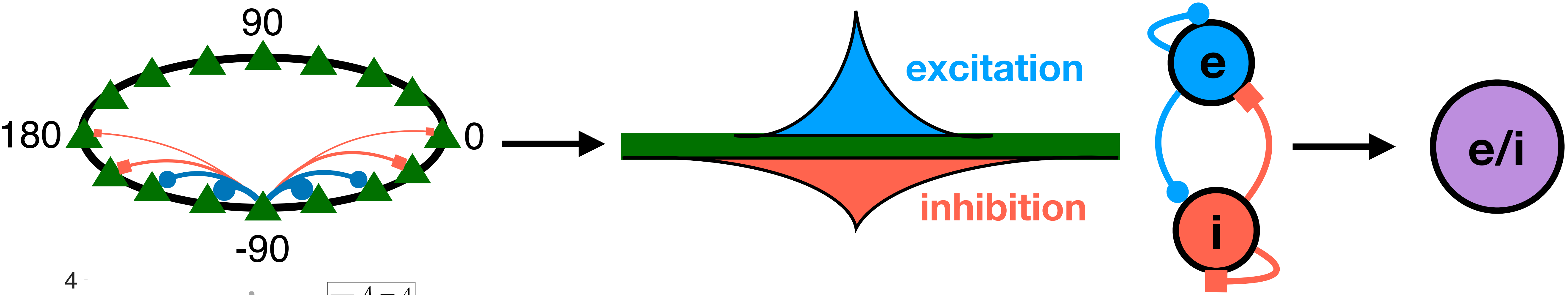

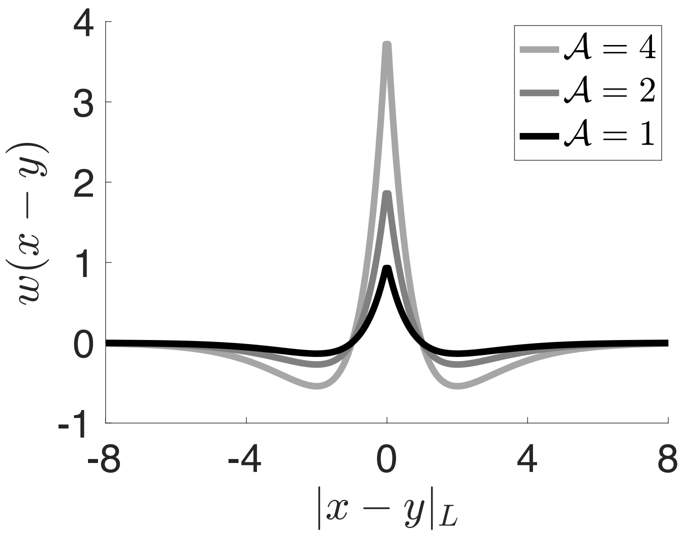

$$w(x) = \mathcal{A}(1 - |x|)\mathrm{e}^{-|x|}$$

$$\frac{\partial u(x,t)}{\partial t} = -u(x,t) + \int_{-180}^{180} w(x-y) f(u(y,t)) \mathrm{d}y$$

$u(x,t)$: population activity at location x

Bump attractor models of working memory

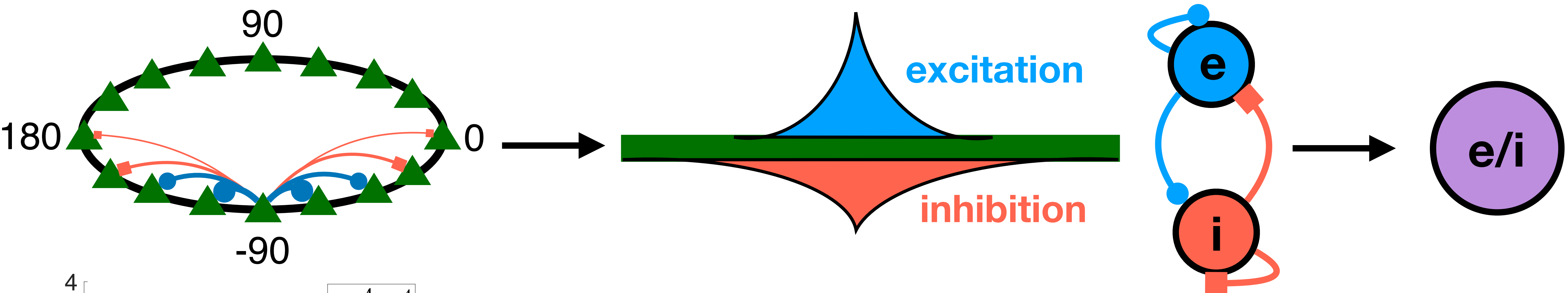

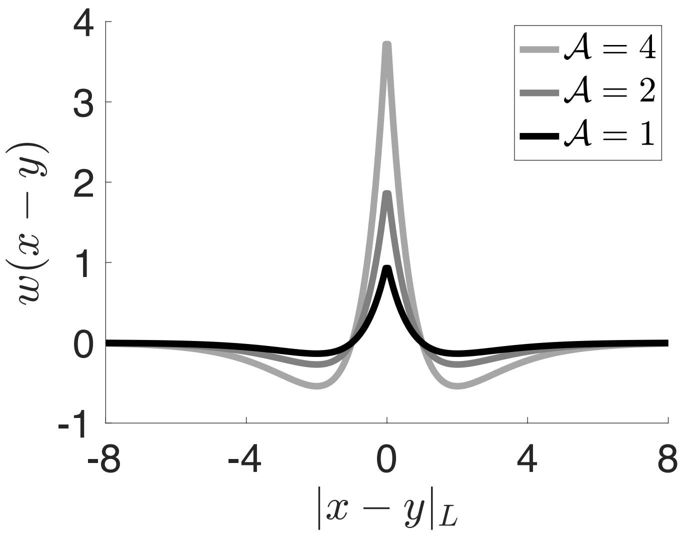

$$w(x) = \mathcal{A}(1-|x|)\mathrm{e}^{-|x|}$$

$$\frac{\partial u(x,t)}{\partial t} = -u(x,t) + \int_{-180}^{180} w(x-y) f(u(y,t))\mathrm{d}y$$

$u(x,t)$: population activity at location x

$w(x-y)$: coupling between two locations

Bump attractor models of working memory

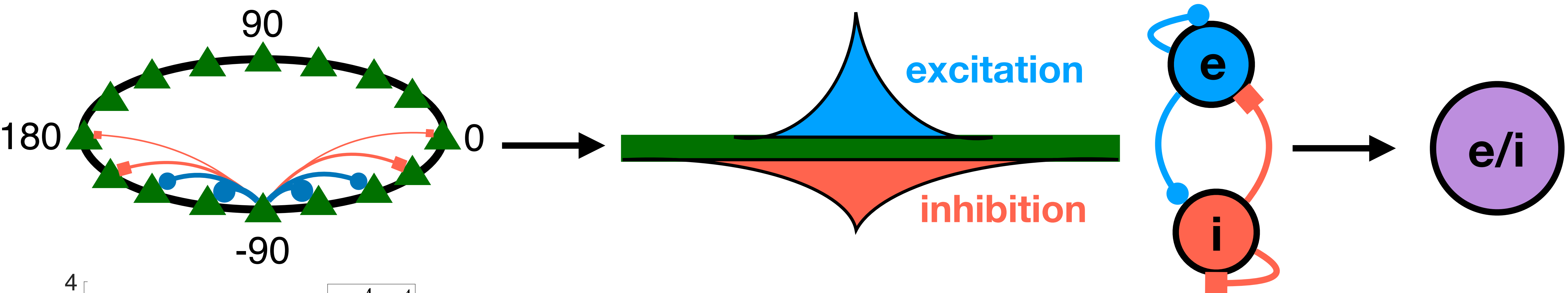

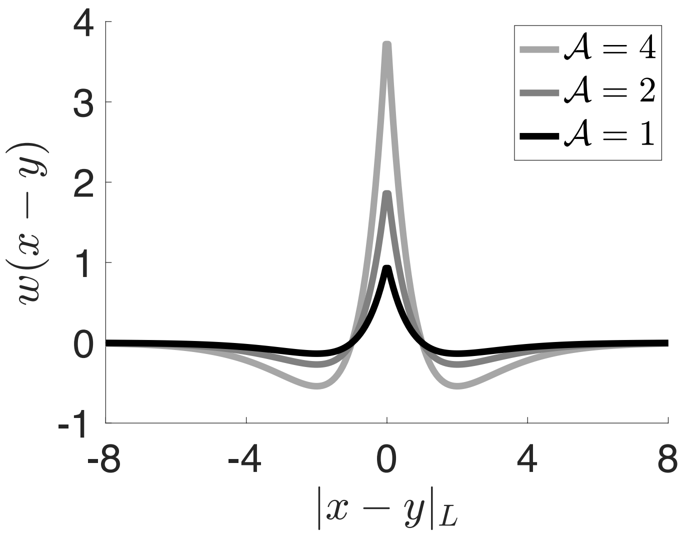

$$w(x) = \mathcal{A}(1-|x|)\mathrm{e}^{-|x|}$$

$$\frac{\partial u(x,t)}{\partial t} = -u(x,t) + \int_{-180}^{180} w(x-y) f(u(y,t))\mathrm{d}y$$

$u(x,t)$: population activity at location x

$w(x-y)$: coupling between two locations

$f(u)$: firing rate nonlinearity converts population activity into synaptic output

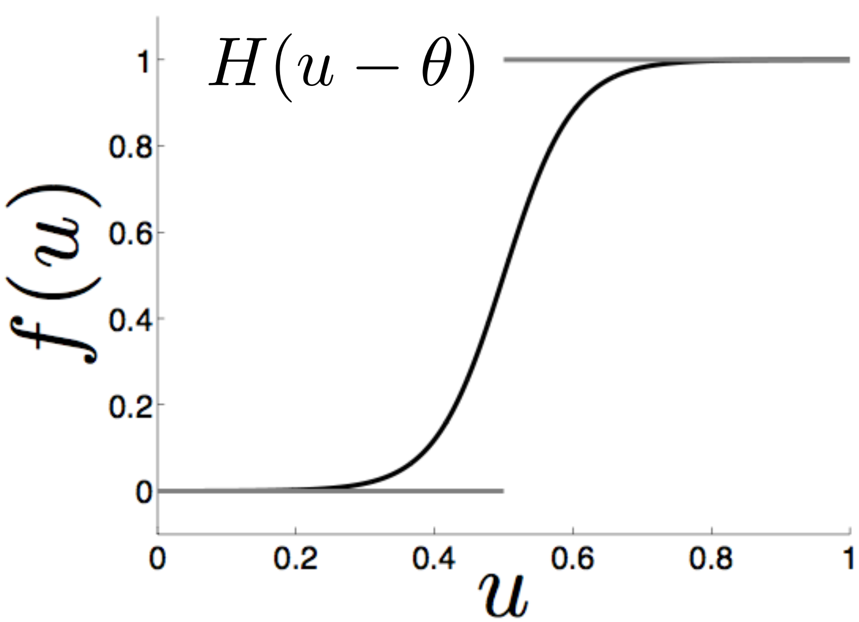

Bump attractor models of working memory

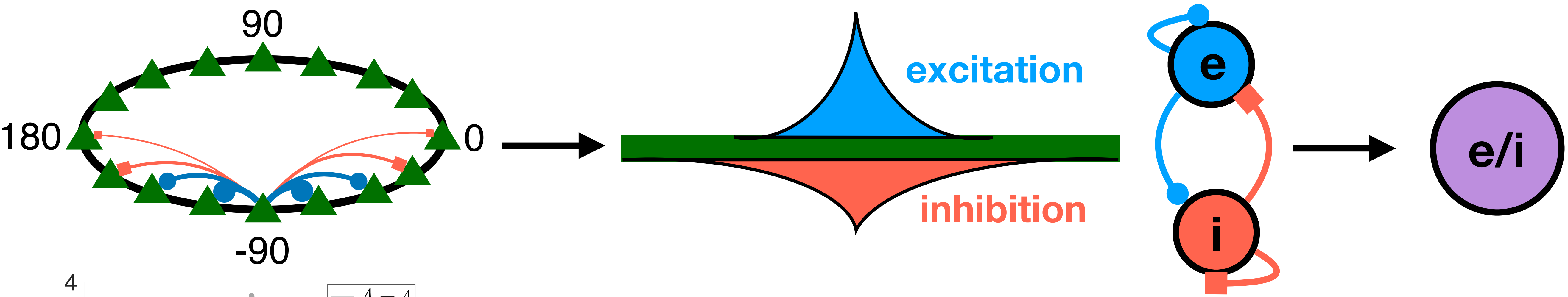

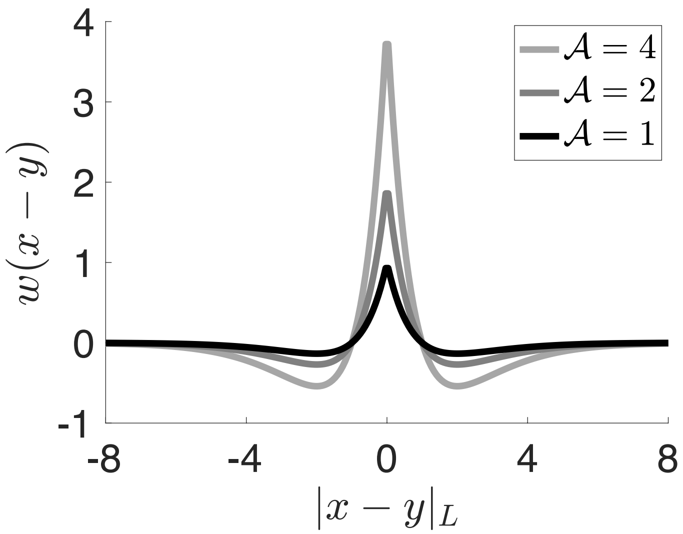

$$\frac{\partial u(x,t)}{\partial t} = -u(x,t) + \int_{-180}^{180} w(x-y) f(u(y,t)) \mathrm{d}y$$

$u(x,t)$: population activity at location x

$$w(x) = \mathcal{A}(1-|x|)\mathrm{e}^{-|x|}$$

$w(x-y)$: coupling between two locations

$f(u)$: firing rate nonlinearity converts population activity into synaptic output

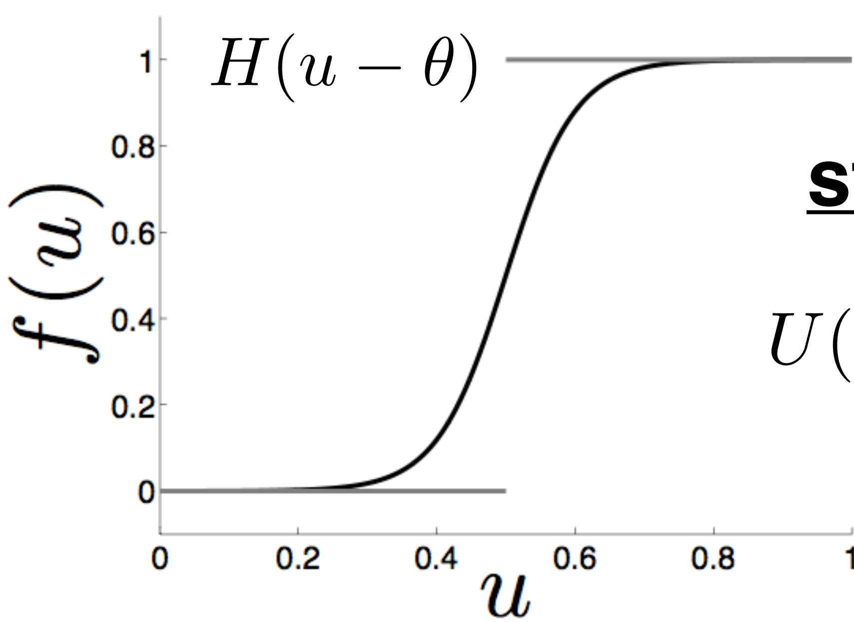

stationary bump solutions

$$U(x) = \int_{-180}^{180} w(x-y) f(U(y)) \mathrm{d}y$$

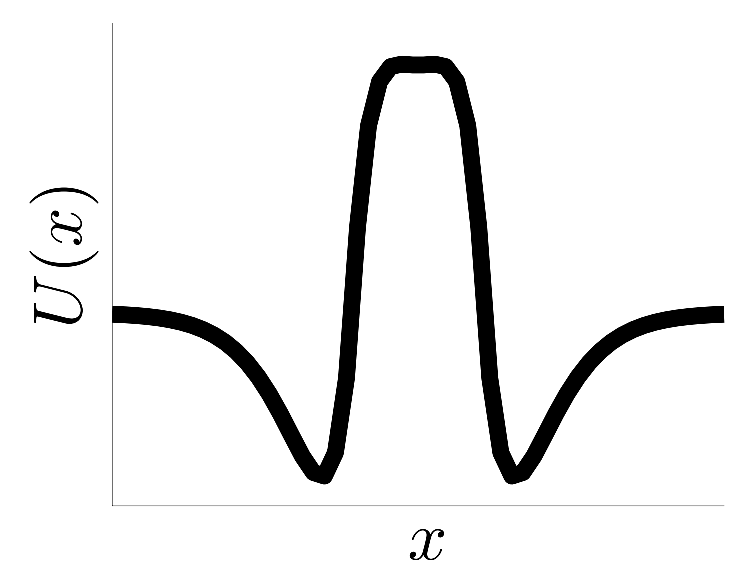

Explicit solutions for Heaviside firing rate

set firing rate nonlinearity

$$f(u) = H(u - \theta)$$

$$[x_1, x_2] = \{x | U(x) \geq \theta\}$$

$$U(x) = \int_{-180}^{180} w(x-y) f(U(y)) \mathrm{d}y \longrightarrow U(x) = \int_{x_1}^{x_2} w(x-y) \mathrm{d}y$$

Explicit solutions for Heaviside firing rate

set firing rate nonlinearity

$$f(u) = H(u - \theta)$$

$$[x_1, x_2] = \{x | U(x) \geq \theta\}$$

$$U(x) = \int_{-180}^{180} w(x-y) f(U(y)) \mathrm{d}y \longrightarrow U(x) = \int_{x_1}^{x_2} w(x-y) \mathrm{d}y$$

so $U(x_1) = U(x_2) = \theta$ $\longrightarrow$ $\theta = \int_0^{2h} w(y) \mathrm{d}y = W(2h)$ implicit eqn defining bump half-width

Explicit solutions for Heaviside firing rate

set firing rate nonlinearity

$$f(u) = H(u-\theta)$$

$$[x_1, x_2] = \{x | U(x) \geq \theta\}$$

$$U(x) = \int_{-180}^{180} w(x-y) f(U(y)) \mathrm{d}y \longrightarrow U(x) = \int_{x_1}^{x_2} w(x-y) \mathrm{d}y$$

so $U(x_1) = U(x_2) = \theta$ $\longrightarrow$ $\theta = \int_0^{2h} w(y) \mathrm{d}y = W(2h)$ implicit eqn defining bump half-width

for $w(x) = \mathcal{A}(1-|x|)\mathrm{e}^{-|x|}$ $\longrightarrow$ $W(2h) = 2\mathcal{A}h\mathrm{e}^{-2h} = \theta$ solved with numerical root finder

Explicit solutions for Heaviside firing rate

set firing rate nonlinearity

$$f(u) = H(u-\theta)$$

$$[x_1, x_2] = \{x | U(x) \geq \theta\}$$

$$U(x) = \int_{-180}^{180} w(x-y) f(U(y)) \mathrm{d}y \longrightarrow U(x) = \int_{x_1}^{x_2} w(x-y)\mathrm{d}y$$

so $U(x_1) = U(x_2) = \theta \longrightarrow \theta = \int_0^{2h} w(y)\mathrm{d}y = W(2h)$ implicit eqn defining bump half-width

for $w(x) = \mathcal{A}(1-|x|)\mathrm{e}^{-|x|} \longrightarrow W(2h) = 2\mathcal{A}h\mathrm{e}^{-2h} = \theta$ solved with numerical root finder

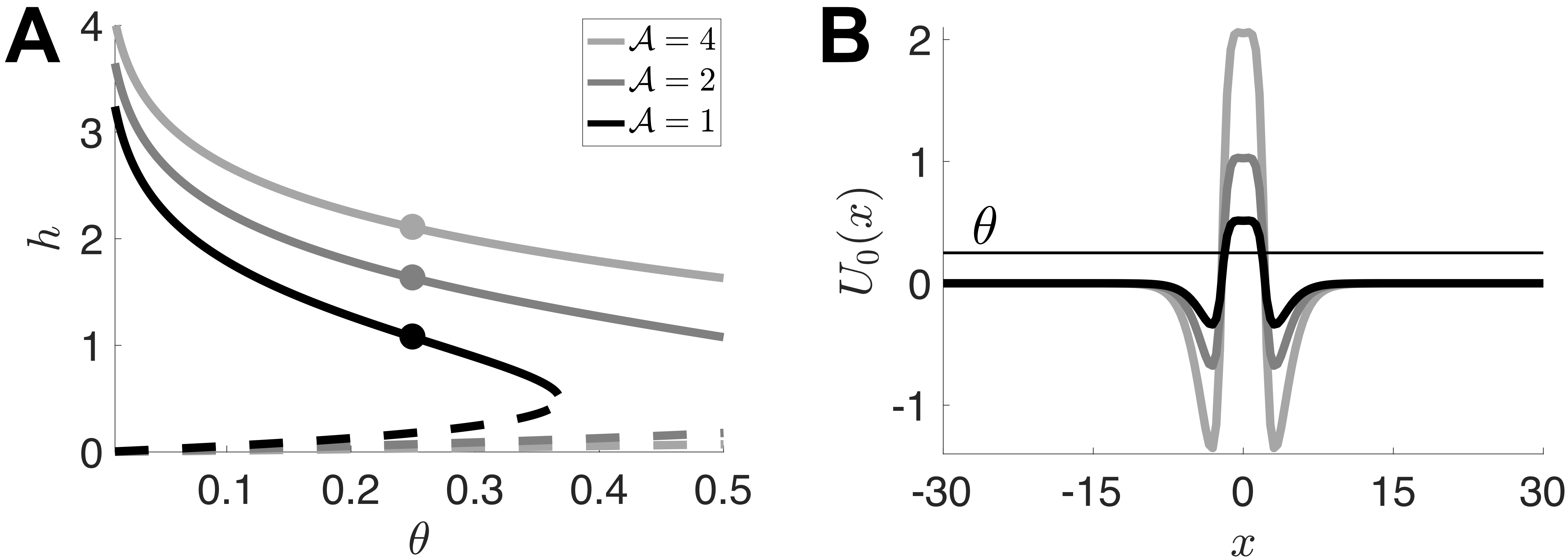

A: two branches of solutions: wide & marginally stable, narrow & unstable

B: bump solutions widen as the strength of coupling is increased

Nonequilibrium dynamics via interface equations

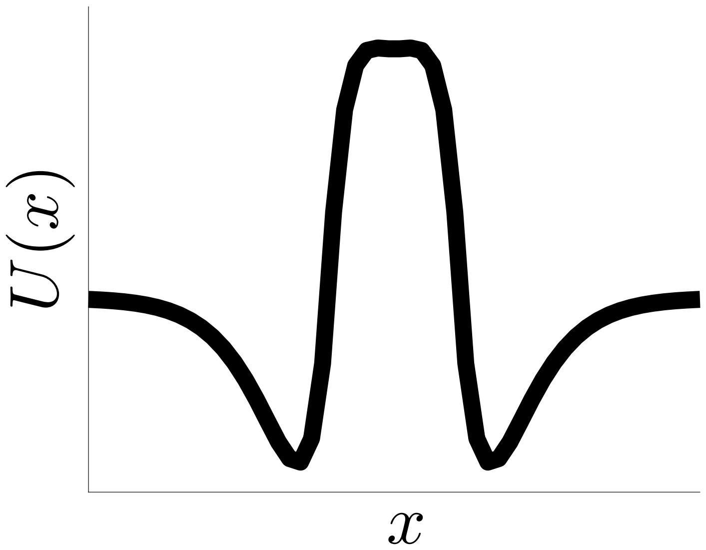

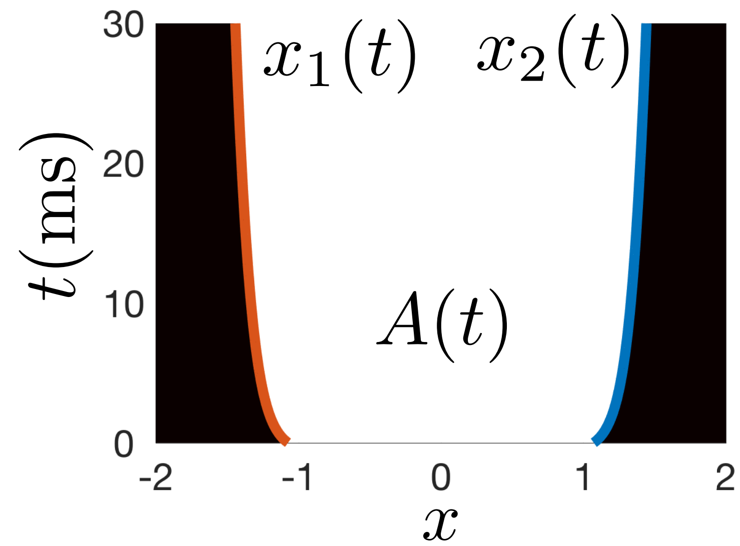

Nonequilibrium dynamics via interface equations

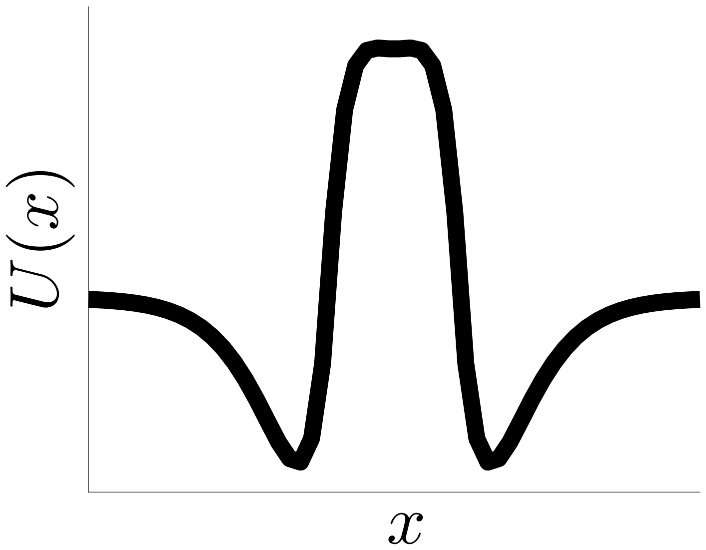

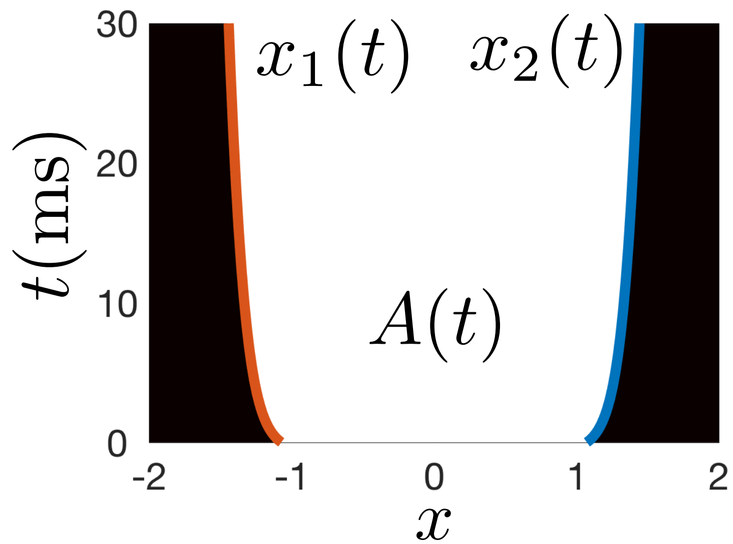

can show interfaces $u(x_j(t),t)=\theta$ determine dynamics of the entire neural field $u(x,t)$

define active region:

$$A(t) = [x_1(t), x_2(t)]$$

Nonequilibrium dynamics via interface equations

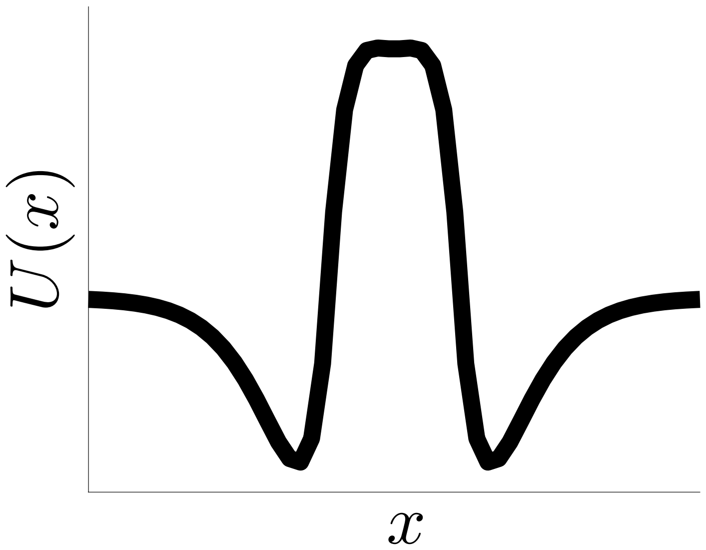

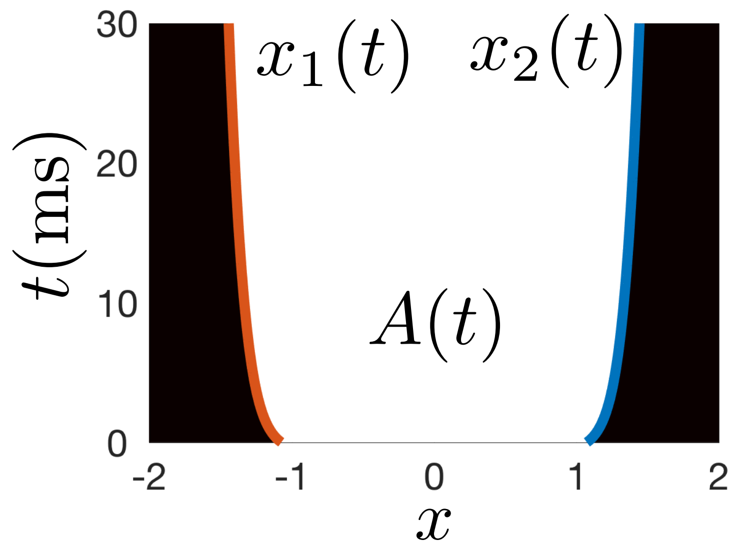

can show interfaces $u(x_j(t),t) = \theta$ determine dynamics of the entire neural field $u(x,t)$

define active region:

$$A(t) = [x_1(t), x_2(t)]$$

differentiate

$$u(x_j(t),t) = \theta \longrightarrow \alpha_j(t)\frac{\mathrm{d}x_j}{\mathrm{d}t} + \frac{\partial u(x_j(t),t)}{\partial t} = 0 \qquad \alpha_j(t) = \frac{\partial u(x_j(t),t)}{\partial x}$$

Nonequilibrium dynamics via interface equations

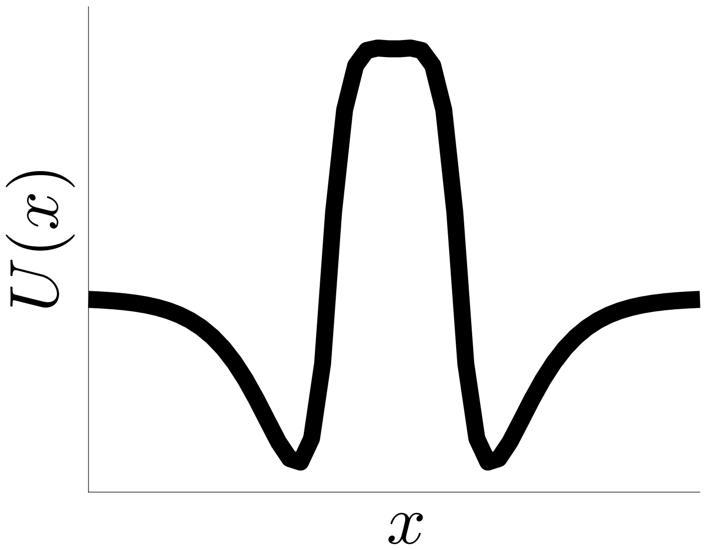

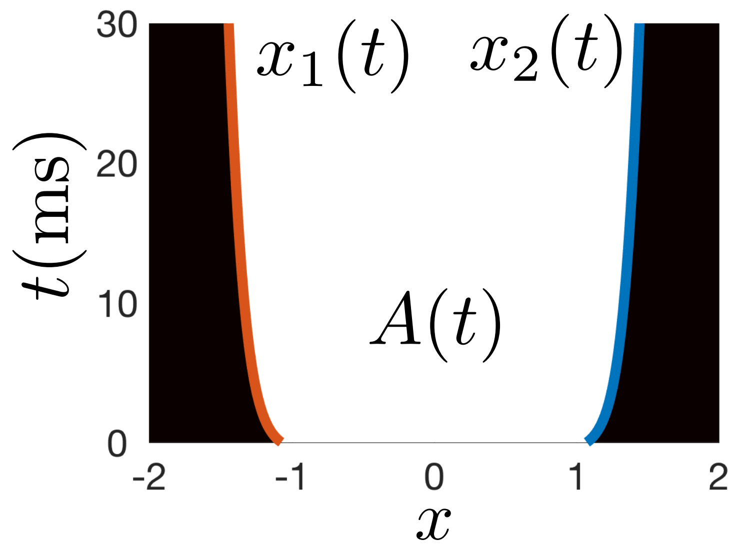

can show interfaces $u(x_j(t),t) = \theta$ determine dynamics of the entire neural field $u(x,t)$

define active region:
$A(t) = [x_1(t), x_2(t)]$

differentiate
$u(x_j(t),t) = \theta$

$$\alpha_j(t)\frac{\mathrm{d}x_j}{\mathrm{d}t} + \frac{\partial u(x_j(t),t)}{\partial t} = 0 \qquad \alpha_j(t) = \frac{\partial u(x_j(t),t)}{\partial x}$$

recall $\dfrac{\partial u(x,t)}{\partial t} = -u(x,t) + \displaystyle\int_{x_1(t)}^{x_2(t)} w(x-y)\mathrm{d}y$

so $\dfrac{\partial u(x_j(t),t)}{\partial t} = -\theta + W(x_2(t) - x_1(t))$ with $W(x) = \displaystyle\int_0^x w(y)\mathrm{d}y$

Nonequilibrium dynamics via interface equations

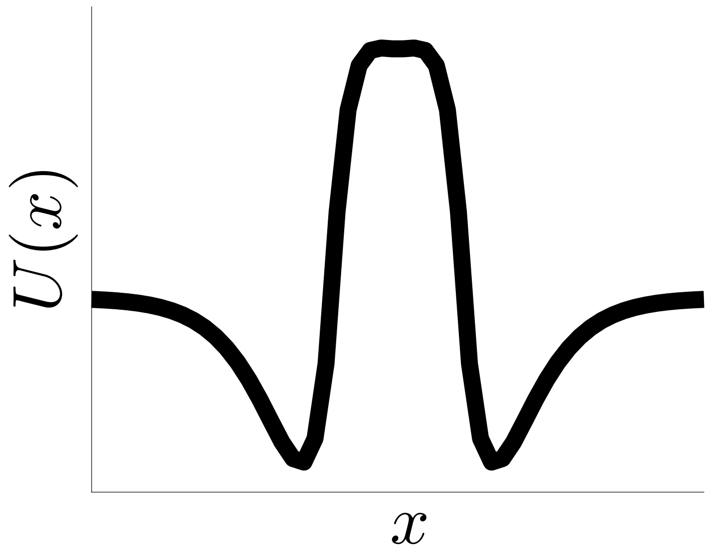

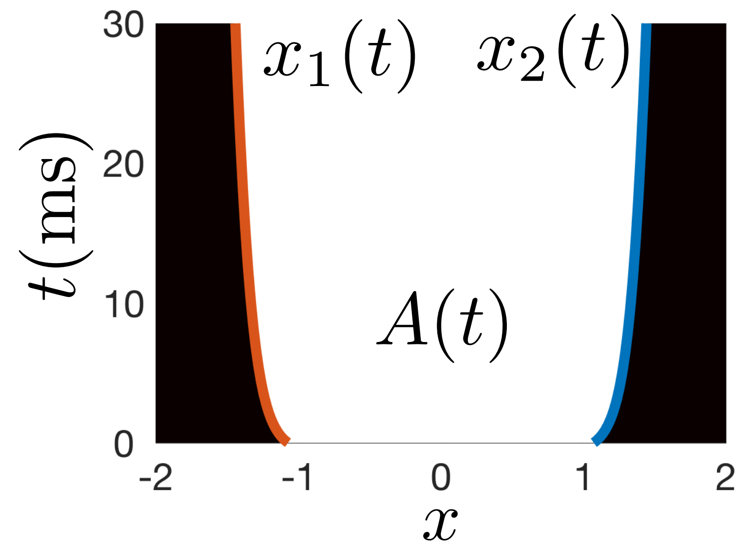

can show interfaces $u(x_j(t), t) = \theta$ determine dynamics of the entire neural field $u(x,t)$

define active region:
$A(t) = [x_1(t), x_2(t)]$

differentiate
$u(x_j(t), t) = \theta$ $\longrightarrow$ $\alpha_j(t) \dfrac{\mathrm{d}x_j}{\mathrm{d}t} + \dfrac{\partial u(x_j(t), t)}{\partial t} = 0$ $\qquad \alpha_j(t) = \dfrac{\partial u(x_j(t), t)}{\partial x}$

recall $\dfrac{\partial u(x,t)}{\partial t} = -u(x,t) + \displaystyle\int_{x_1(t)}^{x_2(t)} w(x-y)\mathrm{d}y$

so $\dfrac{\partial u(x_j(t), t)}{\partial t} = -\theta + W(x_2(t) - x_1(t))$ with $W(x) = \displaystyle\int_0^x w(y)\mathrm{d}y$

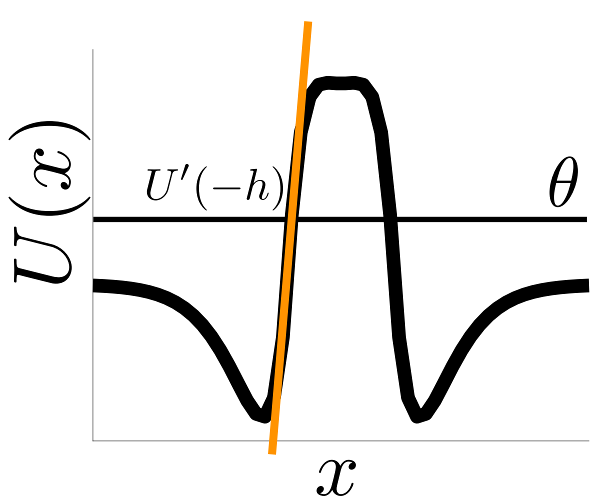

static gradient approximation

$$\alpha_1(t) \approx \bar{\alpha} = U'(-h)$$
$$\alpha_2(t) \approx -\bar{\alpha} = -|U'(h)|$$

(Amari 1977)
(Krishnan, Poll, and ZPK 2017)

$$\dot{x}_1(t) = \bar{\alpha}^{-1}\left[\theta - W(x_2(t) - x_1(t))\right]$$
$$\dot{x}_2(t) = \bar{\alpha}^{-1}\left[-\theta + W(x_2(t) - x_1(t))\right]$$

$W(x_2 - x_1) = \theta: \;\; \dot{x}_1 = \dot{x}_2 = 0$

$W(x_2 - x_1) > \theta: \;\; \dot{x}_1 < 0, \;\; \dot{x}_2 > 0$

$W(x_2 - x_1) < \theta: \;\; \dot{x}_1 > 0, \;\; \dot{x}_2 < 0$

Interface equations for stochastic neural field

$$\mathrm{d}u(x,t) = \left[-u(x,t) + w(x) * H(u(x,t) - \theta)\right]\mathrm{d}t + \sqrt{\epsilon|u(x,t)|}\,\mathrm{d}Z(x,t)$$

$Z(x,t)$: spatially-extended noise with $\langle \mathrm{d}Z(x,t)\mathrm{d}Z(y,s)\rangle = C(x-y)\delta(t-s)\mathrm{d}t\mathrm{d}s$

Interface equations for stochastic neural field

$$\mathrm{d}u(x,t) = \left[-u(x,t) + w(x) * H(u(x,t)-\theta)\right]\mathrm{d}t + \sqrt{\epsilon|u(x,t)|}\,\mathrm{d}Z(x,t)$$

$Z(x,t)$: spatially-extended noise with $\langle \mathrm{d}Z(x,t)\mathrm{d}Z(y,s)\rangle = C(x-y)\delta(t-s)\mathrm{d}t\mathrm{d}s$

interface eqns with static gradient

$$\mathrm{d}x_1 = \bar{\alpha}^{-1}\left[(\theta - W(x_2-x_1))\mathrm{d}t - \sqrt{\epsilon\theta}\,\mathrm{d}Z(x_1(t),t)\right]$$

$$\mathrm{d}x_2 = -\bar{\alpha}^{-1}\left[(\theta - W(x_2-x_1))\mathrm{d}t - \sqrt{\epsilon\theta}\,\mathrm{d}Z(x_2(t),t)\right]$$

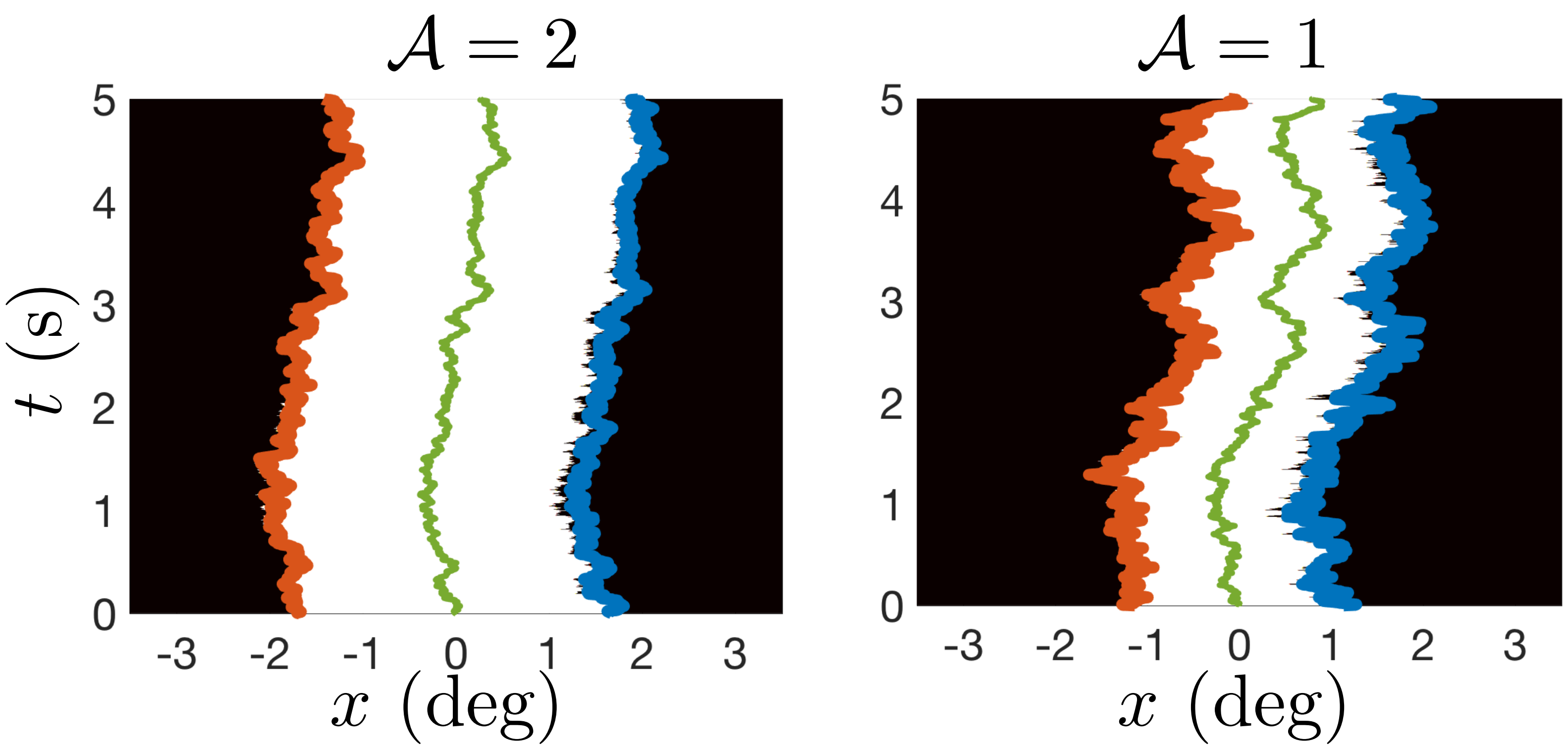

$\Delta(t)$ bump centroid

recall $\mathcal{A}$ is synaptic strength

$$w(x) = \mathcal{A}(1-|x|)\mathrm{e}^{-|x|}$$

Interface equations for stochastic neural field

$$\mathrm{d}u(x,t) = \left[-u(x,t) + w(x) * H(u(x,t)-\theta)\right]\mathrm{d}t + \sqrt{\epsilon|u(x,t)|}\,\mathrm{d}Z(x,t)$$

$Z(x,t)$: spatially-extended noise with $\langle \mathrm{d}Z(x,t)\mathrm{d}Z(y,s)\rangle = C(x-y)\delta(t-s)\mathrm{d}t\mathrm{d}s$

<u>interface eqns</u>
<u>with static gradient</u>

$$\mathrm{d}x_1 = \bar{\alpha}^{-1}\left[(\theta - W(x_2-x_1))\mathrm{d}t - \sqrt{\epsilon\theta}\,\mathrm{d}Z(x_1(t),t)\right]$$

$$\mathrm{d}x_2 = -\bar{\alpha}^{-1}\left[(\theta - W(x_2-x_1))\mathrm{d}t - \sqrt{\epsilon\theta}\,\mathrm{d}Z(x_2(t),t)\right]$$

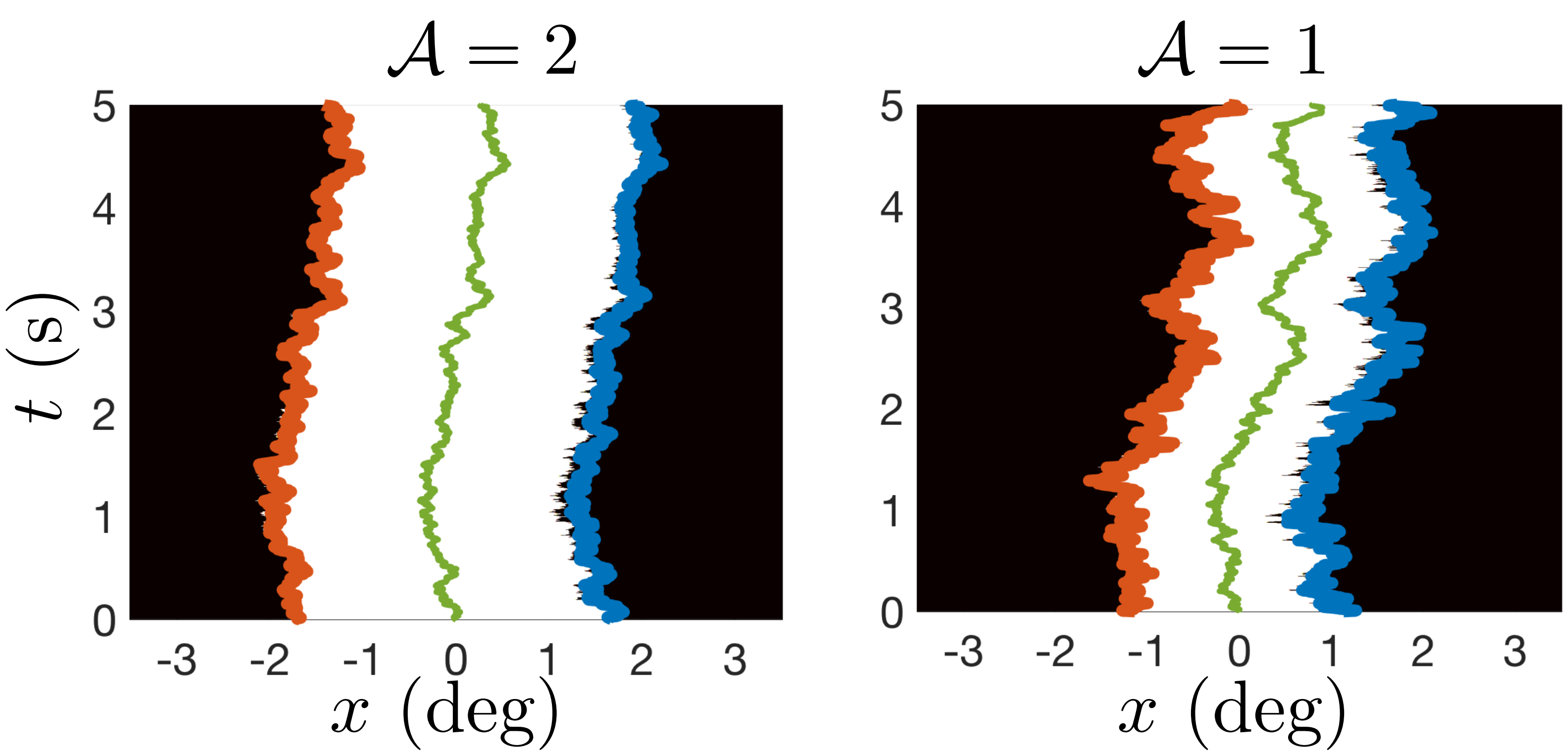

recall $\mathcal{A}$ is synaptic strength

$$\boxed{w(x) = \mathcal{A}(1-|x|)\mathrm{e}^{-|x|}}$$

$\Delta(t)$ bump centroid

$\langle(\Delta(t)-\bar{\Delta})^2\rangle = Dt$ variance decreases with $\mathcal{A}$

$$D \approx \frac{\epsilon\theta}{2\bar{\alpha}^2}\left[C(0) - C(2h)\right]$$

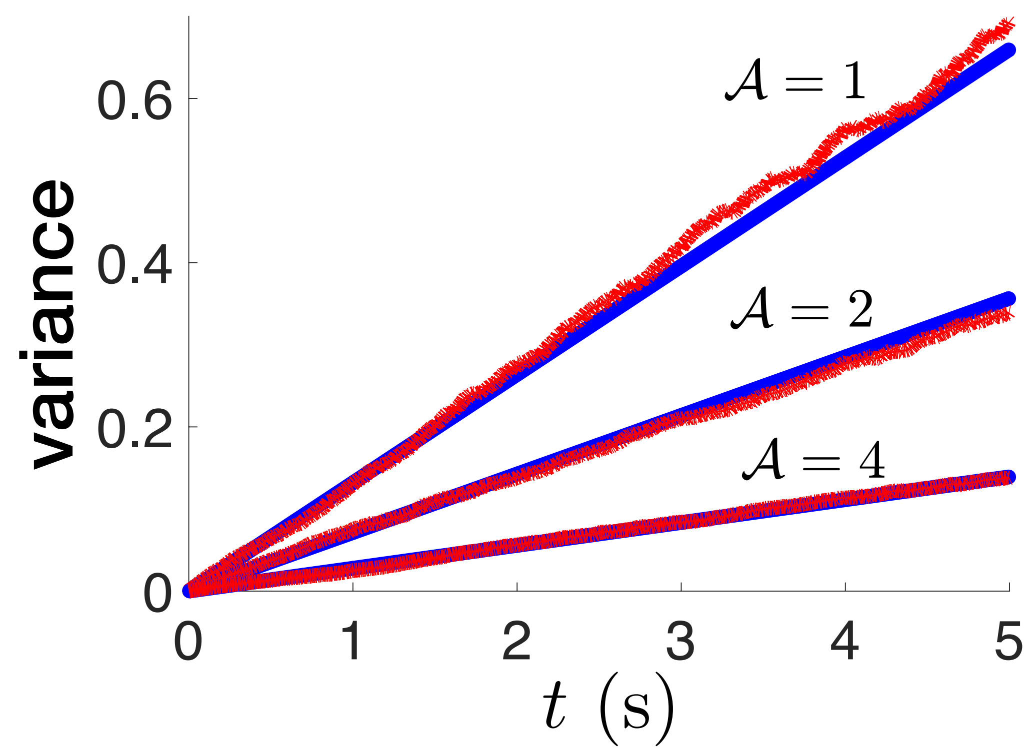

Interface equations for a two interacting bumps

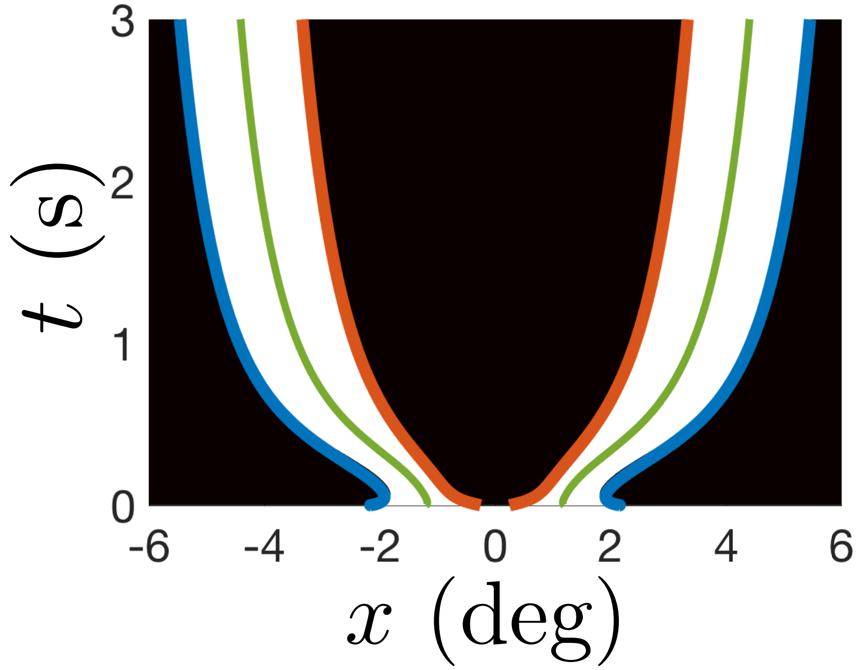

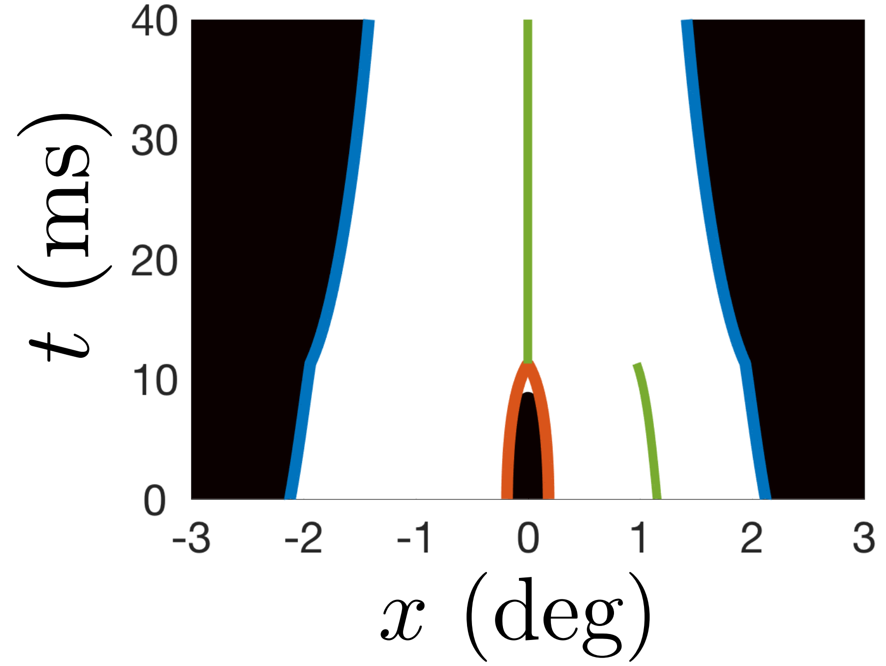

in the absence of noise, bumps will repel or attract one another

similar methods can be used to obtain interface equations

Interface equations for a two interacting bumps

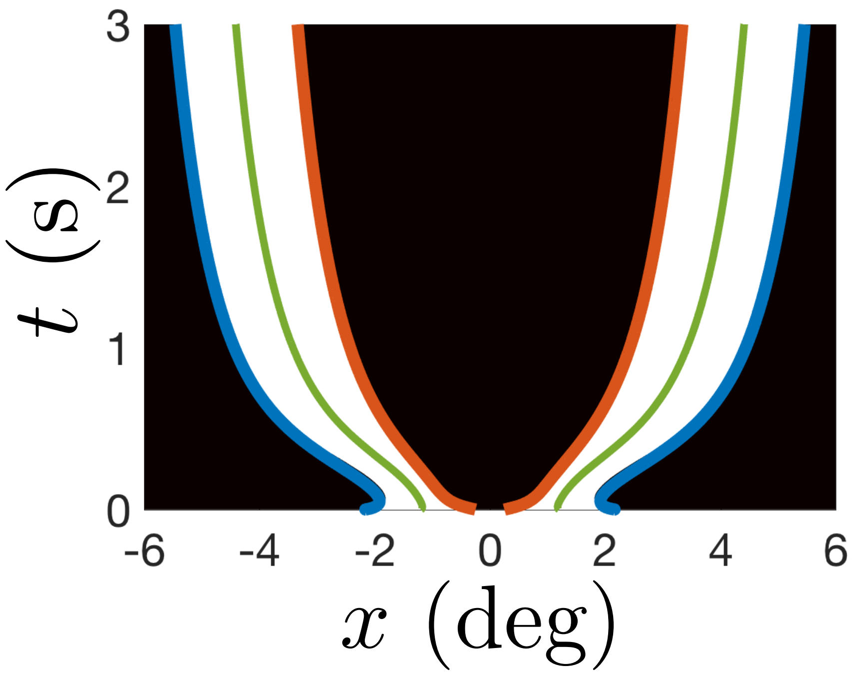

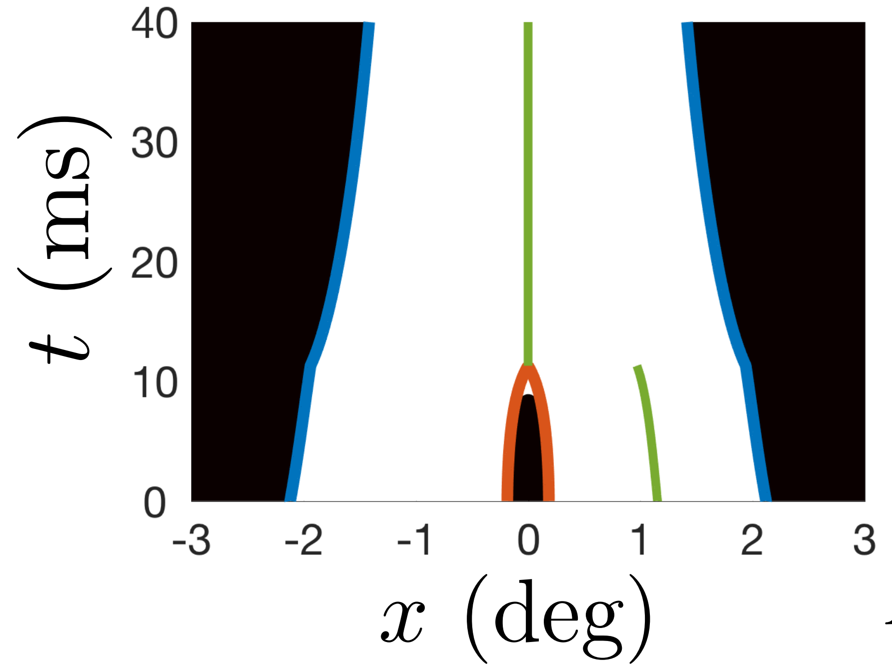

in the absence of noise, bumps will repel or attract one another

similar methods can be used to obtain interface equations

active region

$$A(t) = [x_1(t), x_2(t)] \cup [x_3(t), x_4(t)]$$

$$\frac{\partial u}{\partial t} = -u(x,t) + \int_{x_1(t)}^{x_2(t)} w(x-y)\mathrm{d}y + \int_{x_3(t)}^{x_4(t)} w(x-y)\mathrm{d}y$$

interface eqns will now track 4 edges

Interface equations for a two interacting bumps

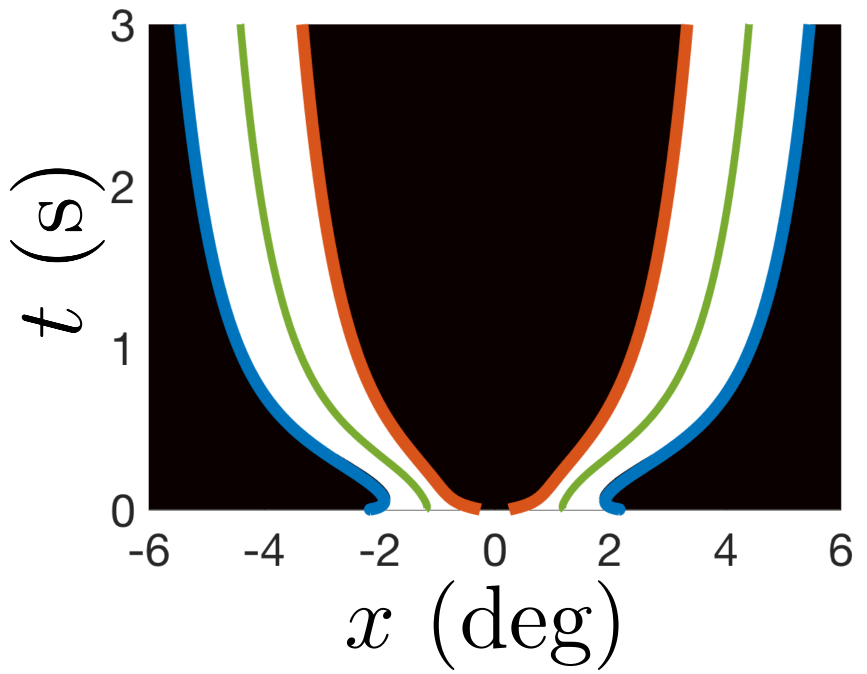

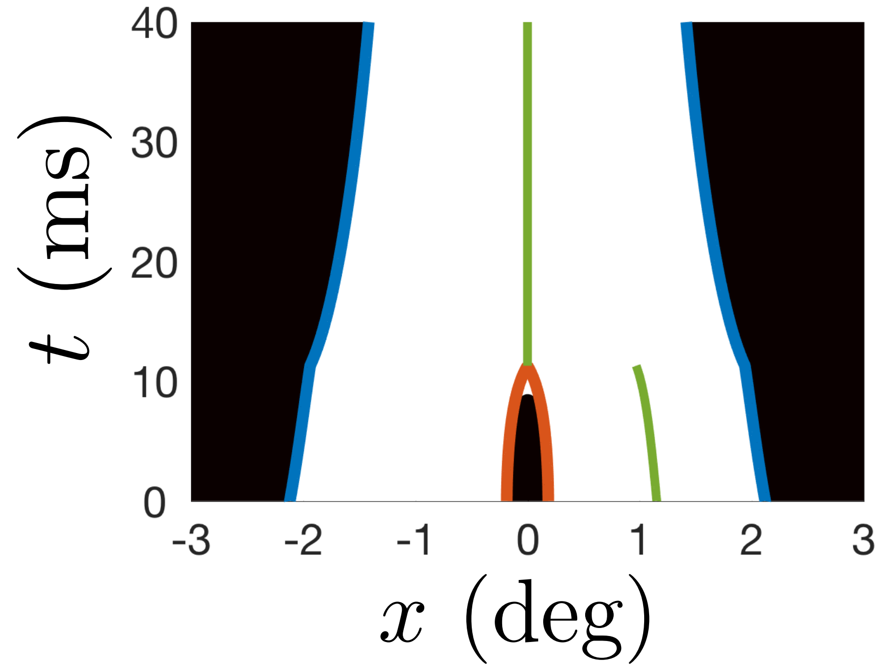

in the absence of noise, bumps will repel or attract one another

similar methods can be used to obtain interface equations

active region

$$A(t) = [x_1(t), x_2(t)] \cup [x_3(t), x_4(t)]$$

$$\frac{\partial u}{\partial t} = -u(x,t) + \int_{x_1(t)}^{x_2(t)} w(x-y)\mathrm{d}y + \int_{x_3(t)}^{x_4(t)} w(x-y)\mathrm{d}y$$

interface eqns will now track 4 edges

for symmetrically initiated bumps

$$a(t) = x_3(t) = -x_2(t)$$
$$b(t) = x_4(t) = -x_1(t)$$
$$\alpha(t) = \alpha_3(t) = -\alpha_2(t)$$
$$\beta(t) = \alpha_1(t) = -\alpha_4(t)$$

$$\dot{a}(t) = \frac{1}{\alpha(t)}\left[\theta - W(b(t)-a(t)) + W(2a(t)) - W(a(t)+b(t))\right],$$

$$\dot{b}(t) = \frac{1}{\beta(t)}\left[W(b(t)-a(t)) - \theta + W(2b(t)) - W(a(t)+b(t))\right]$$

and integral equations for the gradients

Interface equations for a two interacting bumps

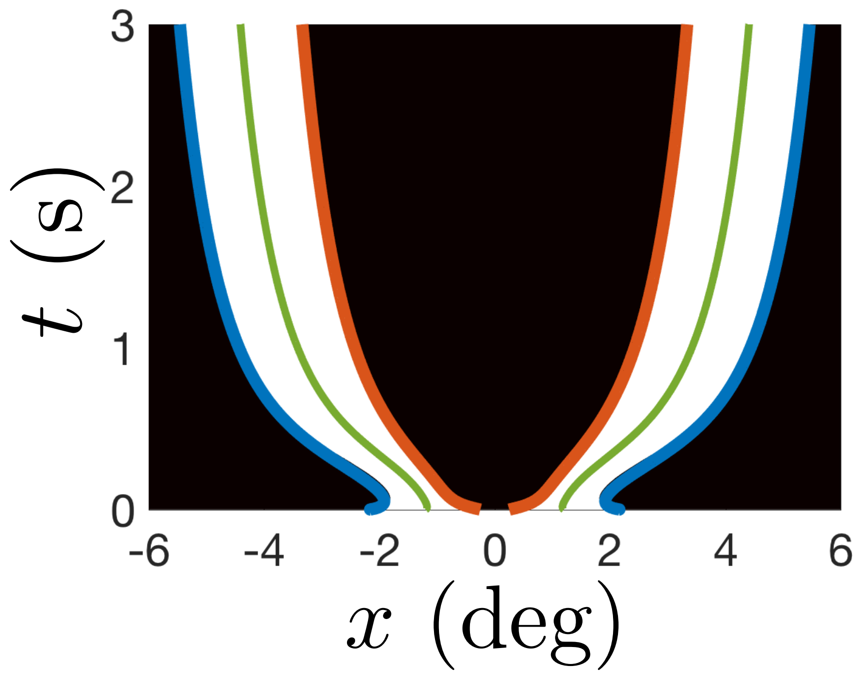

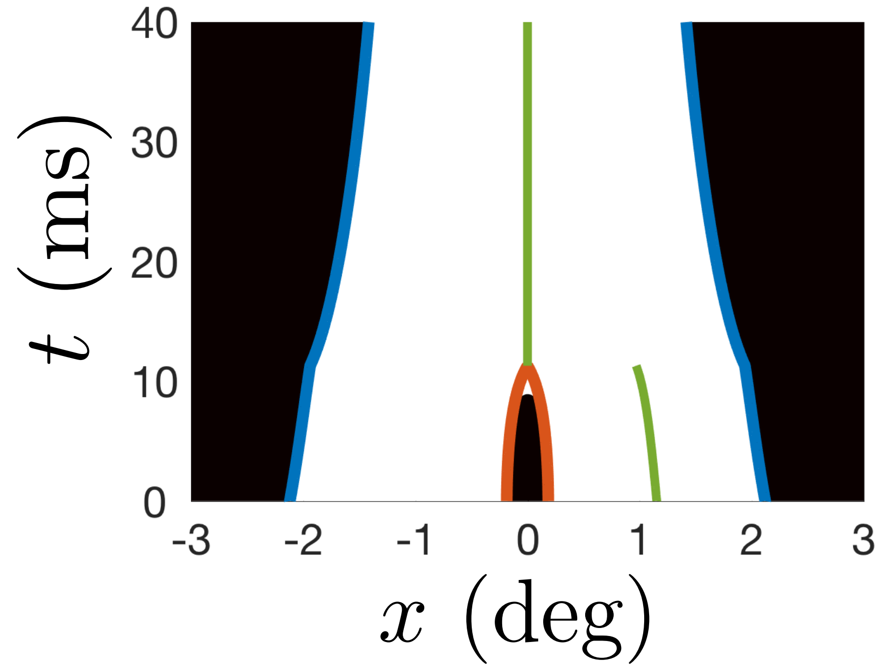

in the absence of noise, bumps will repel or attract one another

similar methods can be used to obtain interface equations

active region

$$A(t) = [x_1(t), x_2(t)] \cup [x_3(t), x_4(t)]$$

$$\frac{\partial u}{\partial t} = -u(x,t) + \int_{x_1(t)}^{x_2(t)} w(x-y)\mathrm{d}y + \int_{x_3(t)}^{x_4(t)} w(x-y)\mathrm{d}y$$

interface eqns will now track 4 edges

for symmetrically initiated bumps

$$a(t) = x_3(t) = -x_2(t)$$
$$b(t) = x_4(t) = -x_1(t)$$
$$\alpha(t) = \alpha_3(t) = -\alpha_2(t)$$
$$\beta(t) = \alpha_1(t) = -\alpha_4(t)$$

$$\dot{a}(t) = \frac{1}{\alpha(t)}\left[\theta - W(b(t)-a(t)) + W(2a(t)) - W(a(t)+b(t))\right],$$

$$\dot{b}(t) = \frac{1}{\beta(t)}\left[W(b(t)-a(t)) - \theta + W(2b(t)) - W(a(t)+b(t))\right]$$

and integral equations for the gradients

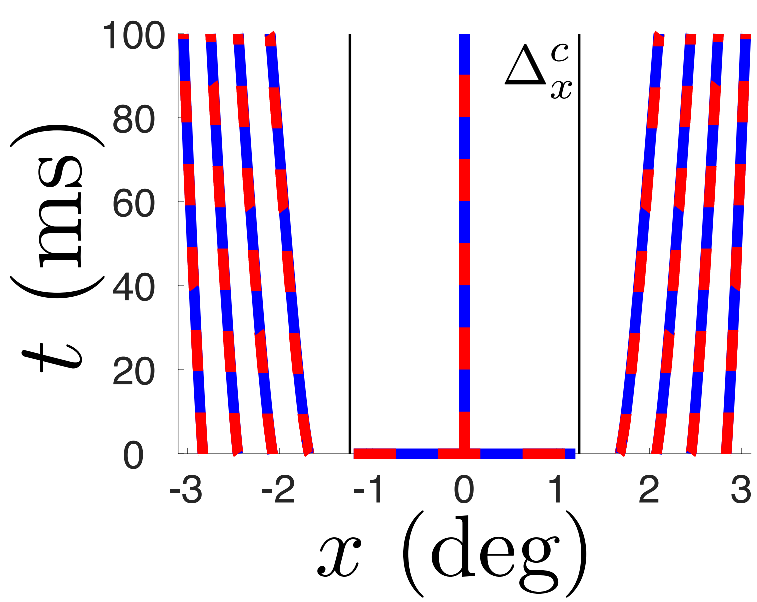

there is a critical distance bump centroids can start apart and not be attracted Δ_x^c

Interface equations for a two interacting bumps

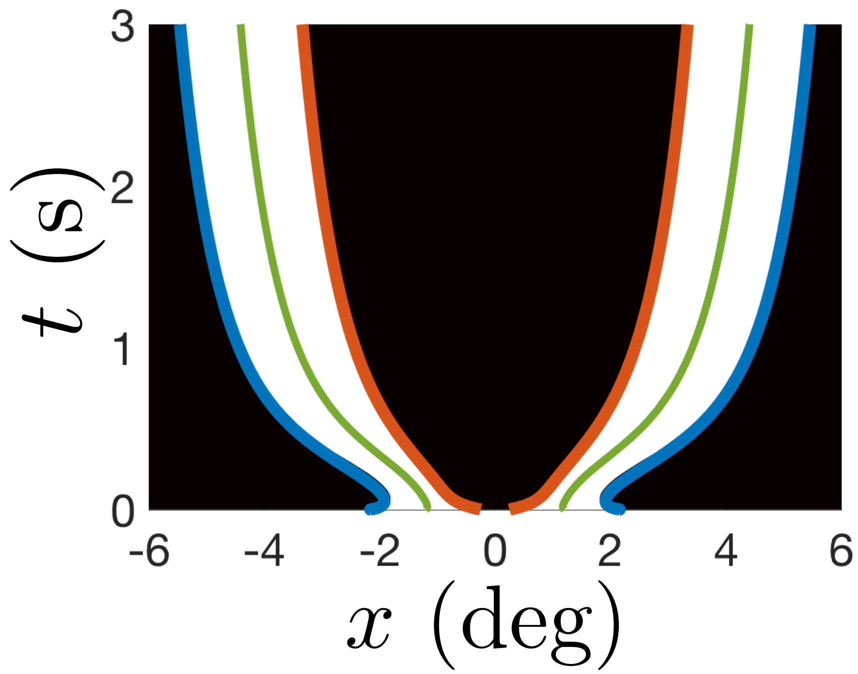

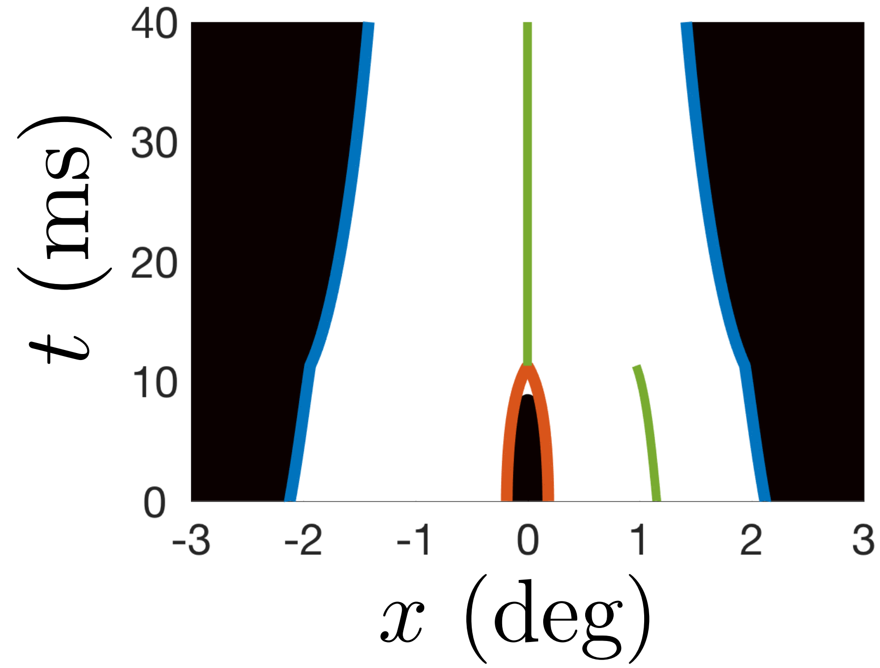

in the absence of noise, bumps will repel or attract one another

similar methods can be used to obtain interface equations

active region

$$A(t) = [x_1(t), x_2(t)] \cup [x_3(t), x_4(t)]$$

$$\frac{\partial u}{\partial t} = -u(x,t) + \int_{x_1(t)}^{x_2(t)} w(x-y)\mathrm{d}y + \int_{x_3(t)}^{x_4(t)} w(x-y)\mathrm{d}y$$

interface eqns will now track 4 edges

for symmetrically initiated bumps

$$a(t) = x_3(t) = -x_2(t)$$
$$b(t) = x_4(t) = -x_1(t)$$
$$\alpha(t) = \alpha_3(t) = -\alpha_2(t)$$
$$\beta(t) = \alpha_1(t) = -\alpha_4(t)$$

$$\dot{a}(t) = \frac{1}{\alpha(t)}\left[\theta - W(b(t)-a(t)) + W(2a(t)) - W(a(t)+b(t))\right],$$

$$\dot{b}(t) = \frac{1}{\beta(t)}\left[W(b(t)-a(t)) - \theta + W(2b(t)) - W(a(t)+b(t))\right]$$

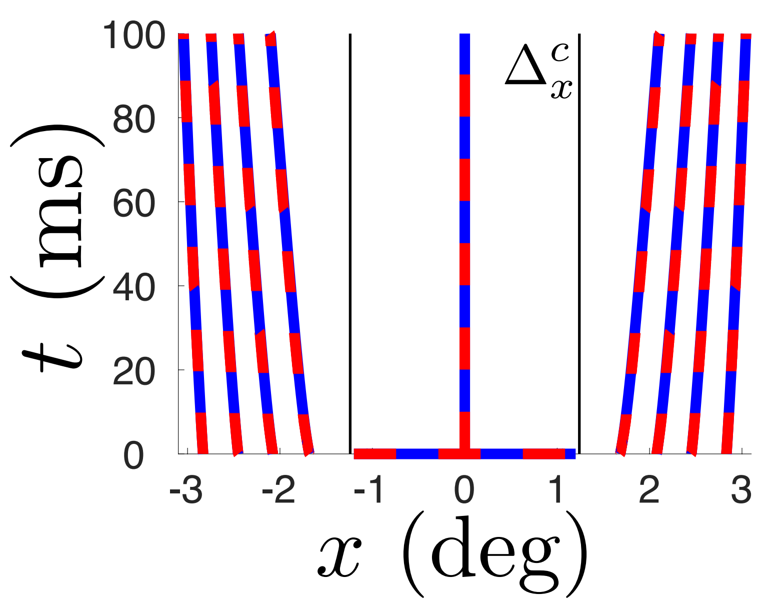

there is a critical distance bump centroids can start apart and not be attracted Δ_x^c

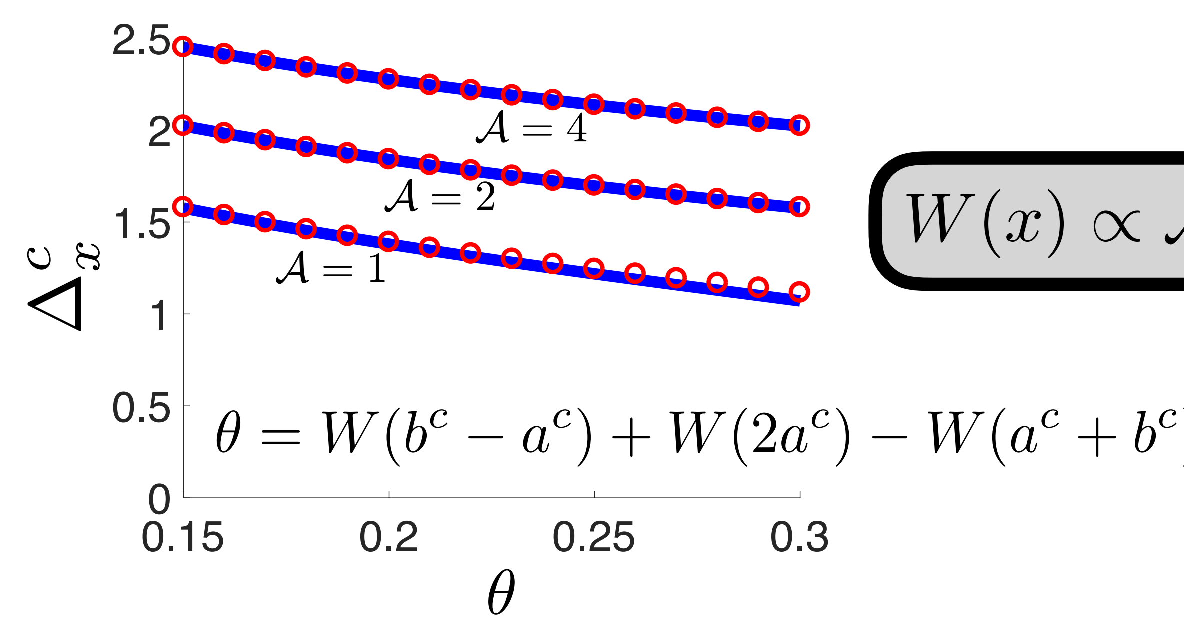

$$W(x) \propto \mathcal{A}$$

Stochastic interface equations for noise-driven bumps

assuming static gradient and considering the stochastic neural field

$$\mathrm{d}x_1 = \bar{\alpha}^{-1}\left[(\theta - W(x_2-x_1) + W(x_3-x_1) - W(x_4-x_1))\,\mathrm{d}t - \sqrt{\epsilon\theta}\,\mathrm{d}Z(x_1,t)\right],$$

$$\mathrm{d}x_2 = -\bar{\alpha}^{-1}\left[(\theta - W(x_2-x_1) + W(x_3-x_2) - W(x_4-x_2))\,\mathrm{d}t - \sqrt{\epsilon\theta}\,\mathrm{d}Z(x_2,t)\right]$$

and similar equations for x_3 & x_4

Stochastic interface equations for noise-driven bumps

assuming static gradient and considering the stochastic neural field

$$\mathrm{d}x_1 = \bar{\alpha}^{-1}\left[(\theta - W(x_2-x_1) + W(x_3-x_1) - W(x_4-x_1))\,\mathrm{d}t - \sqrt{\epsilon\theta}\mathrm{d}Z(x_1,t)\right],$$

$$\mathrm{d}x_2 = -\bar{\alpha}^{-1}\left[(\theta - W(x_2-x_1) + W(x_3-x_2) - W(x_4-x_2))\,\mathrm{d}t - \sqrt{\epsilon\theta}\mathrm{d}Z(x_2,t)\right]$$

and similar equations for x_3 & x_4

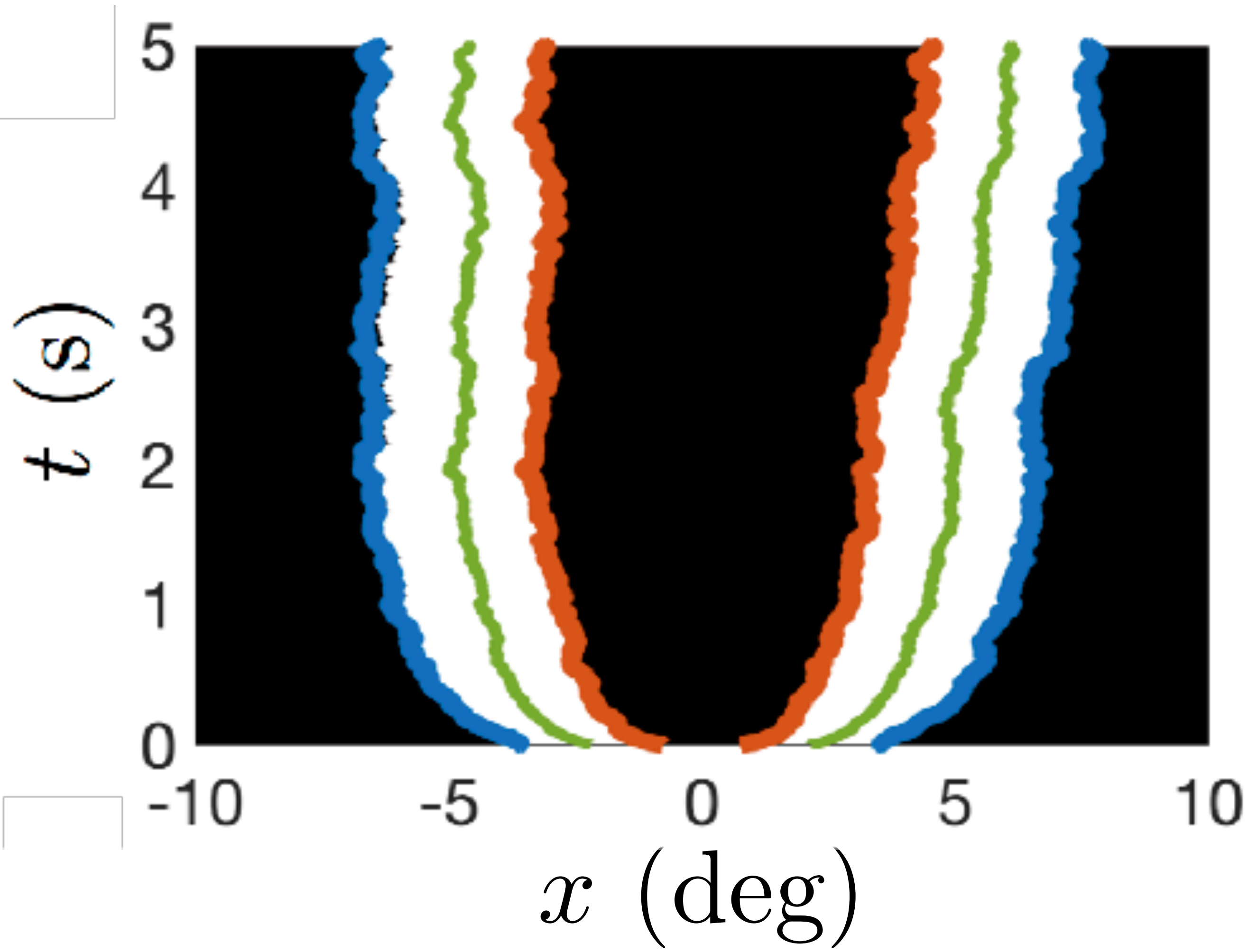

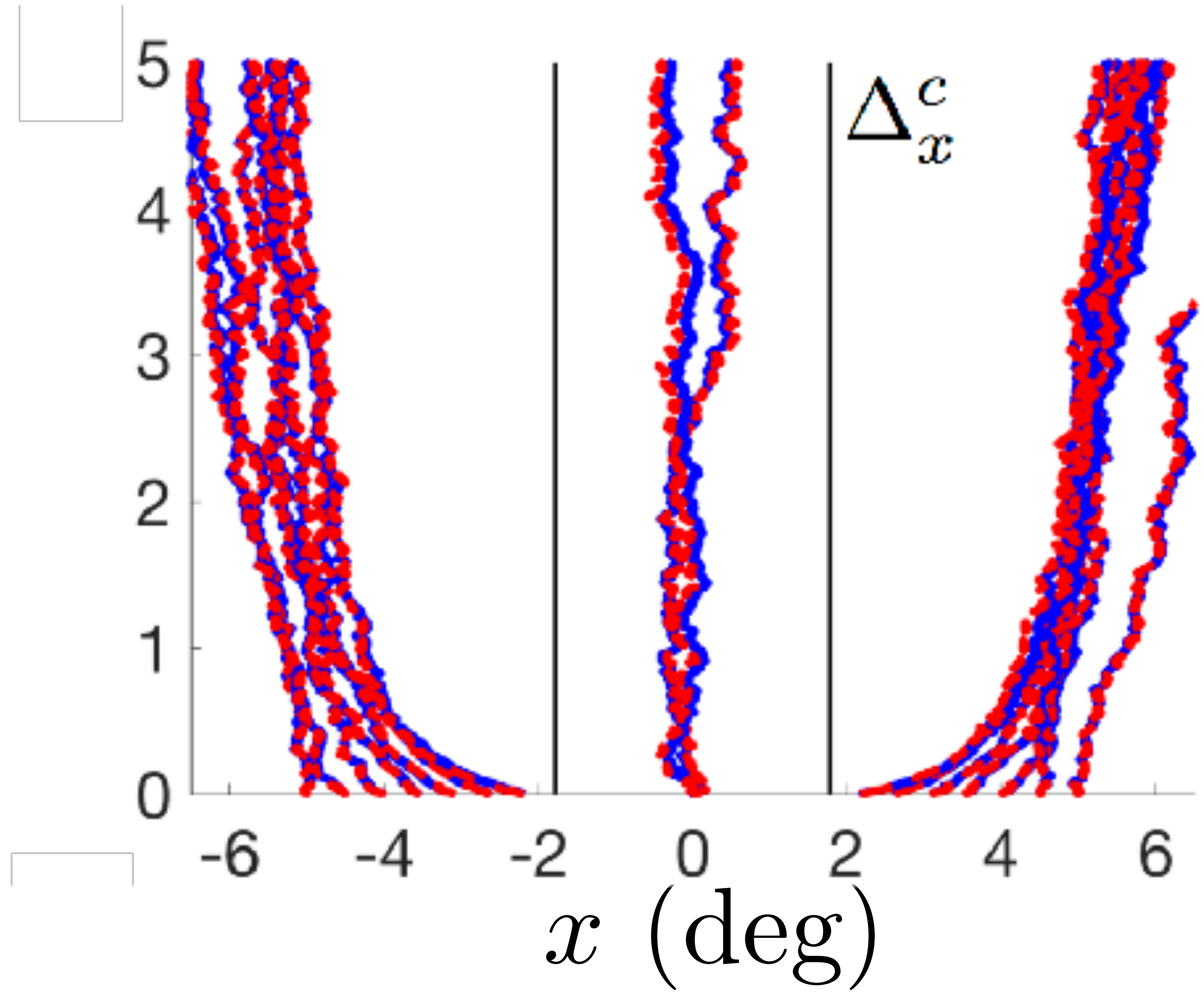

Stochastic interface equations for noise-driven bumps

assuming static gradient and considering the stochastic neural field

$$\mathrm{d}x_1 = \bar{\alpha}^{-1}\left[(\theta - W(x_2 - x_1) + W(x_3 - x_1) - W(x_4 - x_1))\,\mathrm{d}t - \sqrt{\epsilon\theta}\,\mathrm{d}Z(x_1, t)\right],$$

$$\mathrm{d}x_2 = -\bar{\alpha}^{-1}\left[(\theta - W(x_2 - x_1) + W(x_3 - x_2) - W(x_4 - x_2))\,\mathrm{d}t - \sqrt{\epsilon\theta}\,\mathrm{d}Z(x_2, t)\right]$$

and similar equations for x_3 & x_4

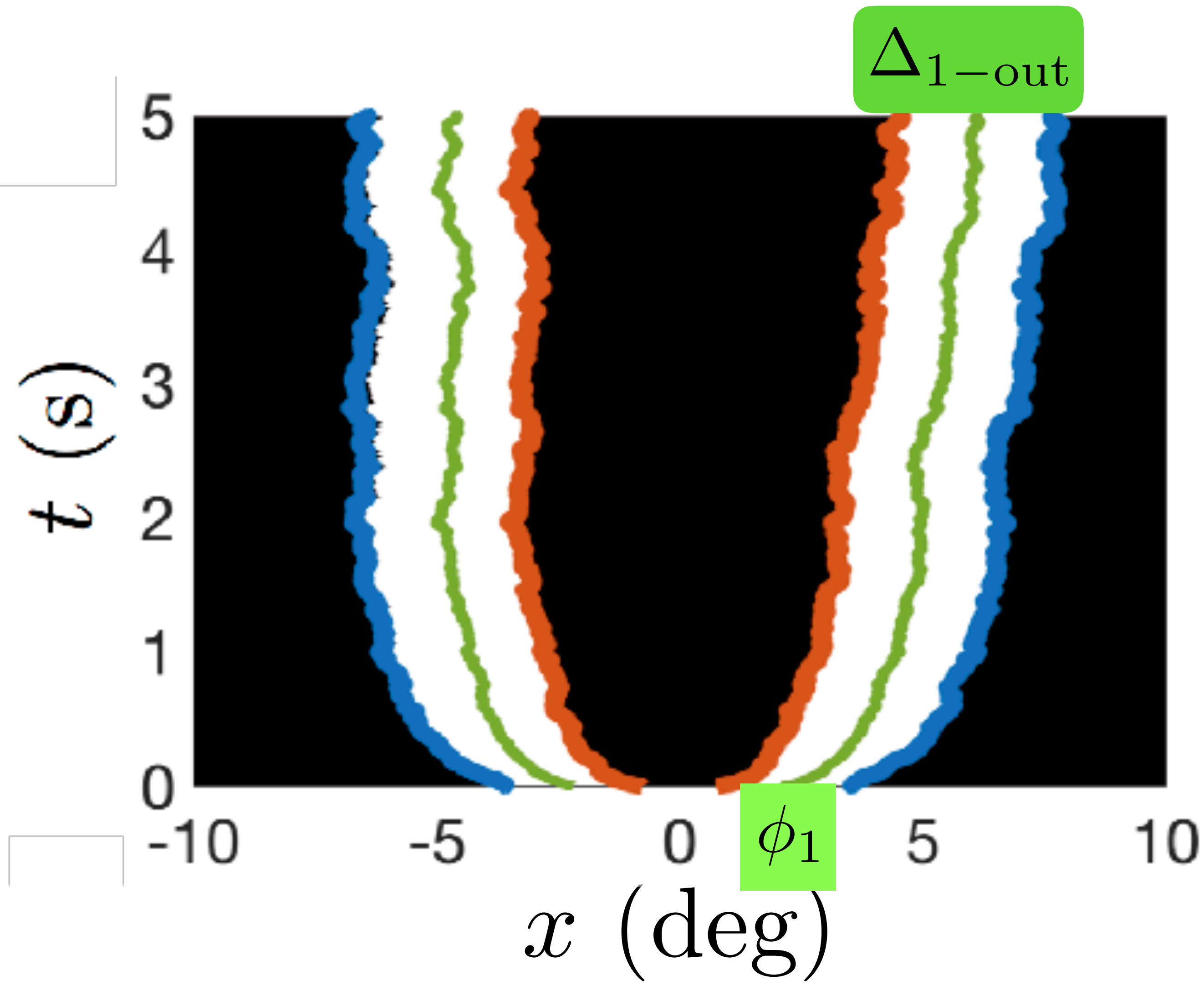

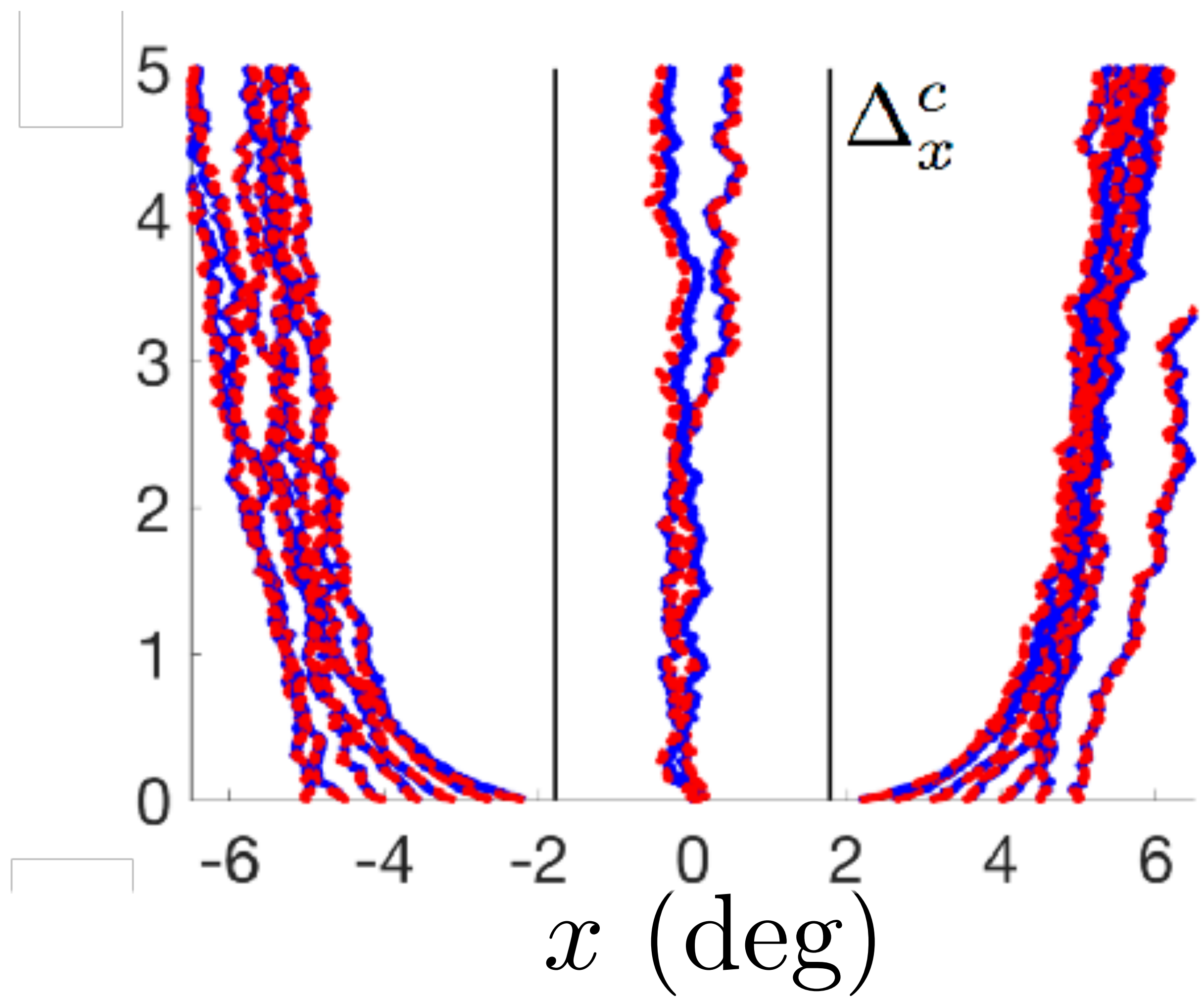

errors in initial condition recall arise from repulsion, absorption, and bump wandering

$$\mathrm{MSE} = \langle(\Delta_{1-\text{out}} - \phi_1)^2\rangle = \frac{1}{K}\sum_{k=1}^{K}(\Delta_{1-\text{out}}^k - \phi_1^k)^2$$

Performance on a two-item working memory task

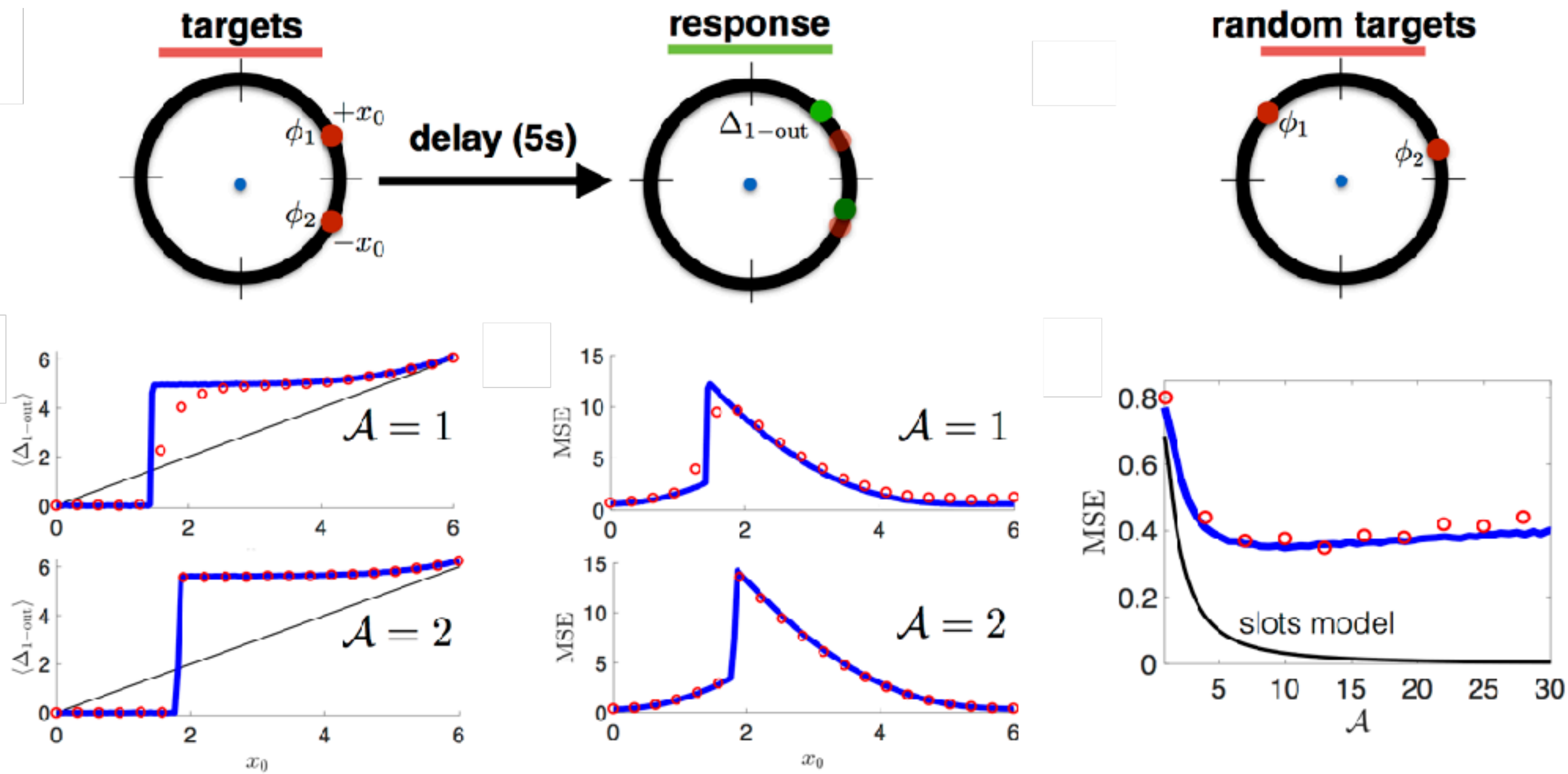

MSE is reduced as two items (bumps) are placed farther apart

Performance on a two-item working memory task

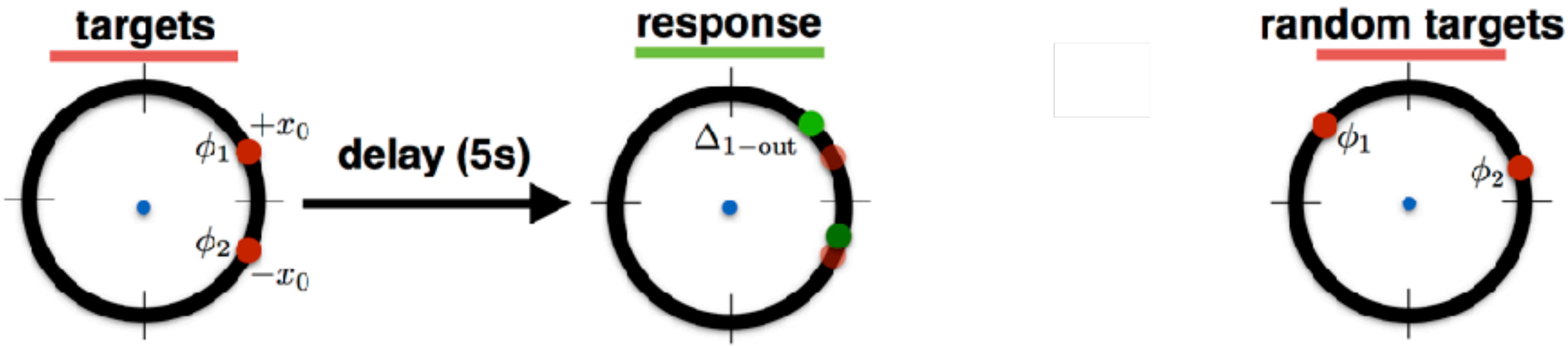

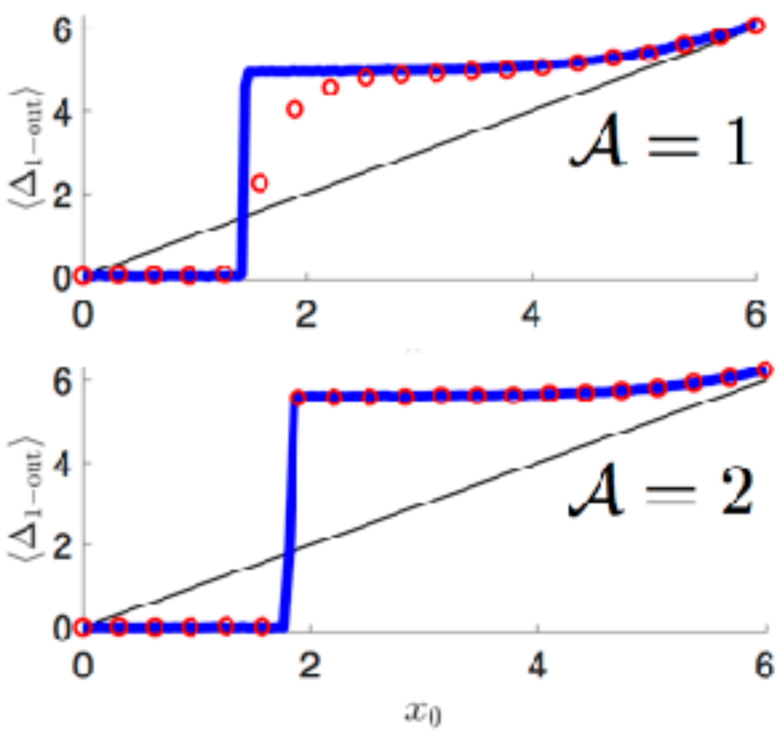

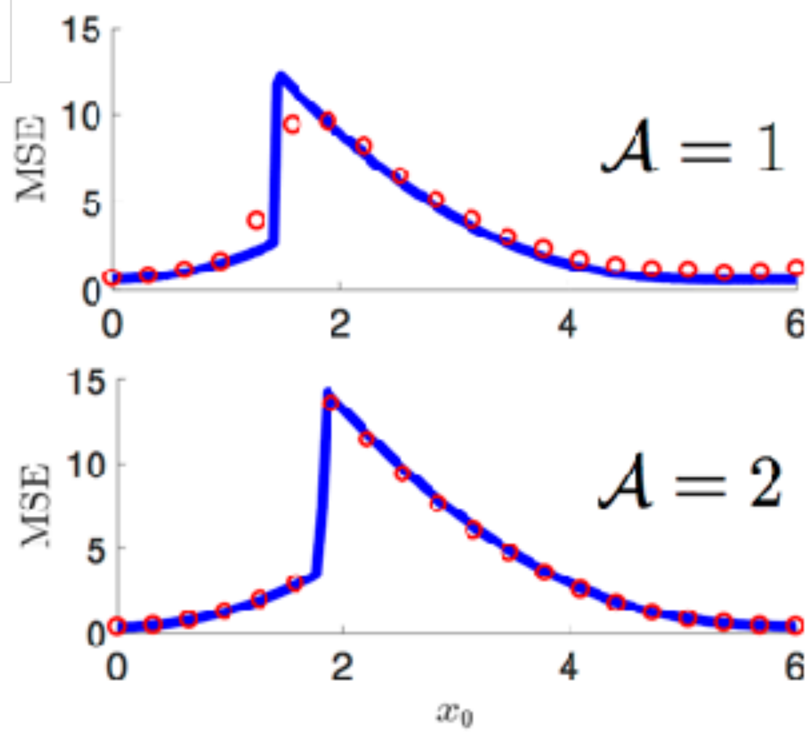

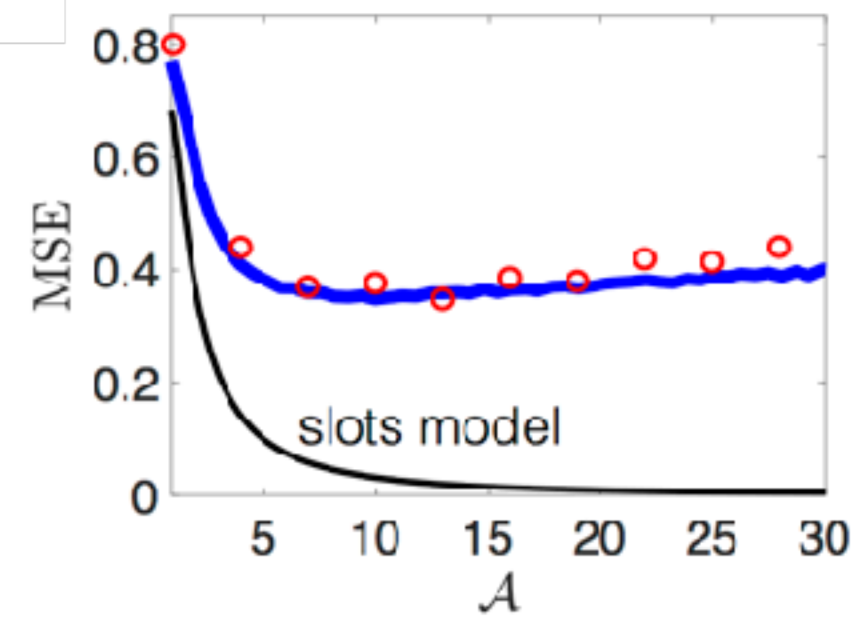

MSE is reduced as two items (bumps) are placed farther apart

optimal choice of synaptic strength $\mathcal{A}$ manages error from fluctuations and interactions

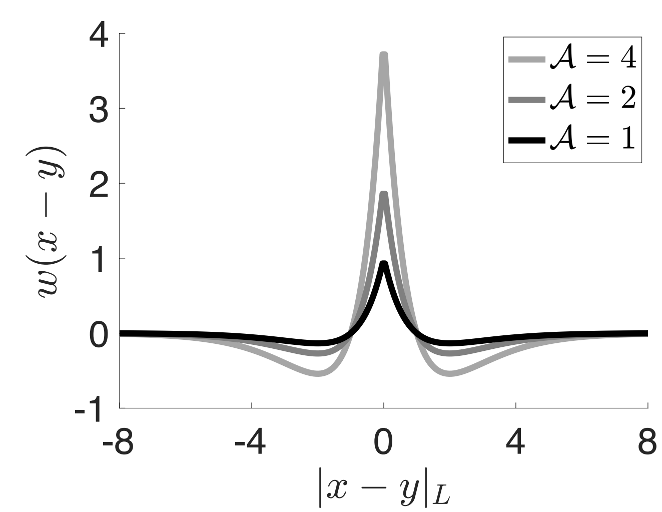

Multiple interacting bumps: Interface equations

active region is given by the union of *N* finite intervals $A(t) = \cup_{j=1}^{N} [a_j(t), b_j(t)]$

effective neural field equation

$$\mathrm{d}u(x,t) = \left[-u(x,t) + \sum_{j=1}^{N} \int_{a_j(t)}^{b_j(t)} w(x-y)\mathrm{d}y \right] \mathrm{d}t + \sqrt{\epsilon |u(x,t)|} \mathrm{d}Z(x,t)$$

Multiple interacting bumps: Interface equations

active region is given by the union of *N* finite intervals $A(t) = \cup_{j=1}^{N} \left[a_j(t), b_j(t)\right]$

effective neural field equation

$$\mathrm{d}u(x,t) = \left[-u(x,t) + \sum_{j=1}^{N} \int_{a_j(t)}^{b_j(t)} w(x-y)\mathrm{d}y \right] \mathrm{d}t + \sqrt{\epsilon |u(x,t)|}\mathrm{d}Z(x,t)$$

stochastic interface eqns

$$\mathrm{d}a_j = \bar{\alpha}^{-1} \left(\left[\theta - \sum_{k=1}^{N} (W(a_j - a_k) - W(a_j - b_k)) \right] \mathrm{d}t - \sqrt{\epsilon}\theta \mathrm{d}Z(a_j, t) \right),$$

$$\mathrm{d}b_j = -\bar{\alpha}^{-1} \left(\left[\theta - \sum_{k=1}^{N} (W(b_j - a_k) - W(b_j - b_k)) \right] \mathrm{d}t - \sqrt{\epsilon}\theta \mathrm{d}Z(b_j, t) \right)$$

Multiple interacting bumps: Interface equations

active region is given by the union of *N* finite intervals $A(t) = \cup_{j=1}^{N} [a_j(t), b_j(t)]$

effective neural field equation

$$\mathrm{d}u(x,t) = \left[-u(x,t) + \sum_{j=1}^{N} \int_{a_j(t)}^{b_j(t)} w(x-y)\mathrm{d}y \right] \mathrm{d}t + \sqrt{\epsilon |u(x,t)|} \mathrm{d}Z(x,t)$$

stochastic interface eqns

$$\mathrm{d}a_j = \bar{\alpha}^{-1} \left(\left[\theta - \sum_{k=1}^{N} (W(a_j - a_k) - W(a_j - b_k)) \right] \mathrm{d}t - \sqrt{\epsilon}\theta \mathrm{d}Z(a_j, t) \right),$$

$$\mathrm{d}b_j = -\bar{\alpha}^{-1} \left(\left[\theta - \sum_{k=1}^{N} (W(b_j - a_k) - W(b_j - b_k)) \right] \mathrm{d}t - \sqrt{\epsilon}\theta \mathrm{d}Z(b_j, t) \right)$$

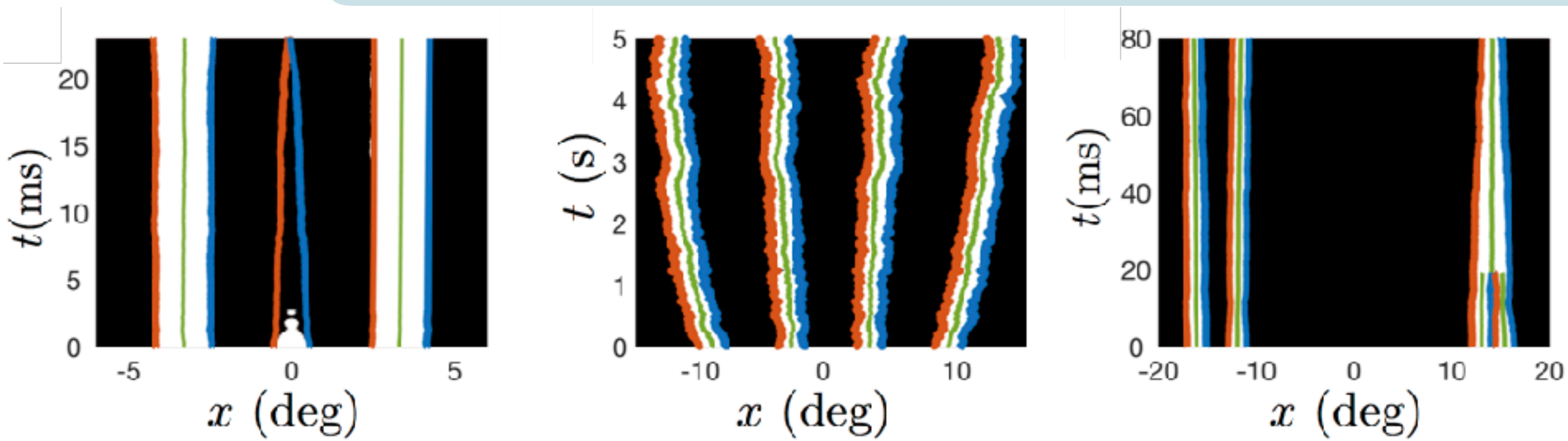

bumps can be annihilated by adjacent bumps in additional to being repelled and merged

Performance in multi-item working memory task

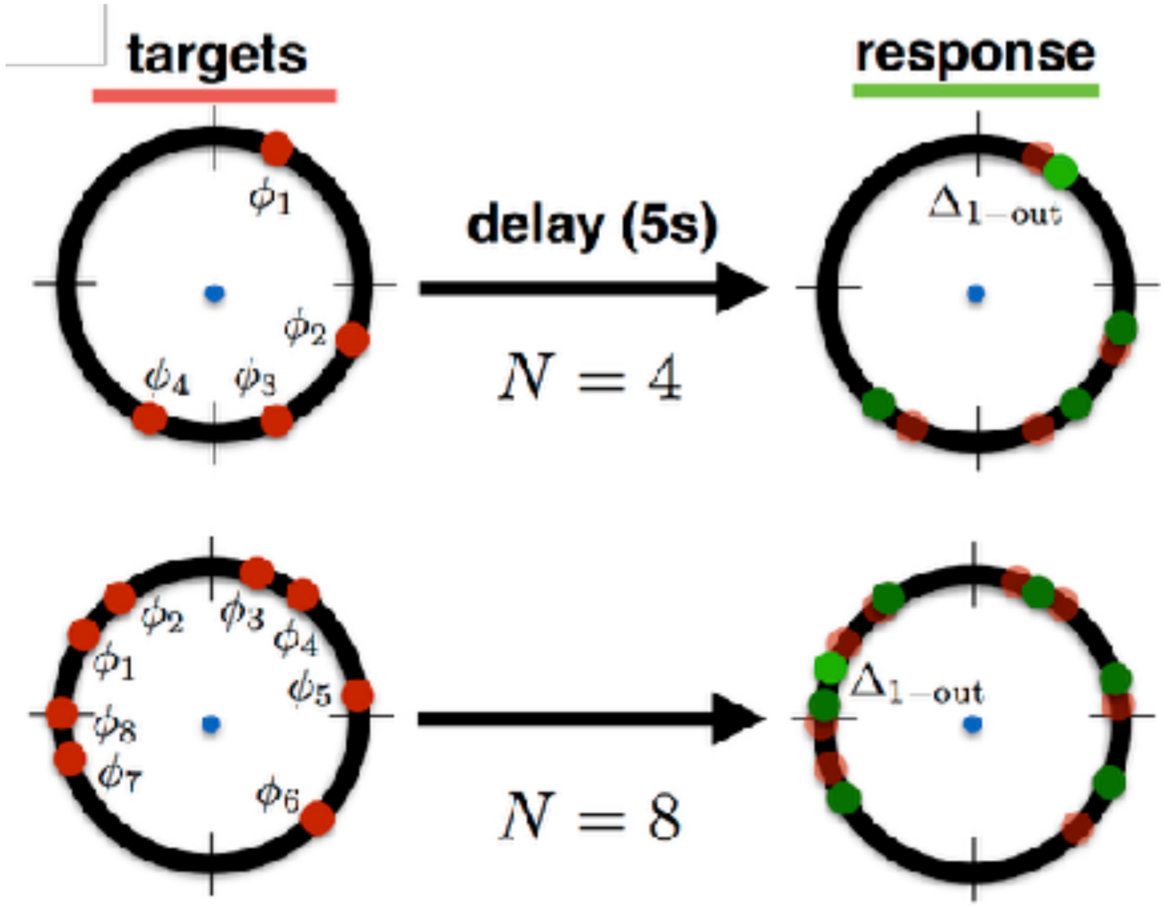

we expect performance to worsen as the number of items to be stored is increased

we also explore the impact of increasing the strength of synaptic connectivity in the network

$$\mathrm{MSE} = \langle (\Delta_{1-\mathrm{out}} - \phi_1)^2 \rangle = \frac{1}{K} \sum_{k=1}^{K} (\Delta^k_{1-\mathrm{out}} - \phi^k_1)^2$$

Performance in multi-item working memory task

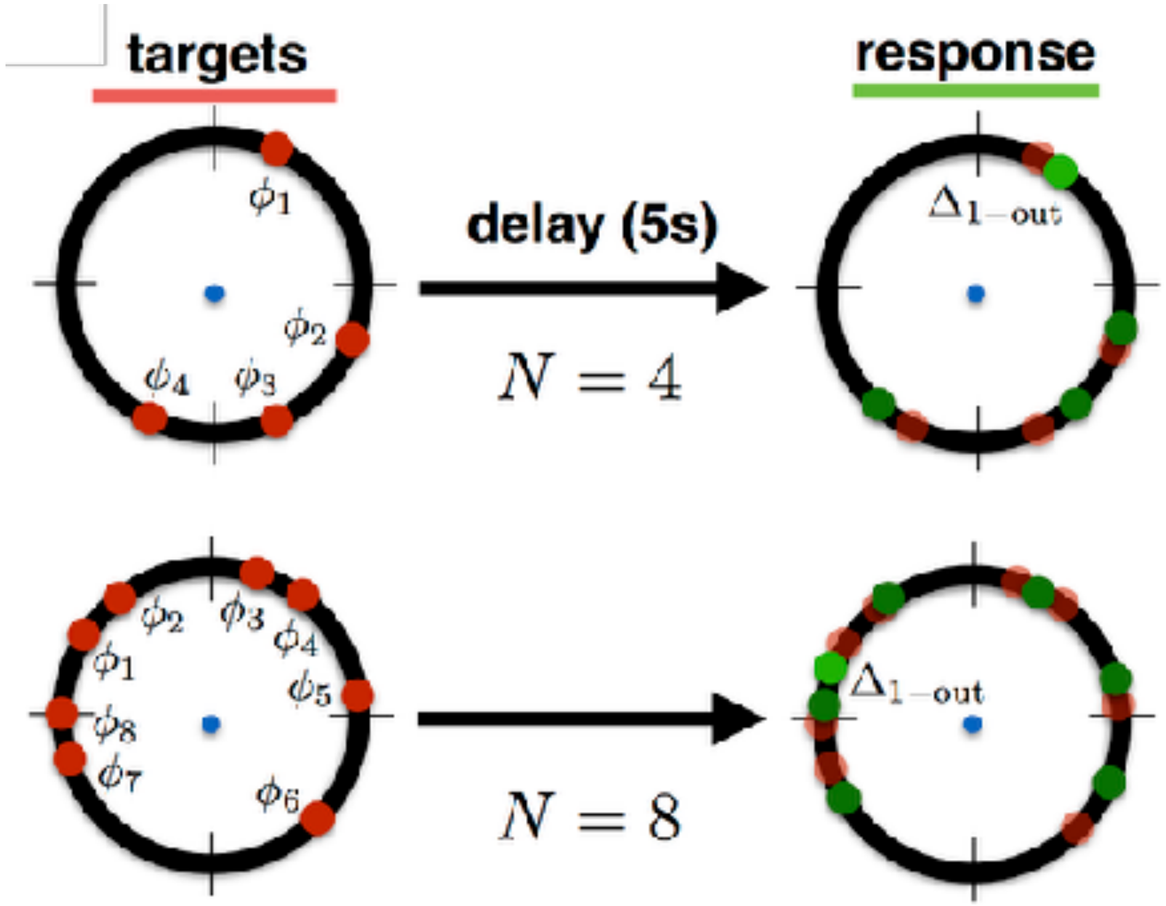

we expect performance to worsen as the number of items to be stored is increased

we also explore the impact of increasing the strength of synaptic connectivity in the network

$$\mathrm{MSE} = \langle (\Delta_{1-\text{out}} - \phi_1)^2 \rangle = \frac{1}{K} \sum_{k=1}^{K} (\Delta^k_{1-\text{out}} - \phi^k_1)^2$$

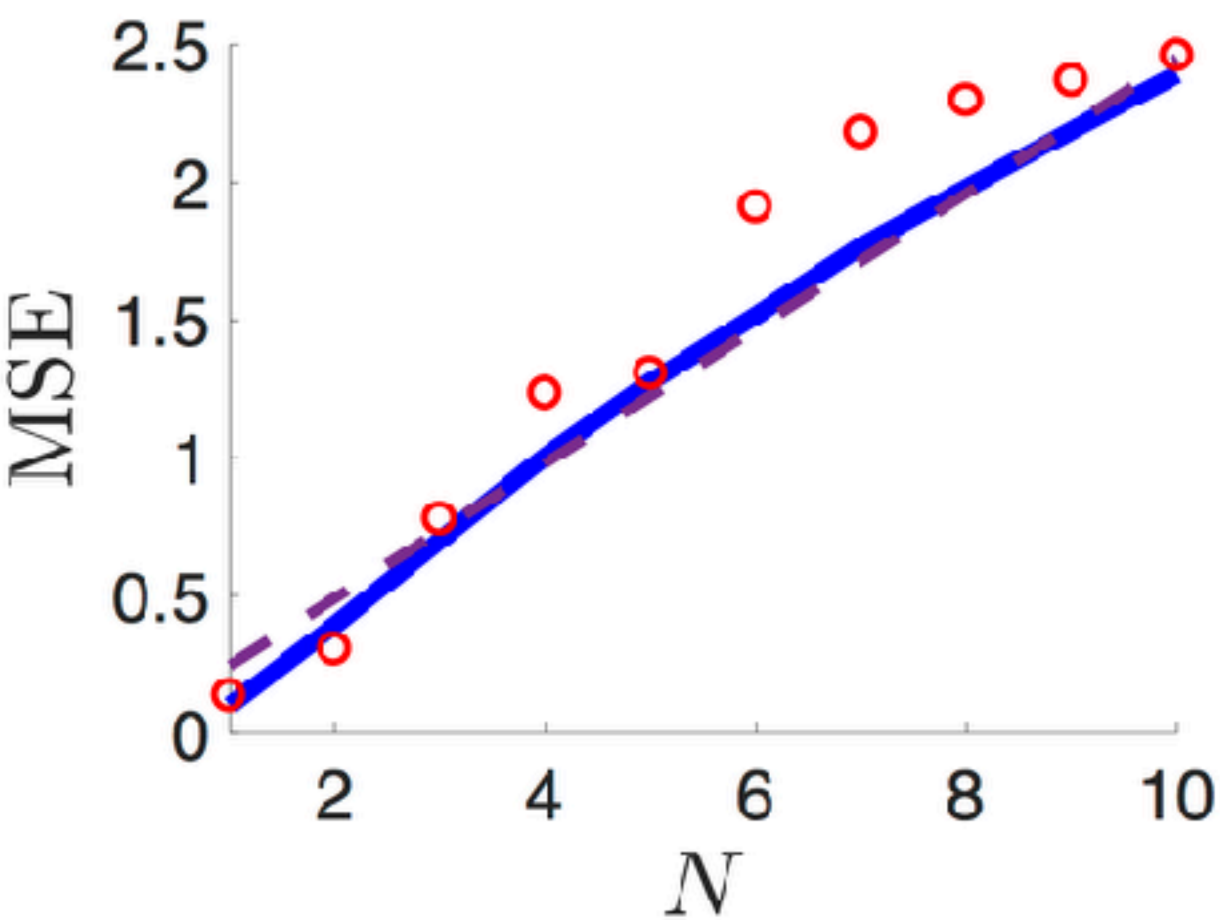

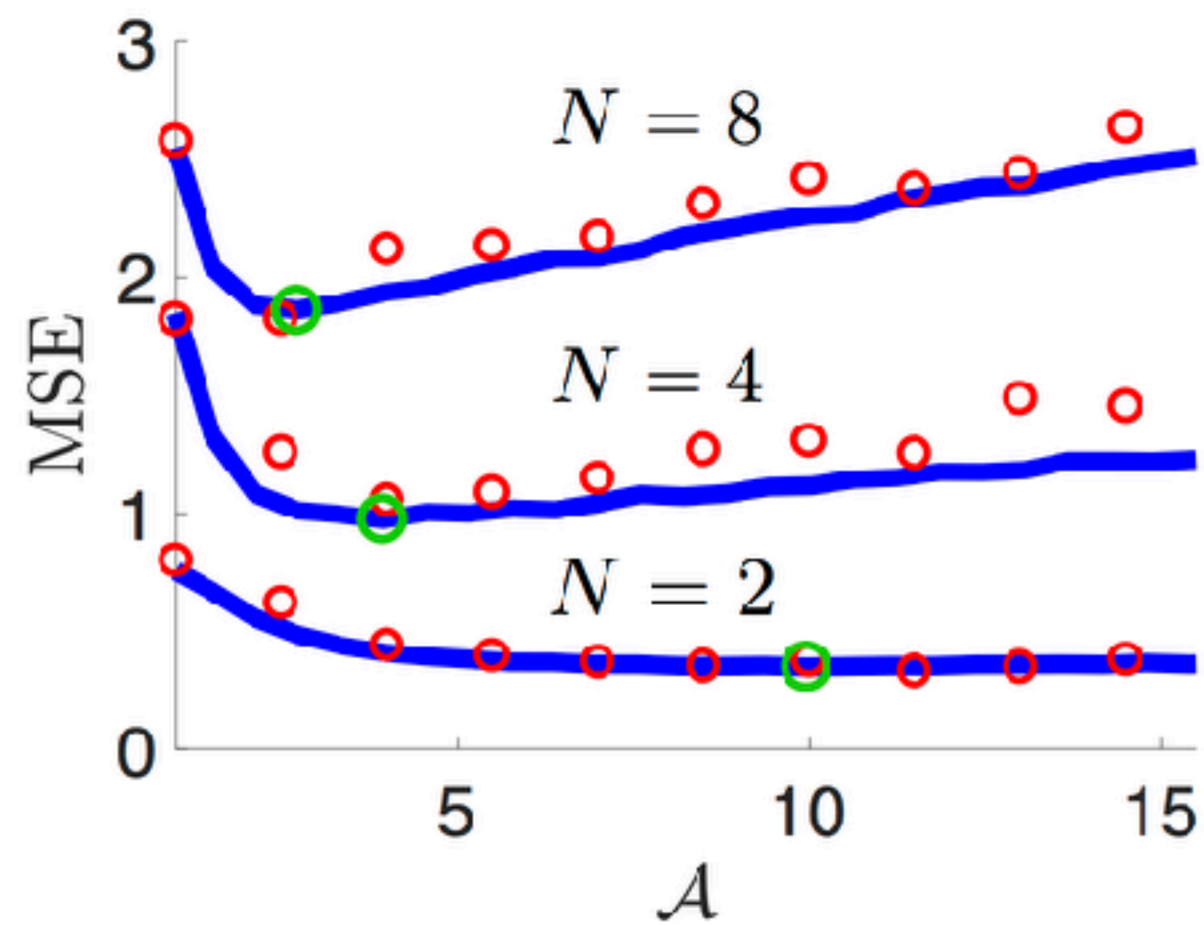

Summary and conclusions

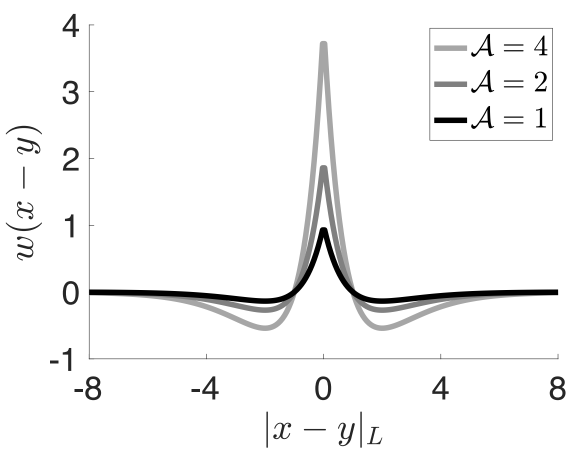

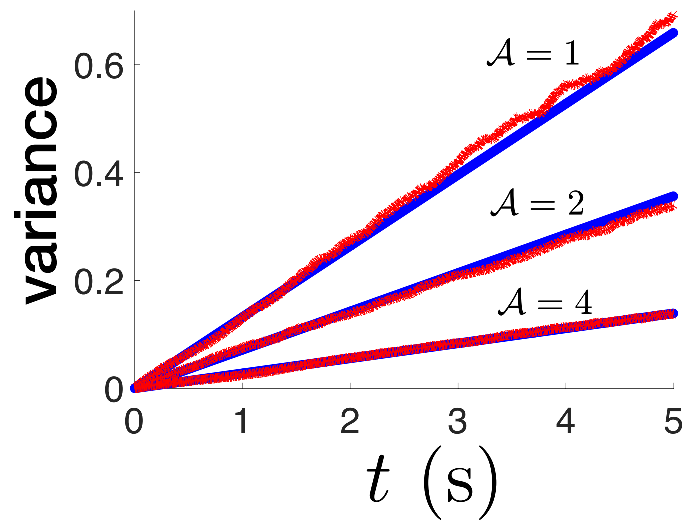

increasing synaptic strength $\mathcal{A}$ leads to decrease in variance for a single bump

N Krishnan, DB Poll, and ZP Kilpatrick. *Interacting bumps model of item limits in working memory. arXiv:1710.11612* (2017).

Summary and conclusions

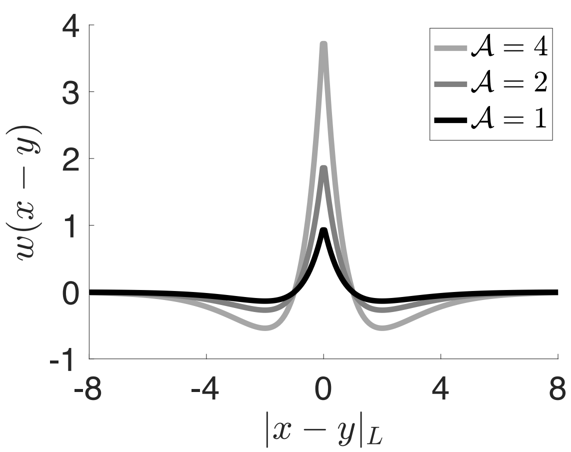

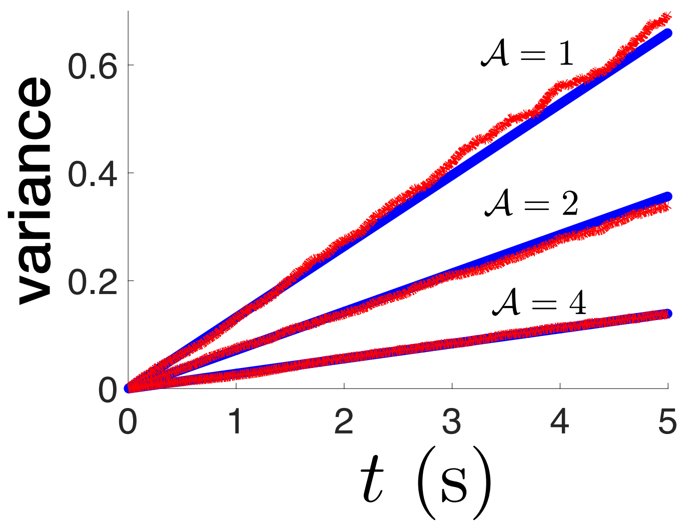

increasing synaptic strength $\mathcal{A}$ leads to decrease in variance for a single bump

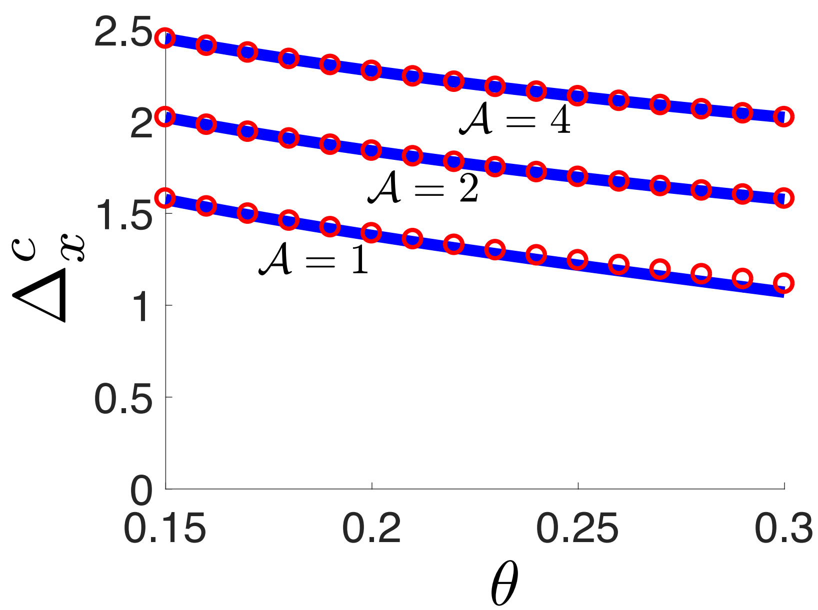

increasing synaptic strength $\mathcal{A}$ leads to wider range of attraction/repulsion for multiple bumps

N Krishnan, DB Poll, and ZP Kilpatrick. *Interacting bumps model of item limits in working memory. arXiv:1710.11612* (2017).

Summary and conclusions

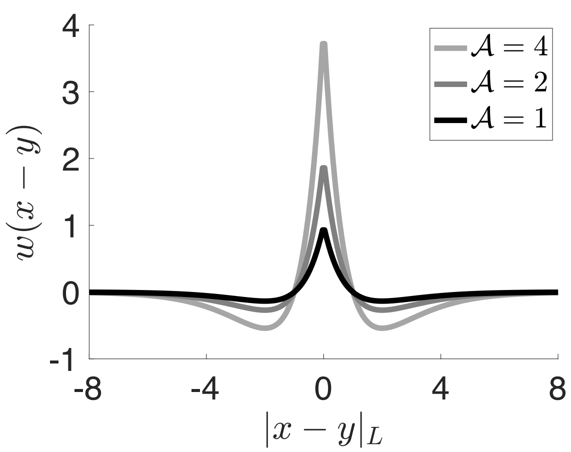

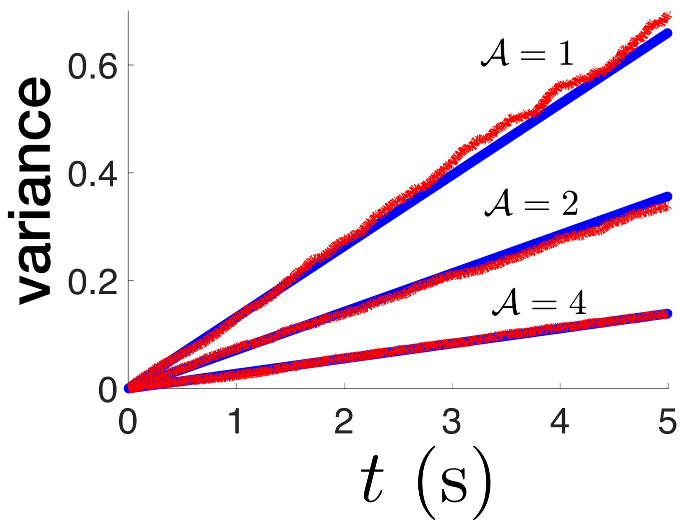

increasing synaptic strength $\mathcal{A}$ leads to decrease in variance for a single bump

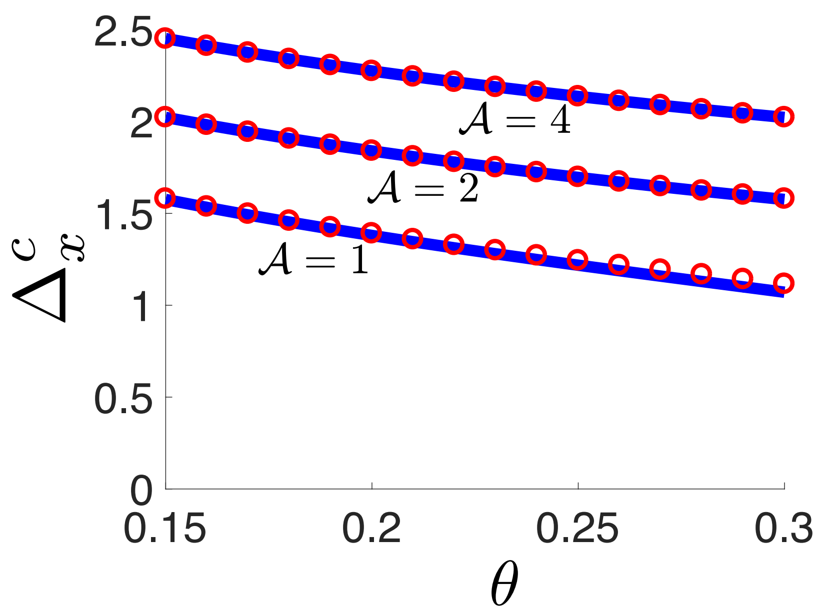

increasing synaptic strength $\mathcal{A}$ leads to wider range of attraction/repulsion for multiple bumps

the optimal $\mathcal{A}$ minimizes MSE by trading off fluctuation and bump-interaction errors

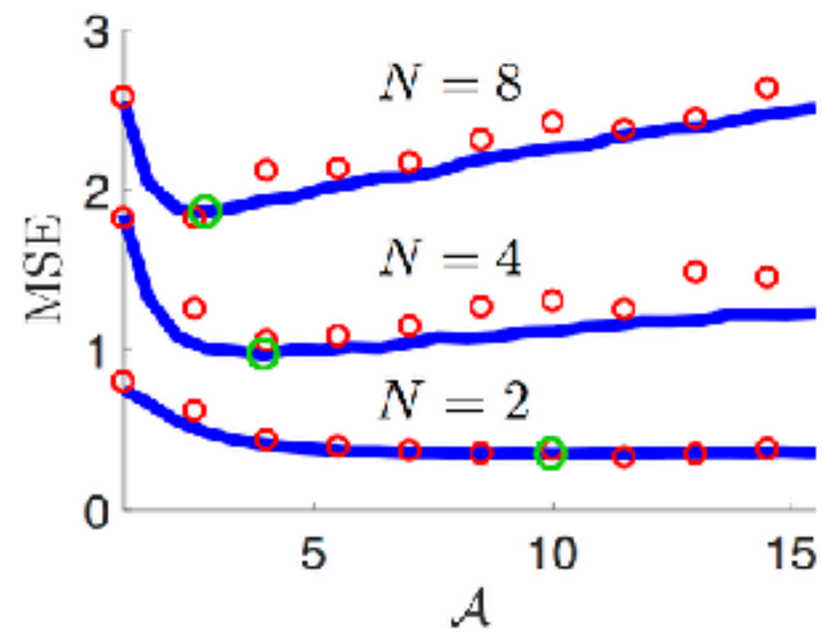

N Krishnan, DB Poll, and ZP Kilpatrick. *Interacting bumps model of item limits in working memory. arXiv:1710.11612* (2017).

Memory-guided search: examples

A

It is, of course, an indispensable part of a scrivener's business to verify the accuracy of his copy, word by word. Where there are two or more scriveners in an office, they assist each other in this examination, one reading from the copy, the other holding the original. It is a very dull, wearisome, and lethargic affair. I can readily imagine that to some sanguine temperaments it would be altogether intolerable.

B

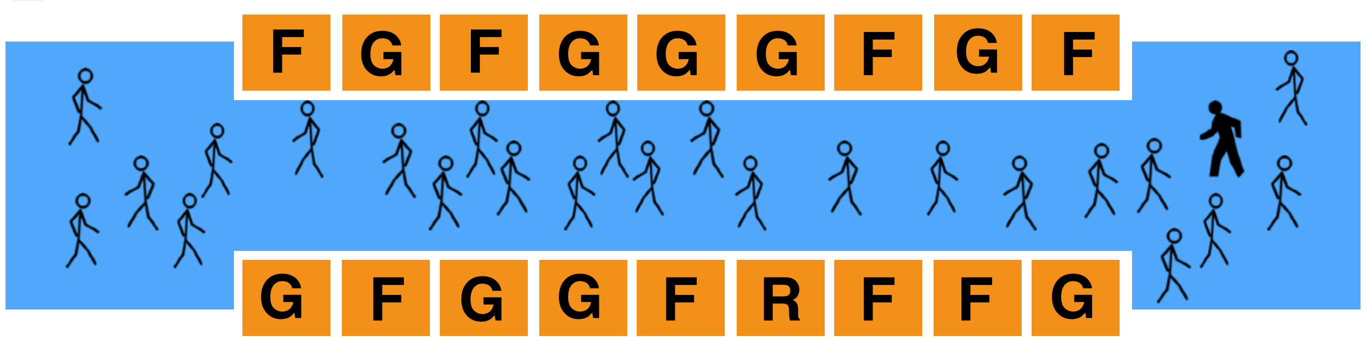

C

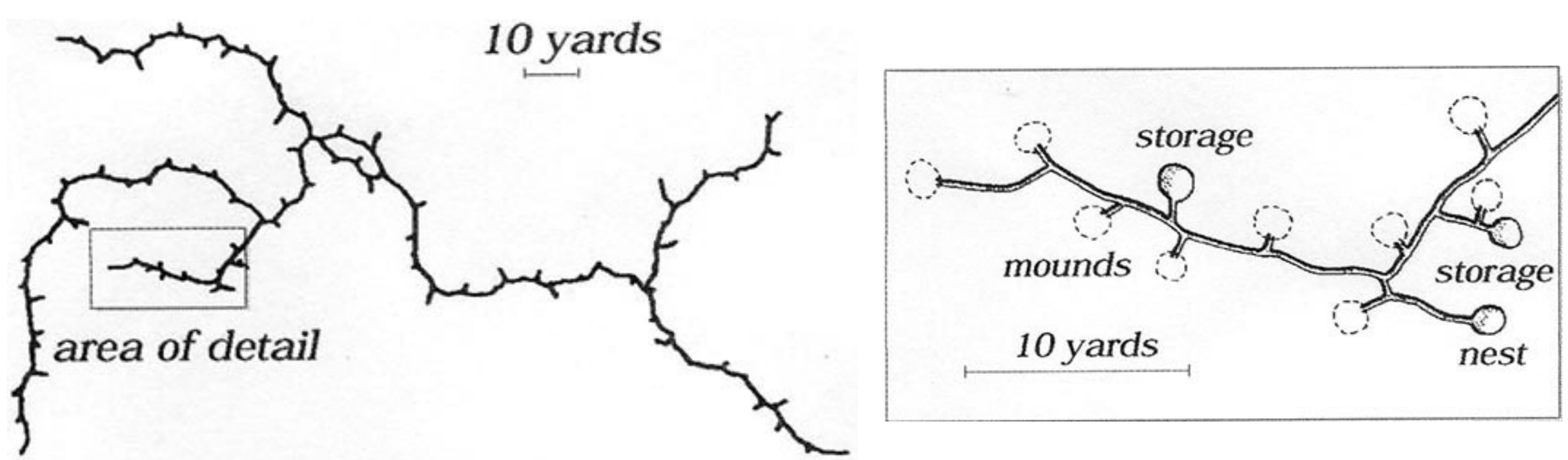

D

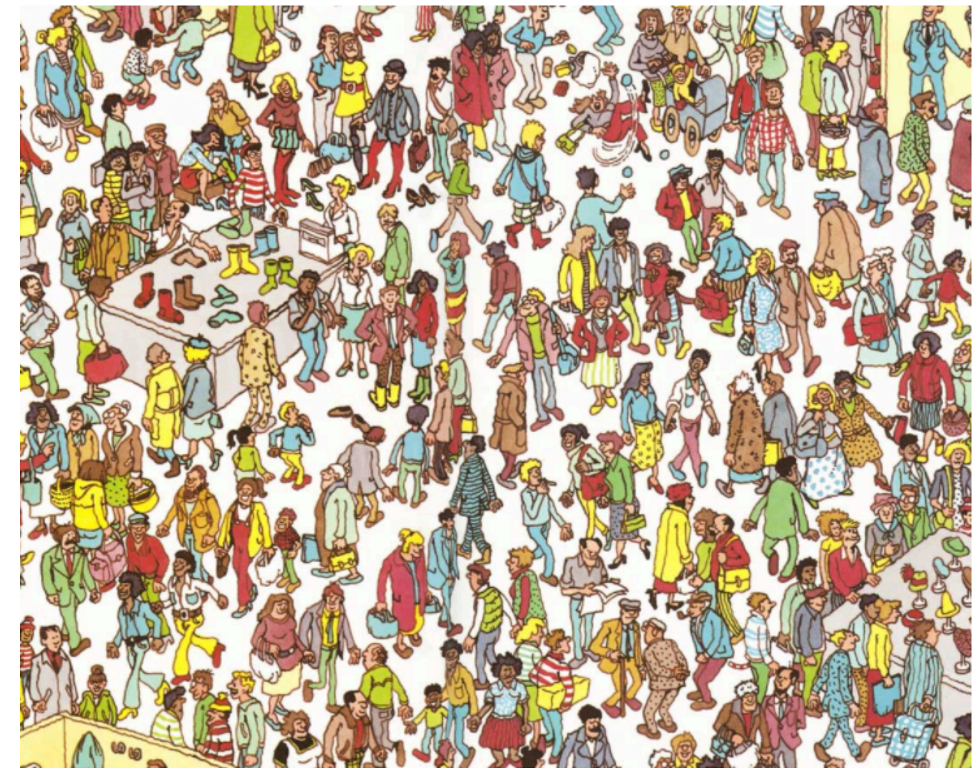

E

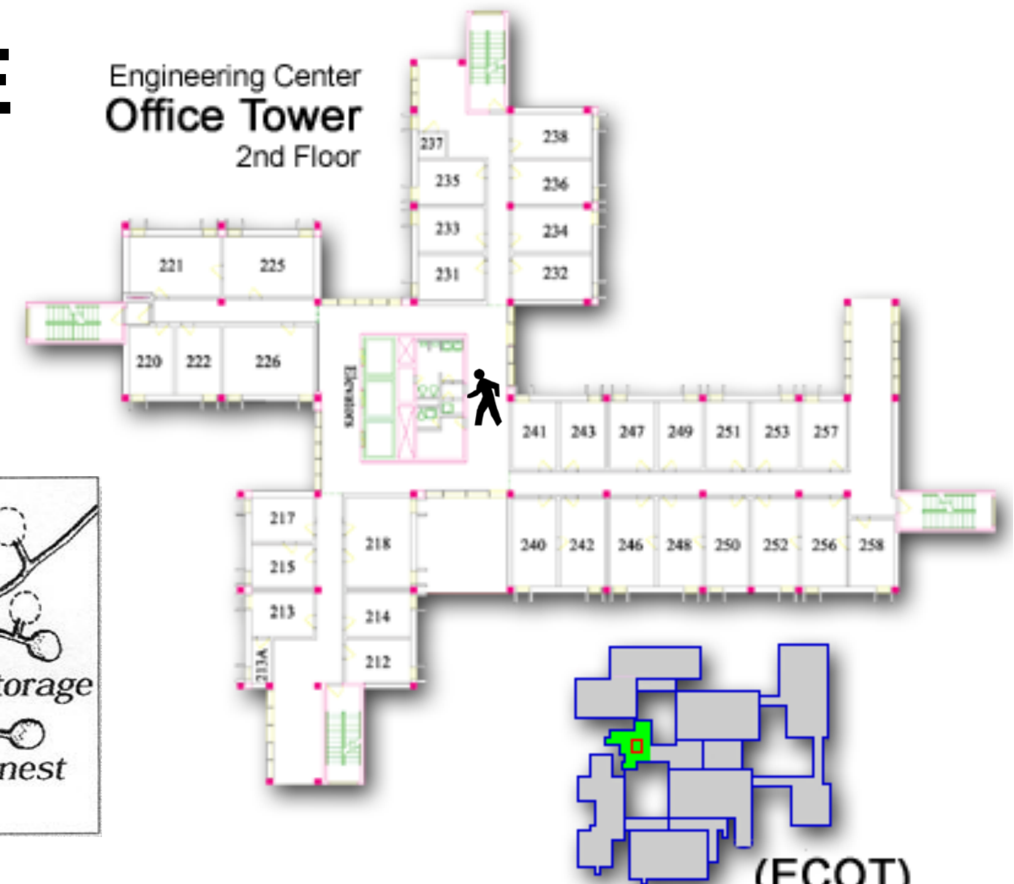

(Kilpatrick & Poll 2017)

Search strategies

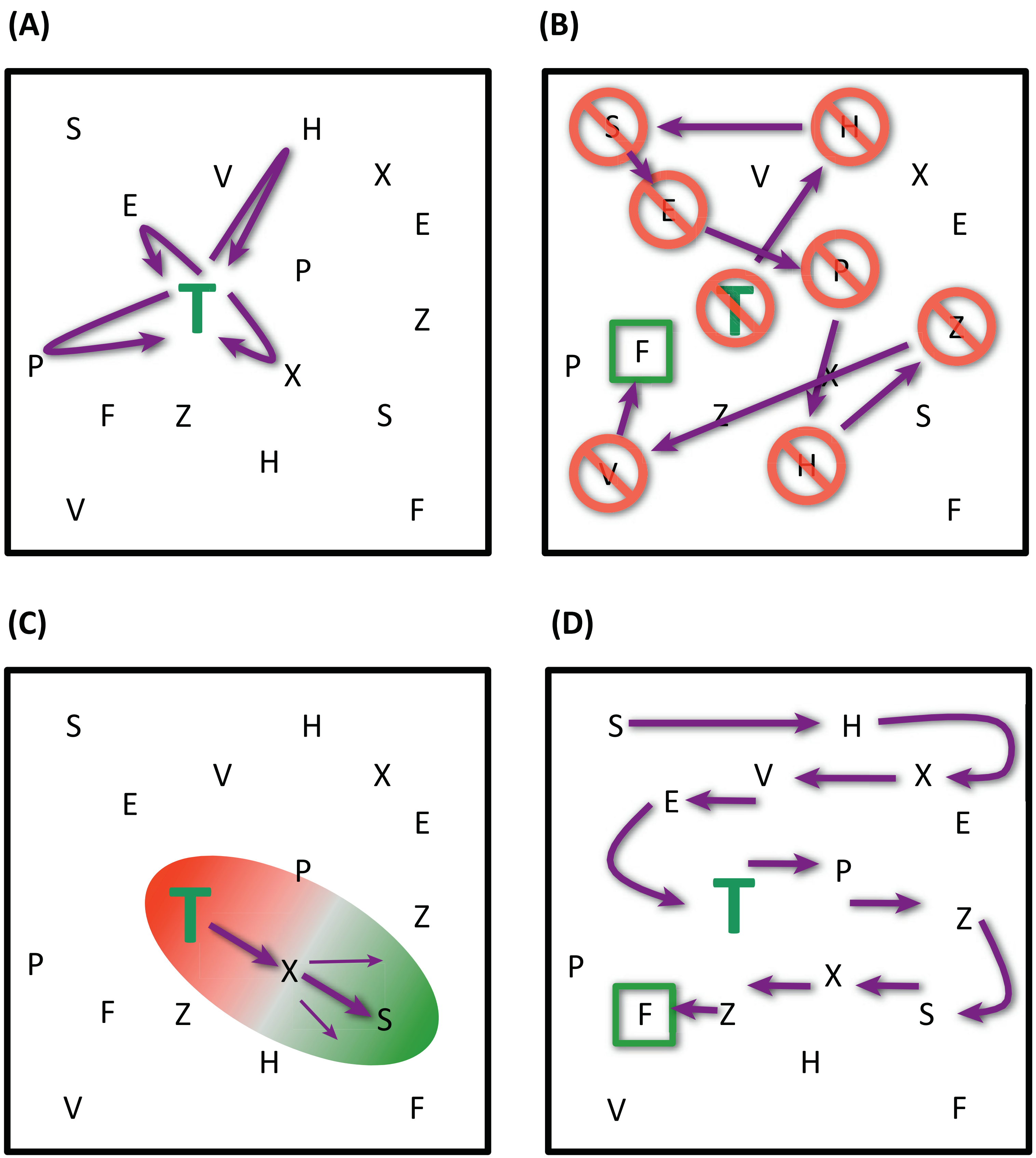

(Hills et al 2015)

- **A**: fixate on salient images
- **B**: ***inhibition-of-return***
- **C**: ***exploration bias***
- **D**: “lawnmower” or “boustrophedonic” strategy

Neural field model of memory-guided search

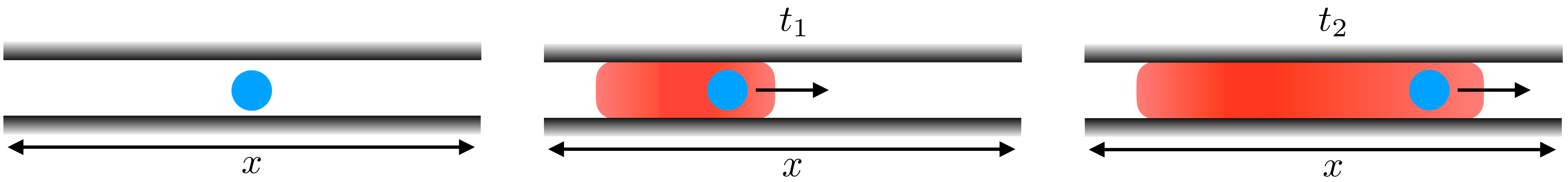

Neural field model of memory-guided search

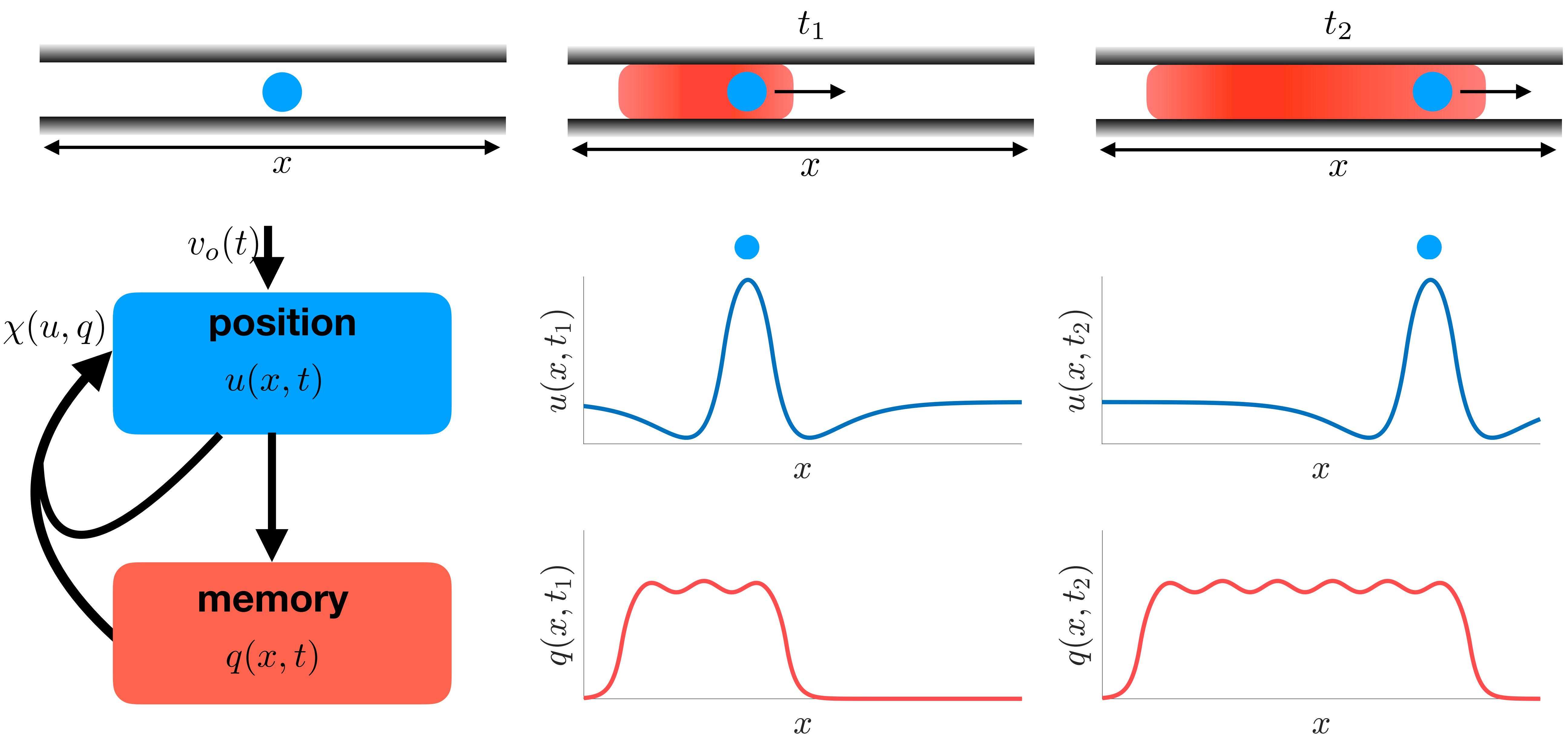

Neural field model of memory-guided search

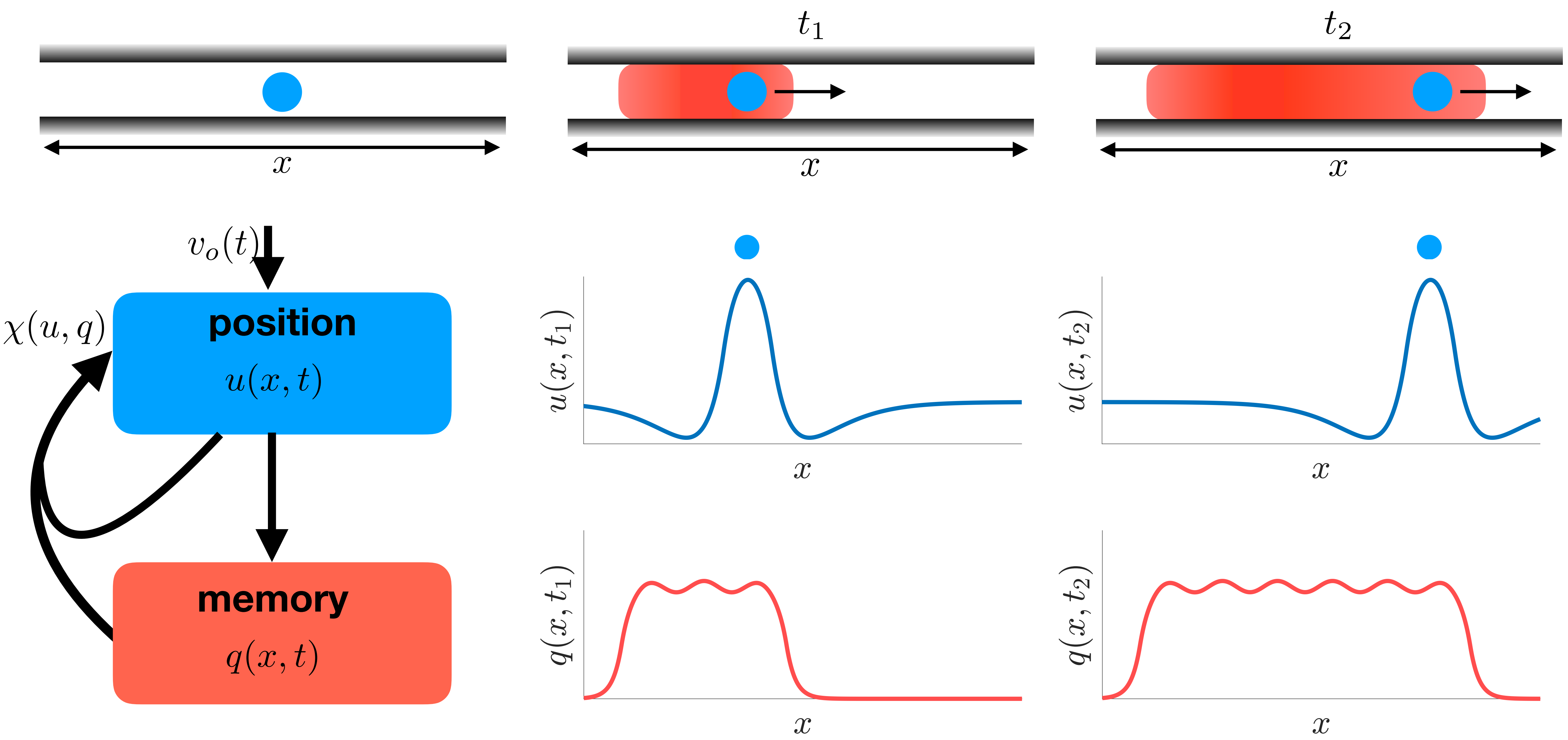

velocity integration

$$u_t = -u + \int_{-L}^{L} \left[w_u(x-y) - v(t) w_u'(x-y) \right] H(u(y,t) - \theta_u) \mathrm{d}y$$

$$q_t = -q + \underbrace{\int_{-L}^{L} w_q(x,y) H(q(y,t) - \theta_q) \mathrm{d}y}_{\text{local connectivity}} + \underbrace{\int_{-L}^{L} w_p(x-y) H(u(y,t) - \theta_u) \mathrm{d}y}_{\text{input from position layer}}$$

Stationary solutions depend on input from position layer

can the memory layer remember visited locations? analyze stationary solns for $v(t) \equiv 0$

$$U(x) = \int_a^b w_u(x-y)\mathrm{d}y$$

$$Q(x) = \int_c^d w_q(x,y)\mathrm{d}y + \int_a^b w_p(x-y)\mathrm{d}y$$

a, b
bump interfaces

c, d
front interfaces

Stationary solutions depend on input from position layer

can the memory layer remember visited locations? analyze stationary solns for $v(t) \equiv 0$

$$U(x) = \int_a^b w_u(x-y)\mathrm{d}y$$

$$Q(x) = \int_c^d w_q(x,y)\mathrm{d}y + \int_a^b w_p(x-y)\mathrm{d}y$$

a, b
bump interfaces

c, d
front interfaces

lateral inhibitory

$$w_u(x) = (1-|x|)\mathrm{e}^{-|x|}$$

locally excitatory

$$w_p(x) = I_0 \frac{\alpha \mathrm{e}^{-\alpha|x|}}{2}$$

$$w_q(x,y) = [1+\sigma\cos(ny)] \cdot \frac{\mathrm{e}^{-|x-y|}}{2}$$

reflects spatial heterogeneity of cortical regions encoding position

Stationary solutions depend on input from position layer

can the memory layer remember visited locations? analyze stationary solns for $v(t) \equiv 0$

$$U(x) = \int_a^b w_u(x-y)\mathrm{d}y$$

$$Q(x) = \int_c^d w_q(x,y)\mathrm{d}y + \int_a^b w_p(x-y)\mathrm{d}y$$

a, b
bump interfaces

c, d
front interfaces

lateral inhibitory

$$w_u(x) = (1-|x|)\mathrm{e}^{-|x|}$$

locally excitatory

$$w_p(x) = I_0 \frac{\alpha \mathrm{e}^{-\alpha|x|}}{2}$$

$$w_q(x,y) = [1+\sigma\cos(ny)] \cdot \frac{\mathrm{e}^{-|x-y|}}{2}$$

reflects spatial heterogeneity of cortical regions encoding position

threshold conditions (self-consistency):

$$U(a) = U(b) = \theta_u,$$

$$Q(c) = Q(d) = \theta_q,$$

evaluated to produce bifurcation plots

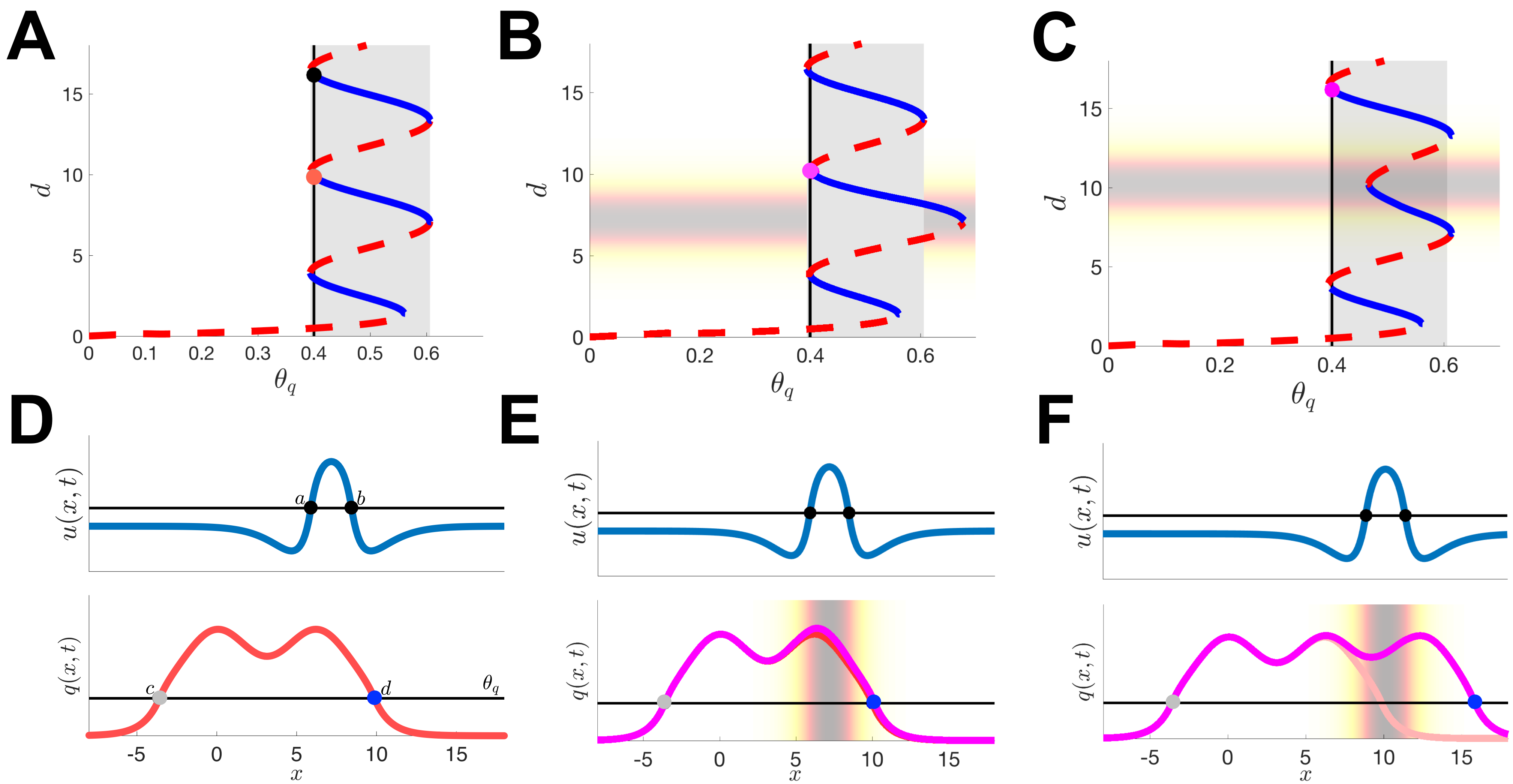

Critical input to propagate the front forward

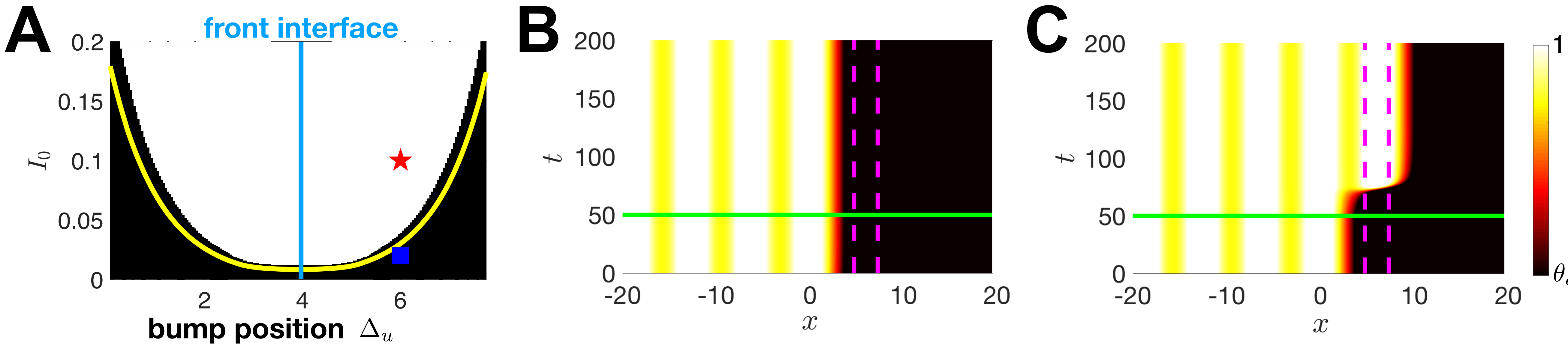

require that $I_0 > I_0^c$ which can be determined by simplifying the threshold equations

$$I_0^c = \frac{2n\sigma}{\alpha(n^2+1)} \cdot \frac{\sin(nd^c) - n\cos(nd^c)}{\mathrm{e}^{-\alpha|d^c-a|} - \mathrm{e}^{-\alpha|d^c-b|}}$$

where d^c is the location of the right front interface at the saddle-node bifurcation

Critical input to propagate the front forward

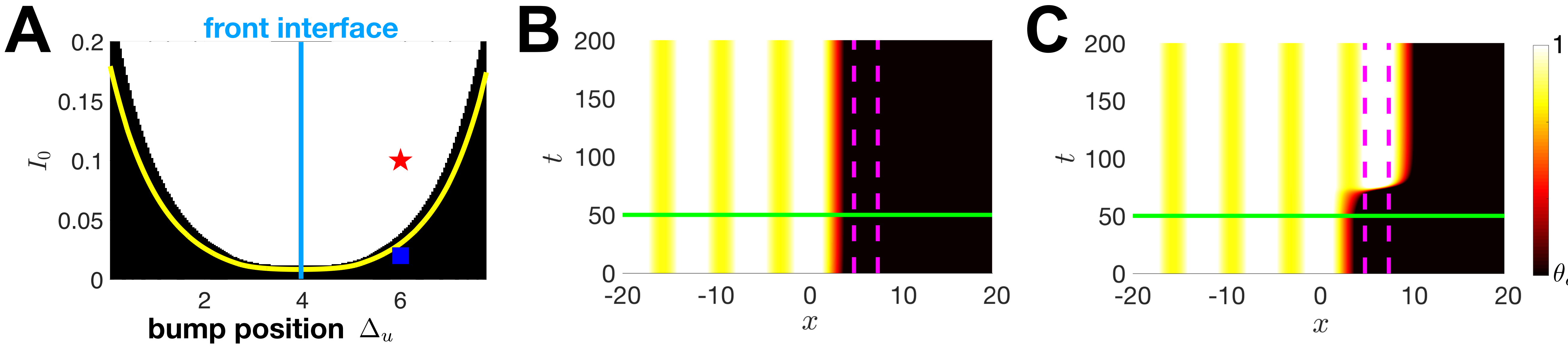

require that $I_0 > I_0^c$ which can be determined by simplifying the threshold equations

$$I_0^c = \frac{2n\sigma}{\alpha(n^2+1)} \cdot \frac{\sin(nd^c) - n\cos(nd^c)}{\mathrm{e}^{-\alpha|d^c-a|} - \mathrm{e}^{-\alpha|d^c-b|}}$$

where d^c is the location of the right front interface at the saddle-node bifurcation

stability is determined by projecting the associated eigenvalue problem to the interfaces

$$u(x,t) = U(x) + \psi(x,t), \;\; q(x,t) = Q(x) + \phi(x,t)$$

$$(\lambda+1)\psi(a) = \gamma_a\left[w_u(0)\psi(a) + w_u(b-a)\psi(b)\right],$$

$$(\lambda+1)\psi(b) = \gamma_a\left[w_u(b-a)\psi(a) + w_u(0)\psi(b)\right].$$

$$(\lambda+1)\phi(c) = \gamma_c w_q(c,c)\phi(c) + \gamma_d w_q(c,d)\phi(d),$$

$$(\lambda+1)\phi(d) = \gamma_c w_q(d,c)\phi(c) + \gamma_d w_q(d,d)\phi(d),$$

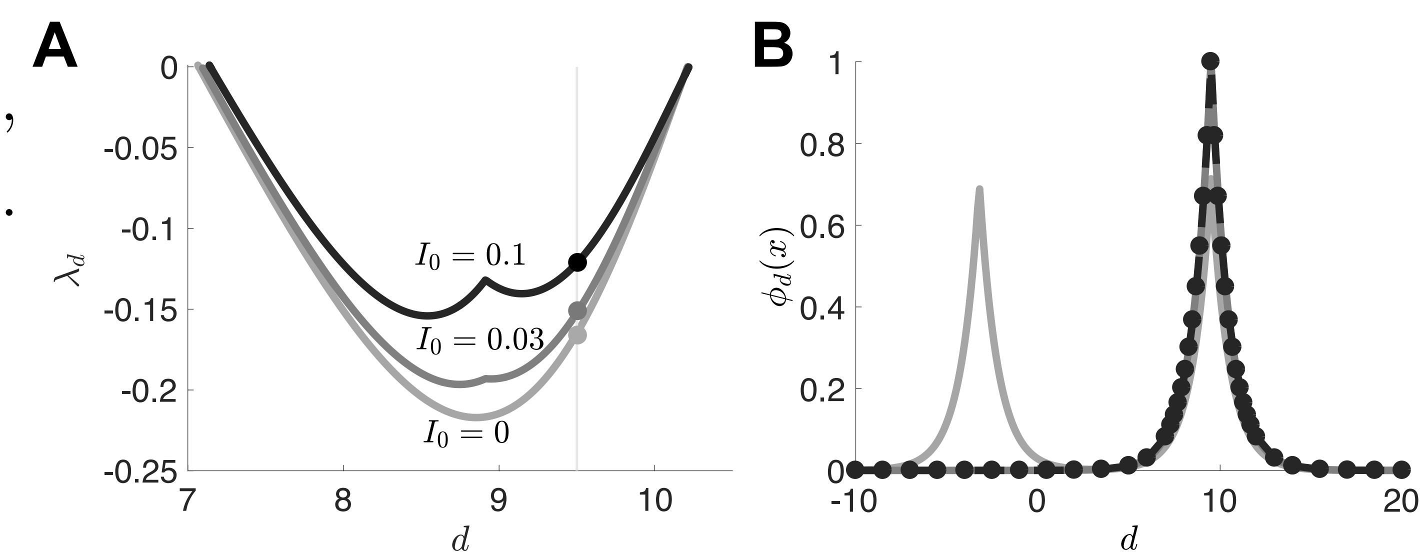

Low-dimensional dynamics via interface methods

idea: $u_t = -u + \int_{-\infty}^{\infty} w_u(x-y) H(u(y,t) - \theta_u) \mathrm{d}y$

has dynamics determined by where

$$u(x_j(t), t) = \theta_u$$

Low-dimensional dynamics via interface methods

idea: $u_t = -u + \int_{-\infty}^{\infty} w_u(x-y) H(u(y,t)-\theta_u)\mathrm{d}y$

has dynamics determined by where

$$u(x_j(t),t) = \theta_u$$

take

$$u_t + u = \int_{A_u(t)} w_u(x-y)\mathrm{d}y - v(t)\int_{A_u(t)} w_u'(x-y)\mathrm{d}y,$$

$$q_t + q = \int_{A_q(t)} w_q(x,y)\mathrm{d}y + \int_{A_u(t)} w_p(x-y)\mathrm{d}y$$

with **active regions**

$$A_u(t) = (x_-(t), x_+(t)),$$

$$A_q(t) = (\Delta_-(t), \Delta_+(t))$$

Low-dimensional dynamics via interface methods

idea: $u_t = -u + \int_{-\infty}^{\infty} w_u(x-y)H(u(y,t)-\theta_u)\mathrm{d}y$ has dynamics determined by where $u(x_j(t),t) = \theta_u$

take

$$u_t + u = \int_{A_u(t)} w_u(x-y)\mathrm{d}y - v(t)\int_{A_u(t)} w_u'(x-y)\mathrm{d}y,$$

$$q_t + q = \int_{A_q(t)} w_q(x,y)\mathrm{d}y + \int_{A_u(t)} w_p(x-y)\mathrm{d}y$$

with **active regions**

$$A_u(t) = (x_-(t), x_+(t)),$$
$$A_q(t) = (\Delta_-(t), \Delta_+(t))$$

derive dynamics of interfaces:

$$\dot{\Delta}_+ = S(\Delta_+) + C(\Delta_+) + G(\Delta_+ - \Delta_u)$$
$$\dot{\Delta}_- = S(\Delta_-) - C(\Delta_-) - G(\Delta_- - \Delta_u)$$

where $\Delta_u(t) = \int_0^t v(s)\mathrm{d}s$ is centroid of bump position

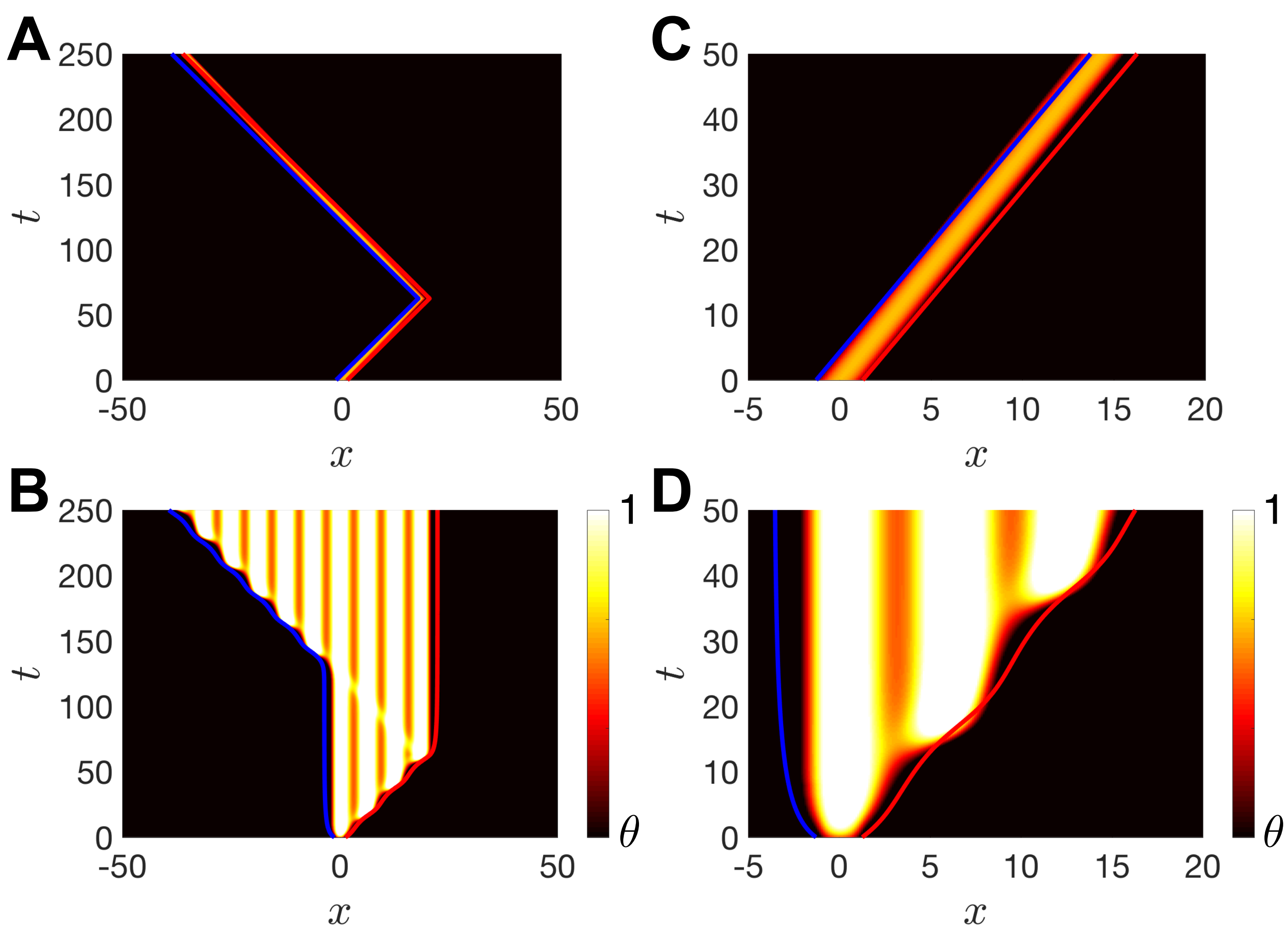

interfaces track bump position as well as expanding front locations

Memory-guided control of search

motor system guides search according to control feedback $v(t) = \chi(u(x,t), q(x,t))$

consider $\tau_\chi \dot{\chi}(t) = 2\langle H(u-\theta_u), H(q-\theta_q)\rangle(\chi_+ - \chi(t)) - \langle H(u-\theta_u)\rangle(\chi_- - \chi(t))$

leads to $v(t) \to v_0$ in novel environments, $v(t) \to v_1$ in searched environments

Memory-guided control of search

motor system guides search according to control feedback $v(t) = \chi(u(x,t), q(x,t))$

consider $\tau_\chi \dot{\chi}(t) = 2\langle H(u-\theta_u), H(q-\theta_q)\rangle(\chi_+ - \chi(t)) - \langle H(u-\theta_u)\rangle(\chi_- - \chi(t))$

leads to $v(t) \to v_0$ in novel environments, $v(t) \to v_1$ in searched environments

on a single track with a hidden target

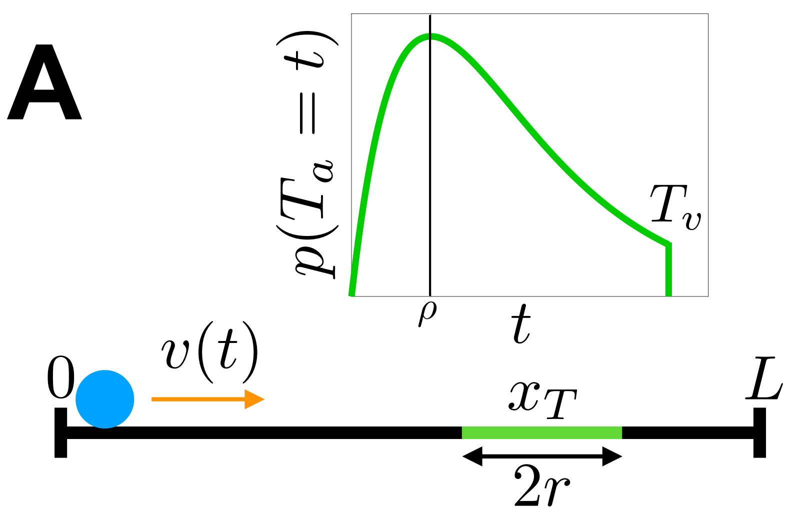

waiting time to discover while over target $\rho^2 t \mathrm{e}^{-\rho t}$

probability of finding on a single visit $P_v = 1 - (1 + \rho T_v)\mathrm{e}^{-\rho T_v}$

Memory-guided control of search

motor system guides search according to control feedback $v(t) = \chi(u(x,t), q(x,t))$

consider $\tau_\chi \dot{\chi}(t) = 2\langle H(u-\theta_u), H(q-\theta_q)\rangle(\chi_+ - \chi(t)) - \langle H(u-\theta_u)\rangle(\chi_- - \chi(t))$

leads to $v(t) \to v_0$ in novel environments, $v(t) \to v_1$ in searched environments

on a single track with a hidden target

waiting time to discover while over target $\rho^2 t \mathrm{e}^{-\rho t}$

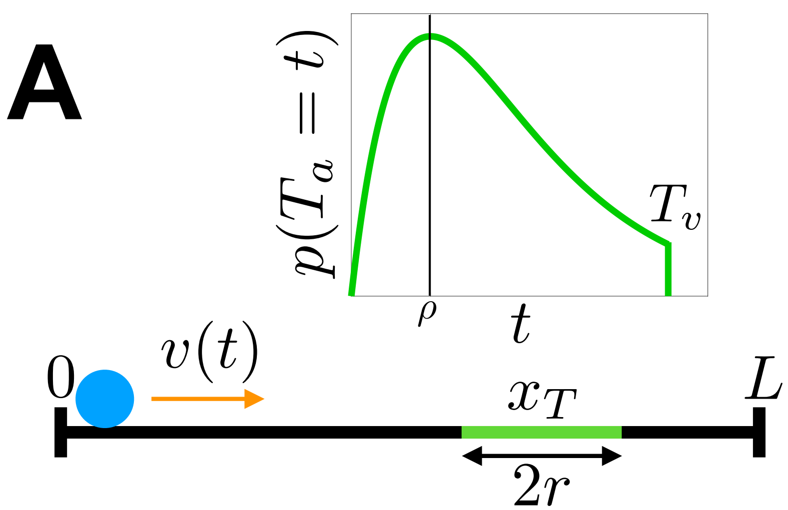

probability of finding on a single visit $P_v = 1 - (1+\rho T_v)\mathrm{e}^{-\rho T_v}$

mean time to find the target

$$\bar{T} = \frac{L-2}{2v_0} + P_{v_0} T_a(v_0) + (1-P_{v_0})\left[\frac{L}{v_1 P_{v_1}} + \left(1+\frac{L}{2}\right)\left(\frac{1}{v_0} - \frac{1}{v_1}\right) + T_a(v_1)\right]$$

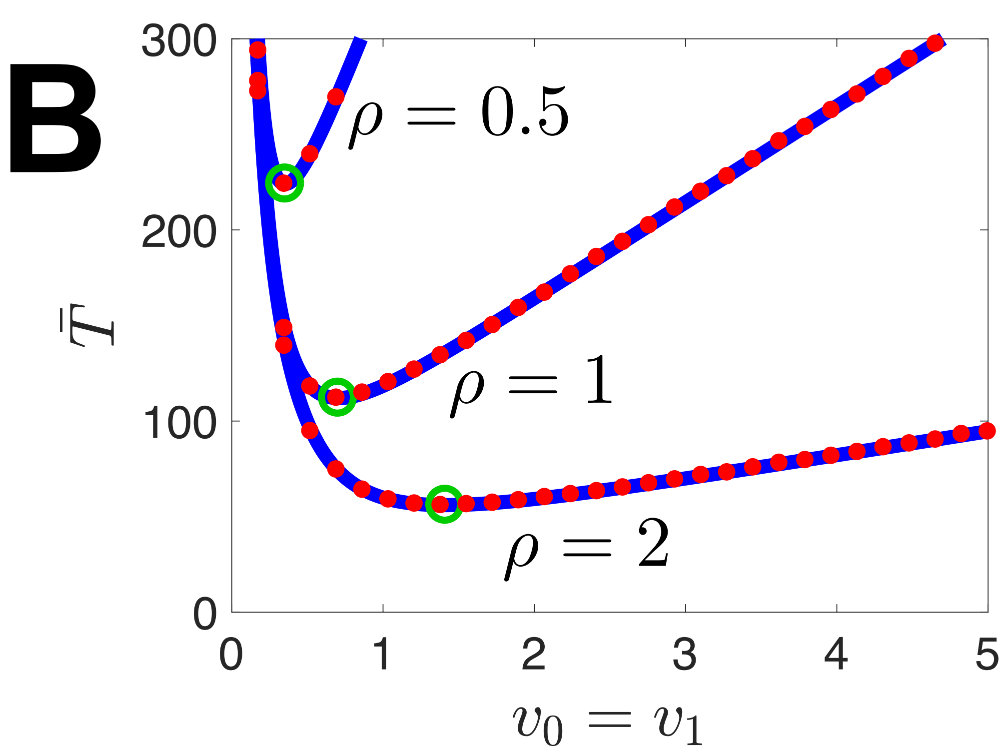

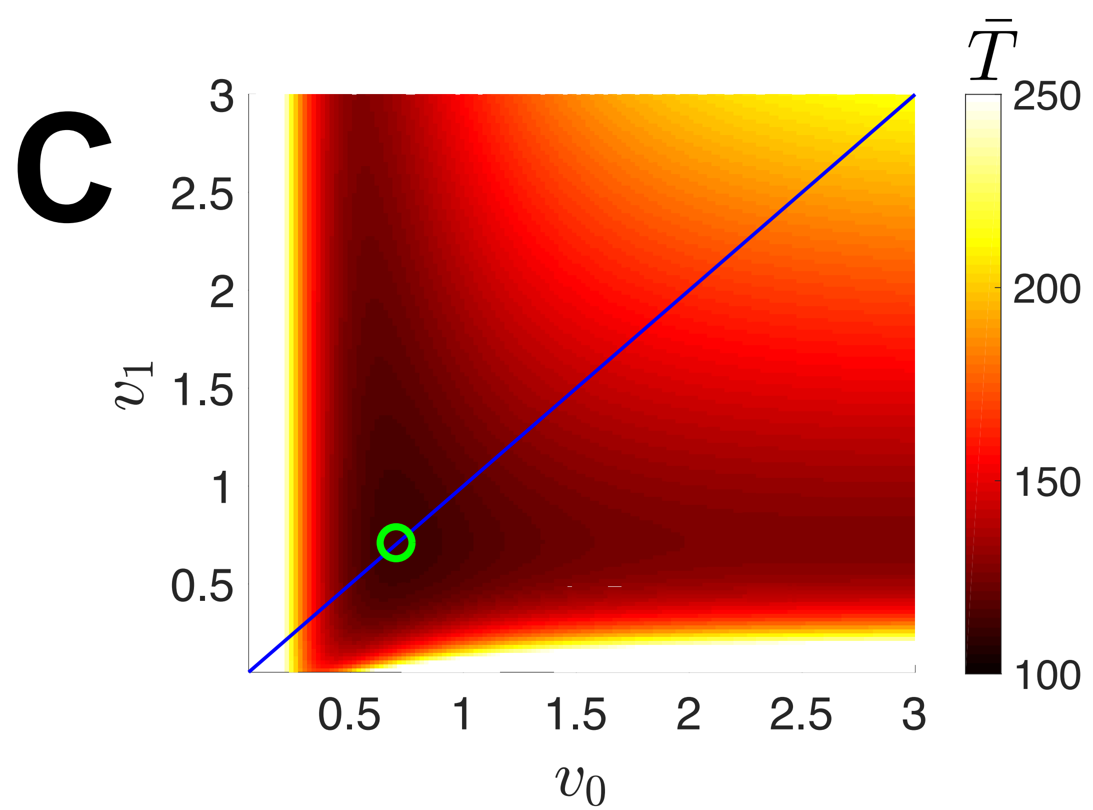

optimal pair

$v_0 \equiv v_1$

IOR has no advantage on single tracks

Inhibition of return in radial arm mazes

A

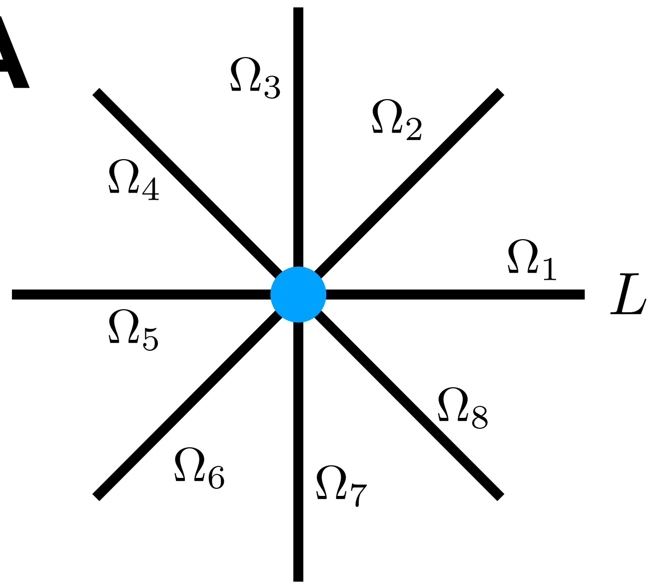

Inhibition of return in radial arm mazes

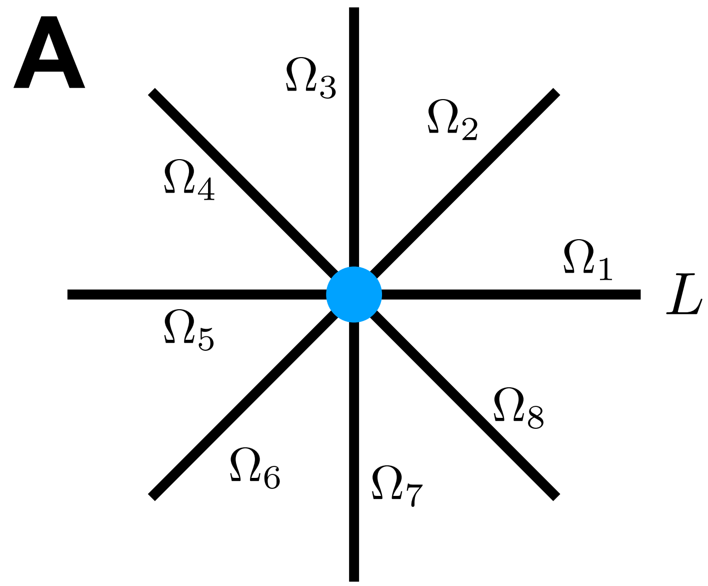

memory population per arm

$$\dot{q}_j(t) = -q_j(t) + H(q_j - \theta_q) + I_j(t)$$

Inhibition of return in radial arm mazes

A

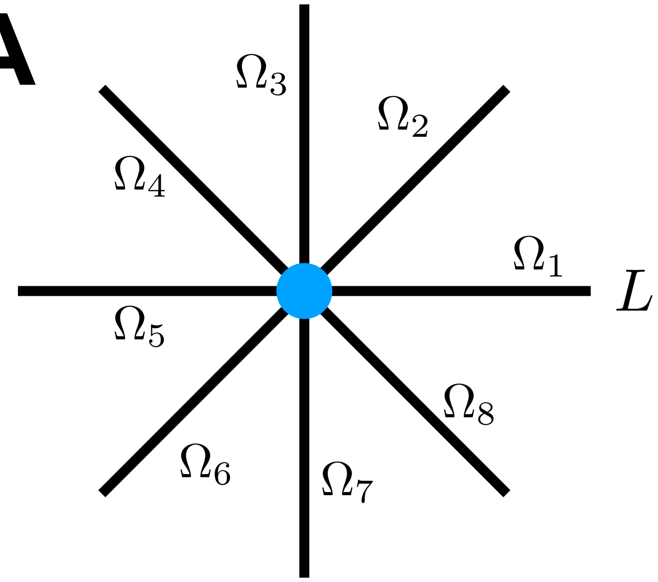

memory population per arm

$$\dot{q}_j(t) = -q_j(t) + H(q_j - \theta_q) + I_j(t)$$

compare random arm selection search strategy to inhibition of return for N arms

$$\bar{T}_{\mathrm{rand}} = \frac{2L(N-1)}{v_0} + \frac{2NL(1-P_{v_0})^2}{P_{v_0}(2-P_{v_0})v_0} + \frac{L(1-P_{v_0})}{(2-P_{v_0})v_0} + \frac{L-2}{2v_0} + T_a(v_0)$$

$$\bar{T}_{\mathrm{IOR}} = \frac{L(N-1)}{v_0} + \frac{2NL(1-P_{v_0})^2}{P_{v_0}(2-P_{v_0})v_0} + \frac{L(1-P_{v_0})}{(2-P_{v_0})v_0} + \frac{L-2}{2v_0} + T_a(v_0)$$

Inhibition of return in radial arm mazes

A

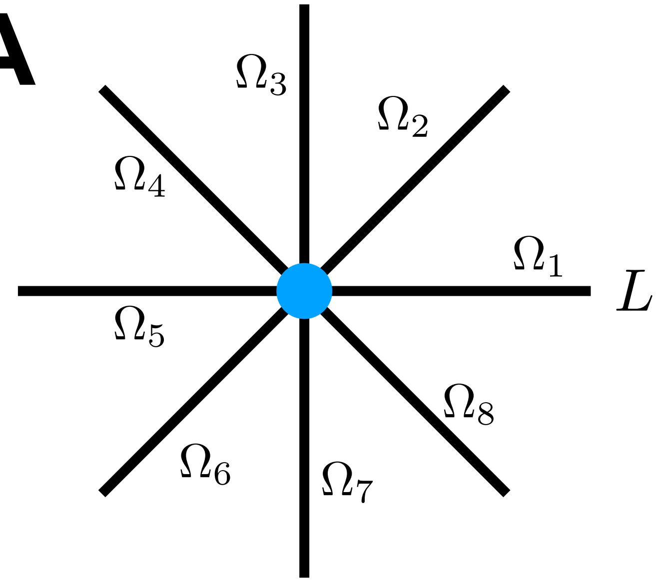

memory population per arm

$$\dot{q}_j(t) = -q_j(t) + H(q_j - \theta_q) + I_j(t)$$

compare random arm selection search strategy to inhibition of return for *N* arms

$$\bar{T}_{\rm rand} = \frac{2L(N-1)}{v_0} + \frac{2NL(1-P_{v_0})^2}{P_{v_0}(2-P_{v_0})v_0} + \frac{L(1-P_{v_0})}{(2-P_{v_0})v_0} + \frac{L-2}{2v_0} + T_a(v_0)$$

$$\bar{T}_{\rm IOR} = \frac{L(N-1)}{v_0} + \frac{2NL(1-P_{v_0})^2}{P_{v_0}(2-P_{v_0})v_0} + \frac{L(1-P_{v_0})}{(2-P_{v_0})v_0} + \frac{L-2}{2v_0} + T_a(v_0)$$

$$\bar{T}_{\rm rand} - \bar{T}_{\rm IOR} = (N-1)\frac{L}{v_0} > 0$$

IOR reduces search time for *N=2* or greater arms

B

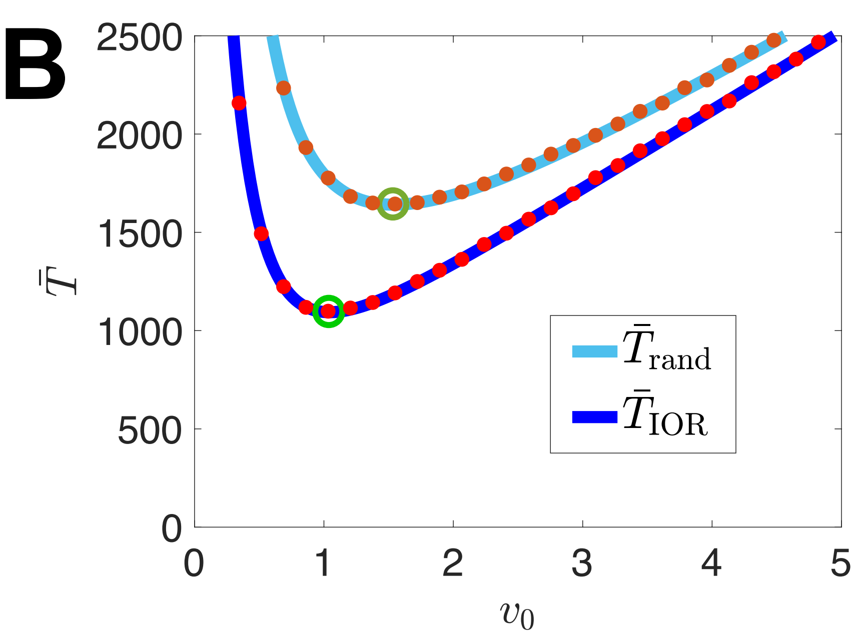

C

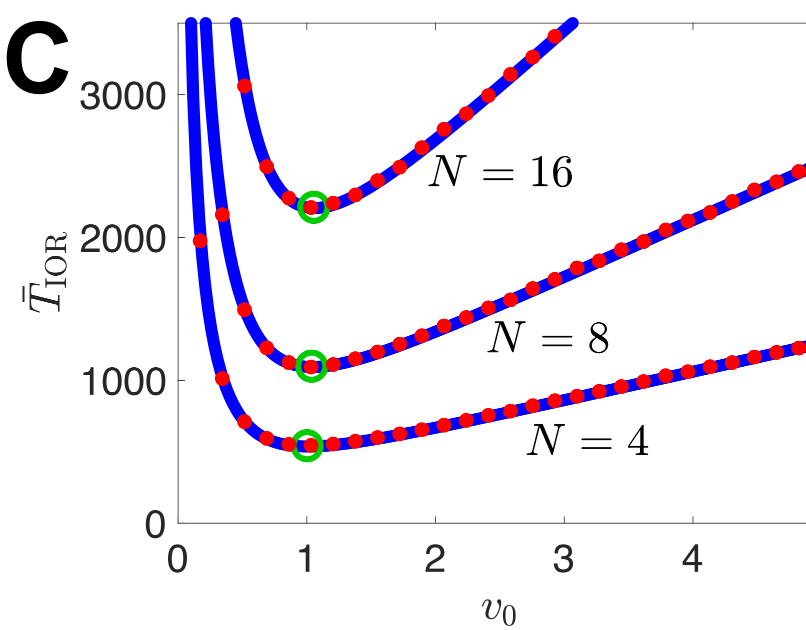

Extensions to two-dimensions

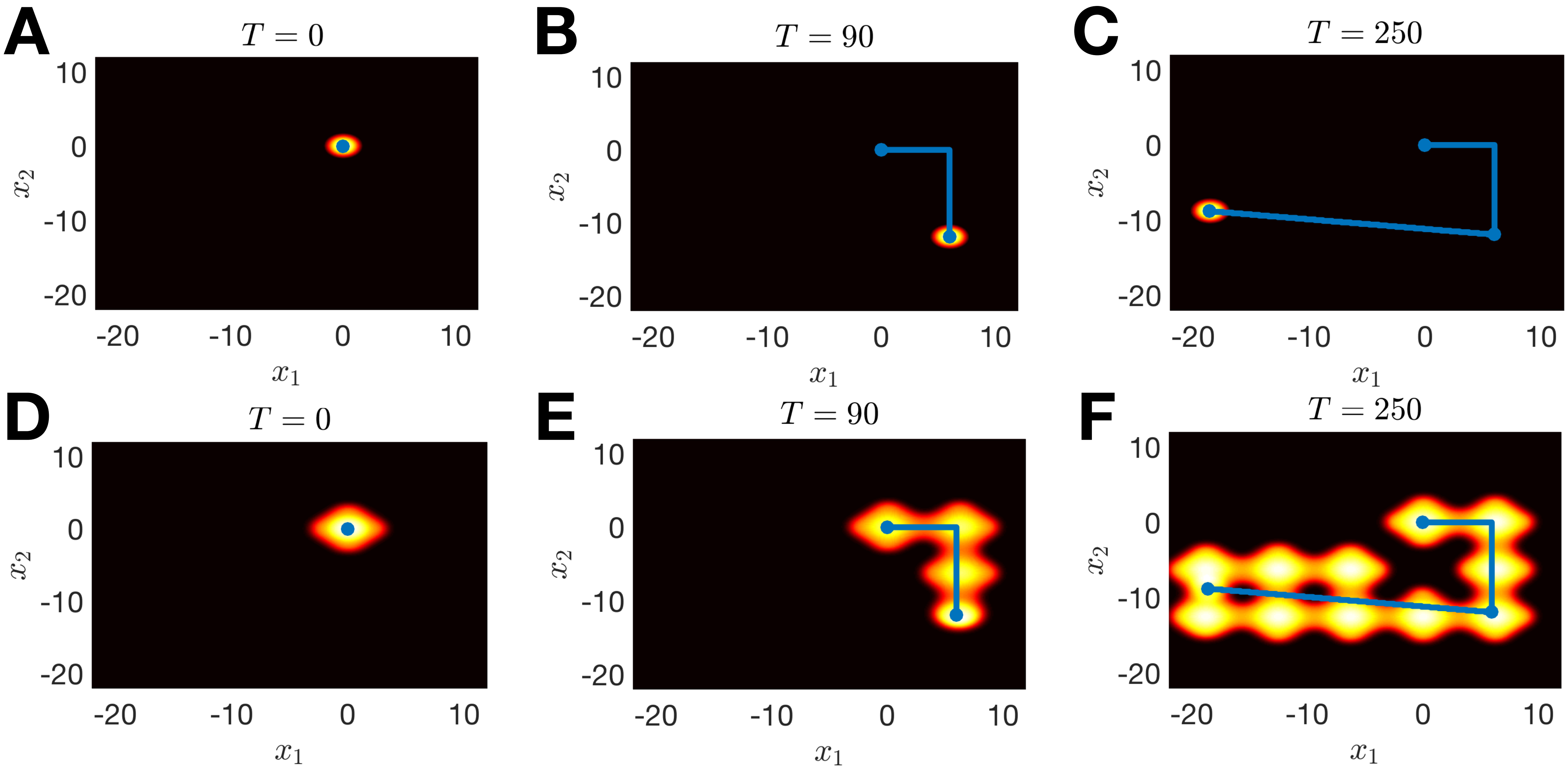

two-dimensional neural field model can track memory

Extensions to two-dimensions

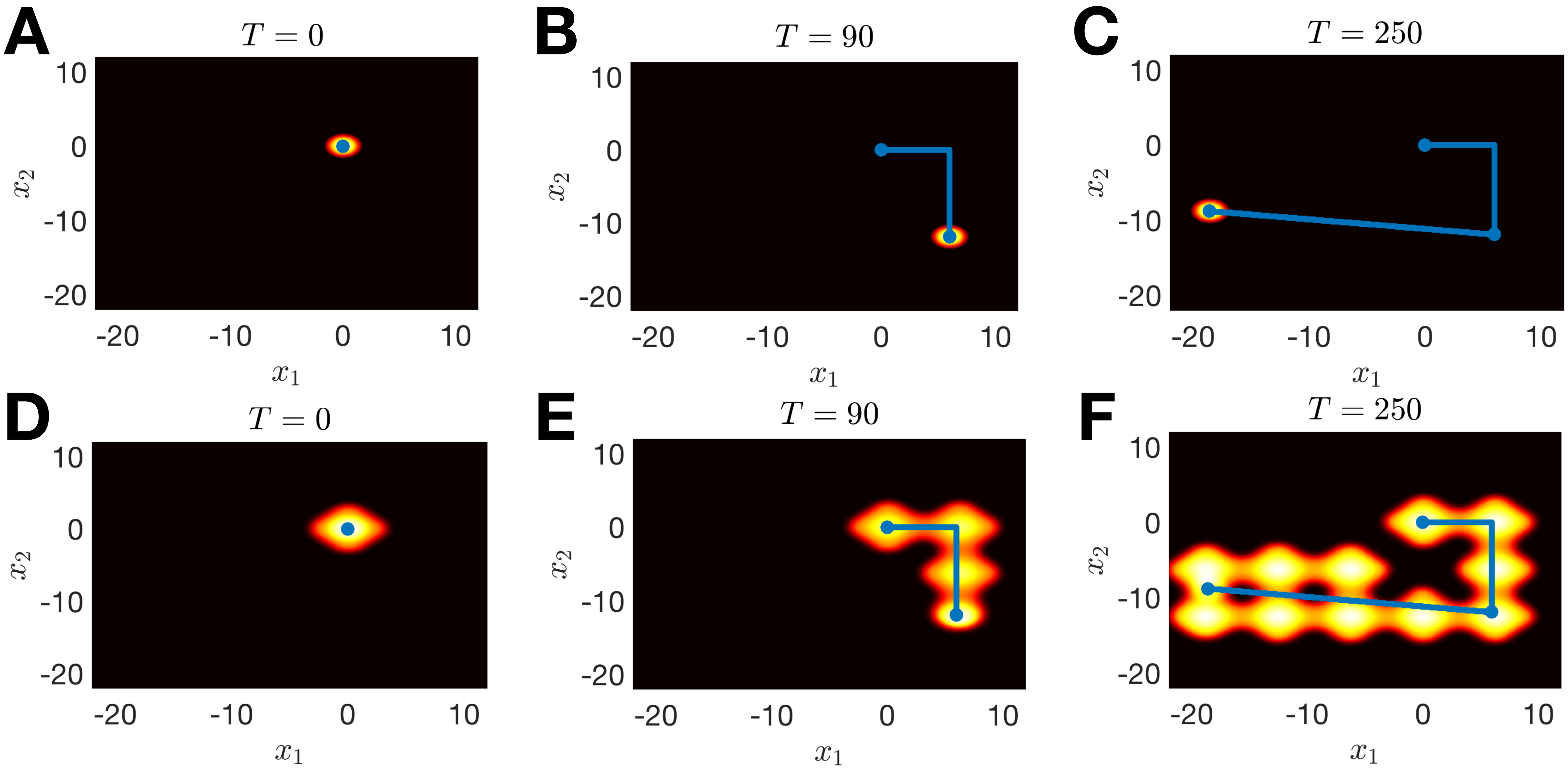

two-dimensional neural field model can track memory

control mechanism could avoid previously visited areas

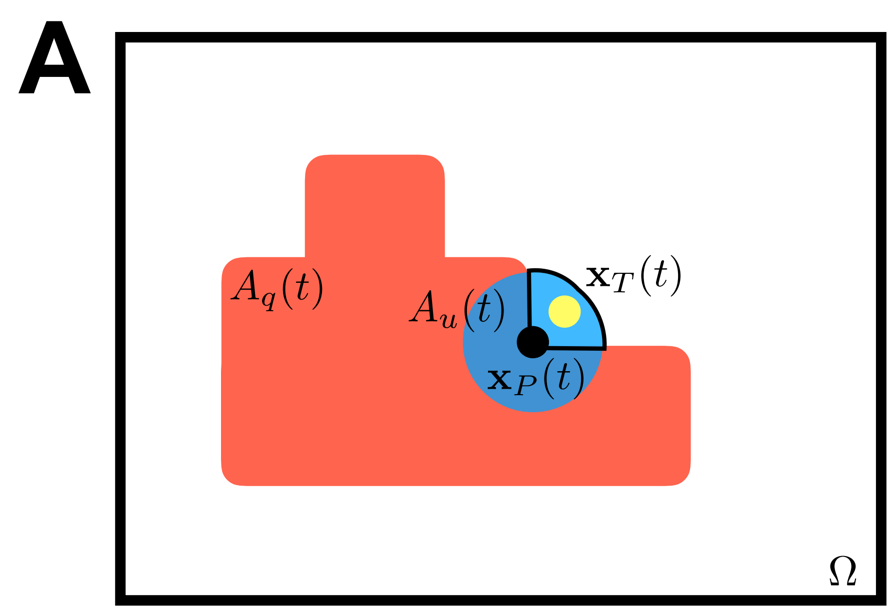

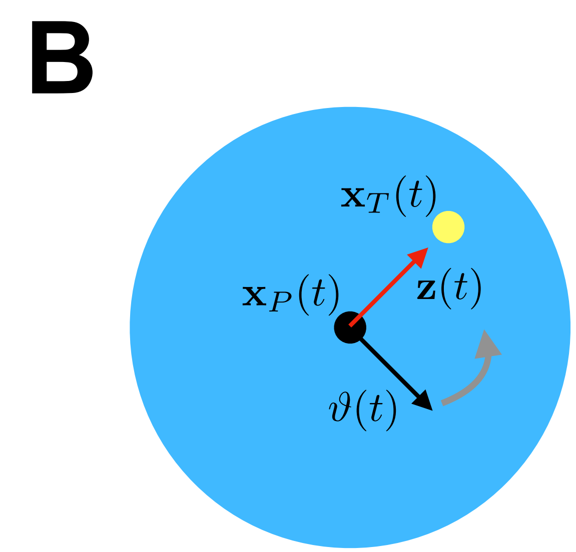

Conclusions

spatiotemporal patterns of neural activity can track current and visited locations

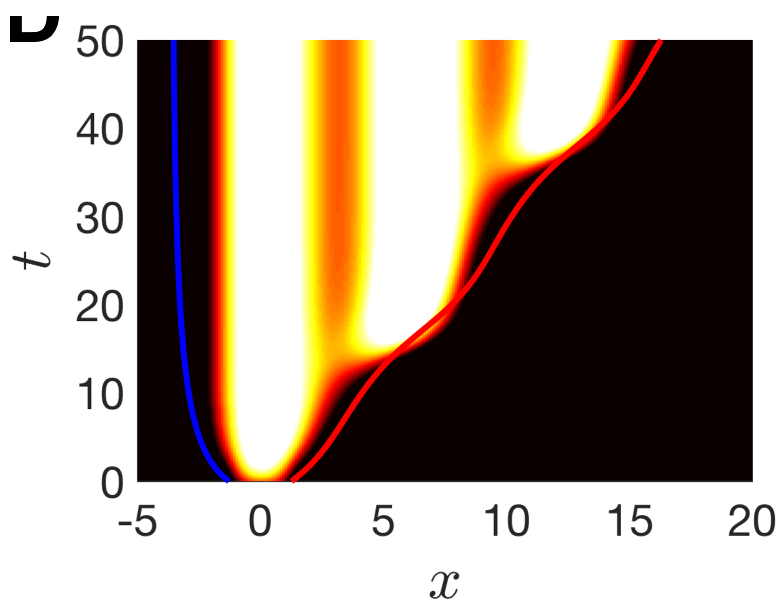

interface equations estimate low-dimensional dynamics

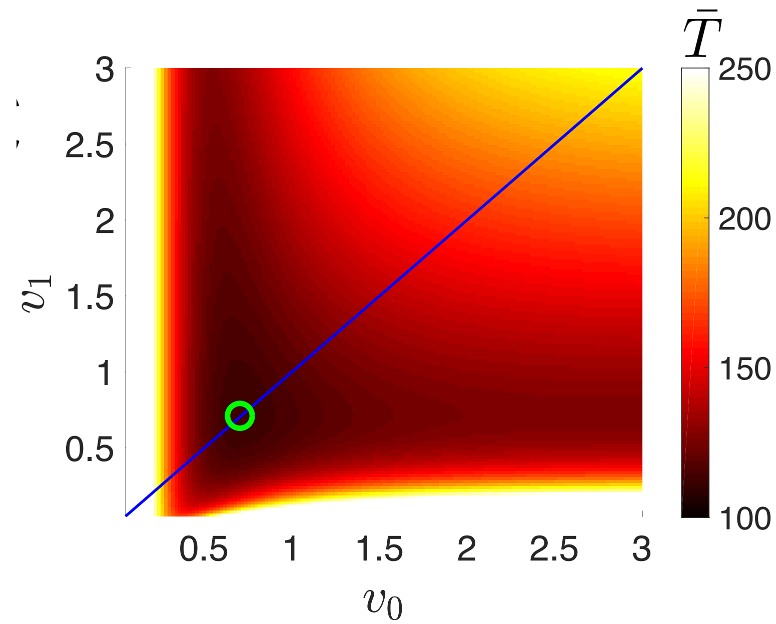

IOR has little advantage along 1D tracks

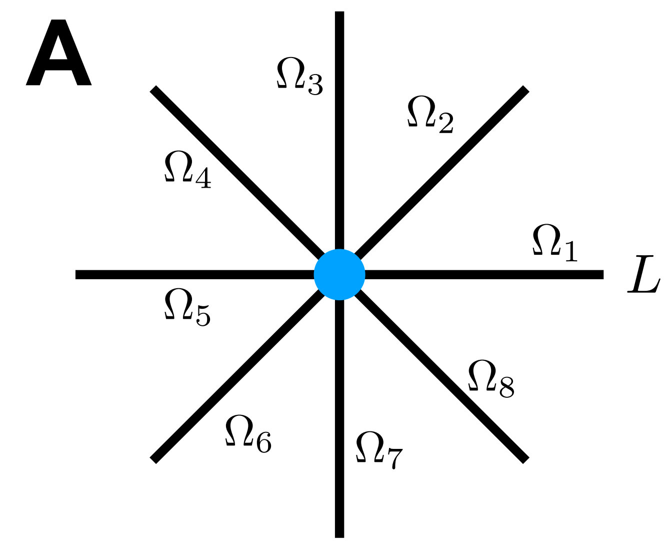

only advantageous on more complex domains

ZP Kilpatrick, DB Poll. *Neural field model of memory-guided search.* Phys. Rev. E (2017) in press.

DB Poll, ZP Kilpatrick. *Persistent search in single and multiple confined domains: a velocity-jump process model.* J Stat. Mech. (2016) 053201.

Conclusions

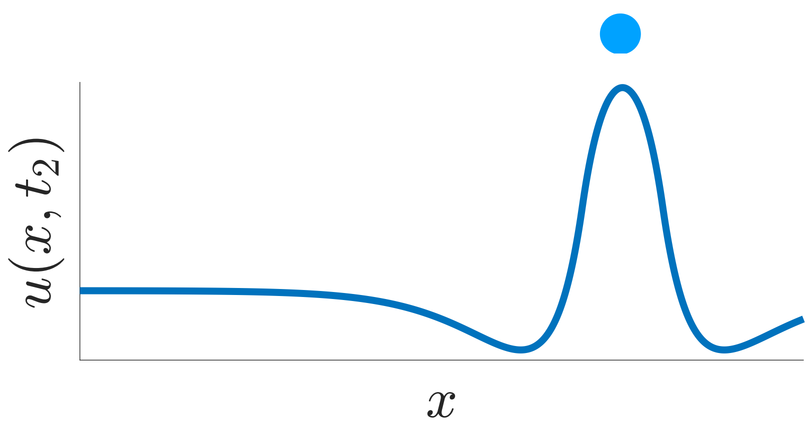

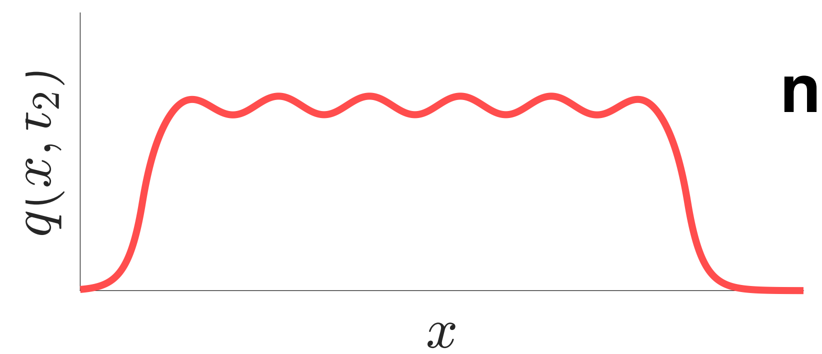

spatiotemporal patterns of neural activity can track current and visited locations

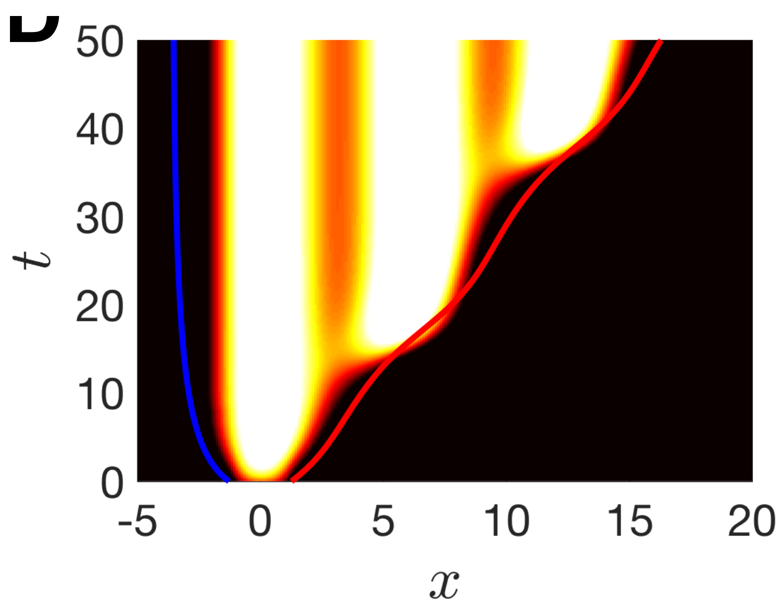

interface equations estimate low-dimensional dynamics

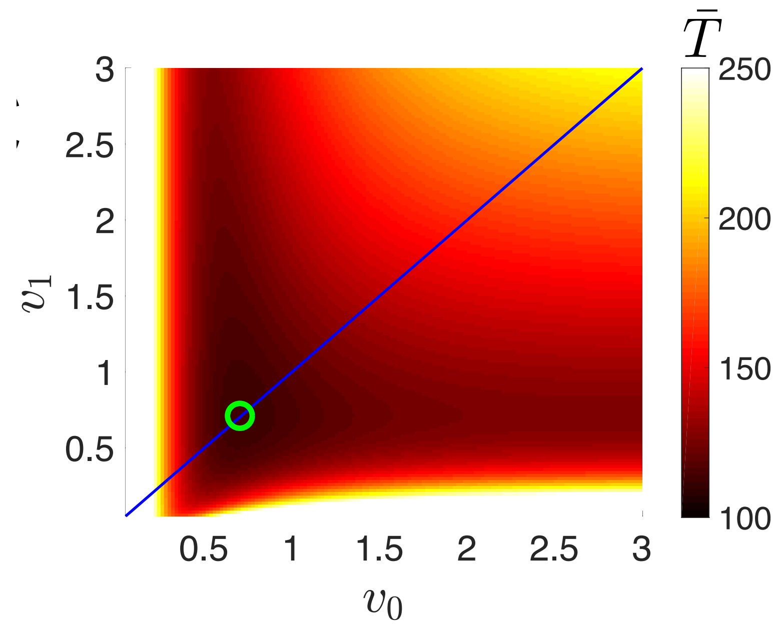

IOR has little advantage along 1D tracks

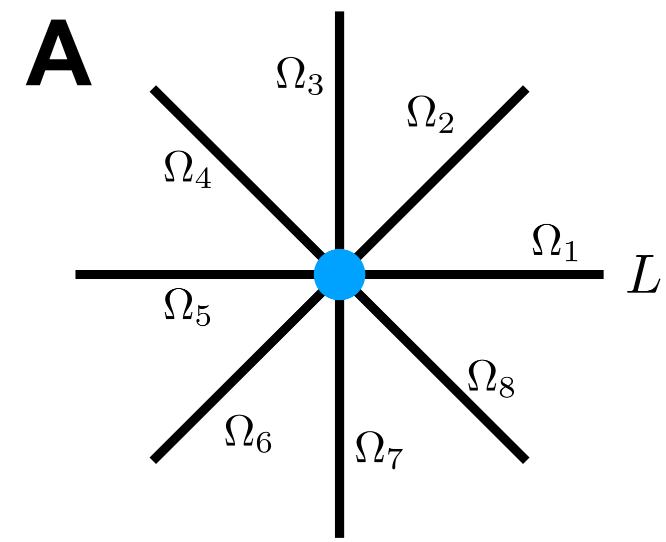

only advantageous on more complex domains

ZP Kilpatrick, DB Poll. *Neural field model of memory-guided search.* Phys. Rev. E (2017) in press.

DB Poll, ZP Kilpatrick. *Persistent search in single and multiple confined domains: a velocity-jump process model.* J Stat. Mech. (2016) 053201.